LUND UNIVERSITY

Study of a Pneumatic Hybrid aided by a FPGA Controlled Free Valve Technology System

Trajkovic, Sasa

2008

[Link to publication](#)

Total number of authors:
1

Study of a Pneumatic Hybrid aided by a FPGA Controlled Free Valve Technology System

Sasa Trajkovic

Thesis for the Degree of Licentiate in Engineering

Division of Combustion Engines
Department of Energy Sciences
Faculty of Engineering
Lund University

To Tatjana

List of Papers

Paper 1

FPGA Controlled Pneumatic Variable Valve Actuation
SAE Technical Paper 2006-01-0041
By Sasa Trajkovic, Alexandar Milosavljevic, Per Tunestål and Bengt Johansson
Presented by Sasa Trajkovic at the SAE World Congress, Detroit, MI, USA, April 2006

Paper 2

Introductory Study of Variable Valve Actuation for Pneumatic Hybridization
SAE Technical Paper 2007-01-0288
By Sasa Trajkovic, Per Tunestål and Bengt Johansson
Presented by Sasa Trajkovic at the SAE World Congress, Detroit, MI, USA, April 2007

Paper 3

Investigation of Different Valve Geometries and Valve Timing Strategies and their Effect on Regenerative Efficiency for a Pneumatic Hybrid with Variable Valve Actuation
SAE Technical Paper 2008-01-1715
By Sasa Trajkovic, Per Tunestål and Bengt Johansson
To be published at the SAE 2008 International Powertrains, Fuels and Lubricants Congress, Shanghai, China, June 2008

Other Publications

HCCI Combustion of Natural Gas and Hydrogen Enriched Natural Gas Combustion Control by Early Direct Injection of Diesel Oil and RME
SAE Technical Paper 2008-01-1657
By I. Saanum, M. Bysveen, J.E. Hustad, P. Tunestål and S. Trajkovic
To be published at the SAE 2008 International Powertrains, Fuels and Lubricants Congress, Shanghai, China, June 2008

Abstract

Urban traffic involves frequent acceleration and deceleration. During deceleration, the energy previously used to accelerate the vehicle is mainly wasted on heat generated by the friction brakes. If this energy that is wasted in traditional IC engines could be saved, the fuel economy would improve. Today there are several solutions to meet the demand for better fuel economy and one of them is the pneumatic hybrids. The idea with pneumatic hybridization is to reduce the fuel consumption by taking advantage of the, otherwise lost, brake energy.

In the work presented in this study a heavy duty Scania D12 engine has been converted to work as a pneumatic hybrid. During pneumatic hybrid operation the engine can be used as a 2-stroke compressor for generation of compressed air during vehicle deceleration (compressor mode) and during vehicle acceleration the engine can be operated as an air-motor driven by the previously stored pressurized air (air-motor mode). The compressed air is stored in a pressure tank connected to one of the inlet ports. One of the engine inlet valves has been modified to work as a tank valve in order to control the pressurized air flow to and from the pressure tank.

In order to switch between different modes of engine operation there is a need for a fully variable valve actuation (FVVA) system. The engine used in this study is equipped with pneumatic valve actuators that use compressed air in order to drive the valves and the motion of the valves are controlled by a combination of electronics and hydraulics.

Since the pneumatic VVA system, used in the work presented in this thesis, was still under development, the need to evaluate the system before any extensive use was more than necessary.

The evaluation of the pneumatic VVA system verified its potential and a stable function was noticed together with great flexibility to manipulate both valve timing and valve lift to fit the desired purpose.

Initial testing concerning the different pneumatic hybrid engine modes of operation was conducted. Both compressor mode (CM) and air-motor mode (AM) were executed successfully. Optimization of CM and AM with regards to valve timing and valve geometry has been done with great improvements in regenerative efficiency which is defined as the ratio between the energy extracted during AM and the energy consumed during CM.

Acknowledgment

Nomenclature

ABDC	After Bottom Dead Centre
AM	Air-motor Mode
APAM	Air-Power-Assist Mode
ATDC	After Top Dead Centre
AVT	Active Valve Train
BDC	
BTDC	Bottom Dead Centre
CA50	Crank Angle for 50% burned
CAD	Crank Angle Degree
CI	Compression Ignition
CM	Compressor Mode
CO	Carbon Monoxide
CO_2	Carbon Dioxide
COV	Coefficient Of Variation
DOHC	Double OverHead Camshaft
EGR	Exhaust Gas Recirculation
EHVA	Electro Hydraulic Valve Actuation
EMVA	Electro Magnetic Valve Actuation
EPVA	Elector Pneumatic Valve Actuation
EVC	Exhaust Valve Closing
EVO	Exhaust Valve Opening
FPGA	Field Programmable Gate Array
FVVA	Fully Variable Valve Actuation
GUI	Graphical User Interface
HCCI	Homogeneous Charge Compression Ignition
HEV	Hybrid Electric Vehicle
HP	Horse Power
HPV	Hybrid Pneumatic Vehicle
ICE	Internal Combustion Engine
IMEP	Indicated Mean Effective Pressure
IVC	Inlet Valve Closing
IVO	Inlet Valve Opening
k	Polytropic exponent [-]
LDT	Linear Displacement Transducer
MIVEC	Mitsubishi Innovative Valve Timing and Lift Electronic Control
OHC	OvherHead Camshaft
OHV	OverHead Valve
p	In-cylinder pressure [bar]
PM	Particulate Matter
PVO	Positive Valve Overlap
NO_x	Nitrogen Oxides
NVO	Negative Valve Overlap
RPM	Revolutions Per Minute
SI	Spark Ignition
TankVC	Tank Valve Closing

TankVO   Tank Valve Opening
TDC   Top Dead Centre
V   Cylinder volume [m^3]
VTEC   Variable valve Timing and lift Electronic Control
VVA   Variable Valve Actuation
VVT   Variable Valve Timing
VVTL-i   Variable Valve Timing and Lift with intelligence

Contents

1 Introduction

1.1 Background

The society of today relies to a great extent on different means of transportation. Never before have people travelled to different parts of the world, far away from their own, as today. This massive traveling is a heavy load on our nature. The cars that increase in numbers every day, emit toxic emissions on our highways and the airplanes consume huge amounts of fossil fuels. In recent years the awareness of the effect of pollution on the environment and climate has increased. People are more conscious of the situation and are looking for alternative means of transportation with less impact on the environment. The exhaust emission standards are getting more and more stringent and there now exists a discussion about the introduction of a mandatory emissions standard for CO2 [1], a green house gas that contributes to the climate change which is an issue of growing international concern. This demand for lower exhaust emission levels together with increasing fuel prices leads to the demand of combustion engines with better fuel economy, which forces engine developers to find and investigate more efficient alternative engine management.

Today there exist several solutions to achieve lower exhaust emissions and better fuel economy. Some of them are well known while others are still in development. Some examples of such solutions are VVA (Variable Valve Actuation), EGR (Exhaust Gas Recirculation), direct injection, hybridization of vehicles, just to mention a few. In this work the emphasis has been put on VVA and vehicle hybridization.

A VVA system adds several degrees of freedom to the control of the combustion engine. VVA makes it possible to use valve strategies that affect the combustion in such a way that the exhaust emissions are decreased. The valve lift and duration are automatically altered in a VVA system to the optimum setting for the actual engine speed and load, and thereby the fuel consumption is lowered. With VVA it is possible to deactivate some of the engine´s cylinders when they are not needed which results in higher engine efficiency and thereby lower fuel consumption.

Vehicle hybridization can be done in various ways. The maybe best known example of vehicle hybridization is the electric hybrid. However other hybrids like fuel cell hybrids and pneumatic hybrids are being investigated. The main idea with electric hybridization is to reduce the fuel consumption by taking advantage of the otherwise lost brake energy. Hybrid operation also allows the combustion engine to operate at its most optimal operating point in terms of load and speed. The main disadvantage with electric hybrids is that they require an extra propulsion system and large heavy batteries with a limited life-cycle. This introduces extra manufacturing costs which are compensated by a higher end-product price comparable to the price of high end vehicles. One way of keeping the extra cost as low as possible and thereby increase customer attractiveness, is the introduction of the pneumatic hybrid. It does not require an expensive extra propulsion source and it works in a way similar to the electric hybrid. Tai et al. [2] describes simulations of a pneumatic hybrid with a so called "round-trip" efficiency of 36% and an improvement of 64% on fuel economy in city driving. Simulations made by Andersson et al. [3] show a regenerative efficiency as high as 55% for a dual pressure tank system for heavy duty vehicles.

1.2 Outline

The work presented in this thesis can be divided into two parts. The first part deals with a new type of VVA system, namely an electro-pneumatic VVA system and the second part describes experimental studies done on an engine converted to work as a pneumatic hybrid.

1.2.1 Pneumatic valve actuation

Variable valve actuation influences many parameters in an engine and is therefore of great importance. The problem with VVA systems has so far been that they are quite complicated and introduce higher production costs compared to conventional camshaft-driven engine valves. Another issue is that not all of the various VVA systems on the market are fully variable valve actuating (FVVA) systems, i.e. valve timing, duration and lift height can not be controlled independently. This problem can be solved with hydraulic VVA systems. The disadvantage with such systems is that they are quite expensive to manufacture because of the high precision needed and has unacceptably high energy consumption. The pneumatic VVA system used in the project described in this thesis, offers fully variable valve lift height and valve duration at an energy consumption well below the consumption of a hydraulic system (less than 4 kW at 6000 rpm with a 4-cylinder engine) and it is also well suited to mass production with relatively few moving parts, which makes it very cost effective [4]. In the present thesis the pneumatic VVA system has been evaluated and different valve strategies have been tested in order to ensure proper operation in a real combustion engine [5].

1.2.2 Pneumatic hybrid

Electric hybrids have become very popular over the last couple of years thanks to increasing concern for our environment. The attractiveness of the electric hybrid is its low fuel consumption which in turn leads to lower levels of exhaust emissions. What stops the electric hybrid car from becoming every man's property is its price. The extra propulsion system and batteries add up to the manufacturing cost, which in turn the customer has to pay for. A more cost effective alternative would be the pneumatic hybrid. It works in a way similar to the electric hybrid, but since it does not require an extra propulsion source and batteries, the additional manufacturing price can be kept at a reasonable level, thus making it an attractive choice for the customers. Simulations have showed that the pneumatic hybrid has a great potential in saving fuel, at least during city driving [2, 3, 6, 7, 8]. The second part of the present thesis describes experimental studies done on a single-cylinder Scania D12 diesel engine converted to work as a pneumatic hybrid [9] and optimization of the valve timings in order to maximize the efficiency of pneumatic hybrid operation [10].

1.3 Method

Since there have already been some simulations done regarding pneumatic hybridization by other researchers, it has been decided that the first part of the author´s PhD work presented in this thesis should be conducted as an experimental study in order to investigate the feasibility of the pneumatic hybrid concept. The second part of the authors PhD work will, among other things, include simulations based on results from real engine experiments, however it will not be dealt with in the present thesis.

2 The internal combustion engine

For more than 100 years the internal combustion engine (ICE) has been the primary source of propulsion in ground vehicles and it is remarkable that this old design is still what propels the vehicles of today. Ever since the beginning of the ICE era various inventors have tried to find a better alternative solution but with no great success. The reason is that although the ICE has a relatively low efficiency, it has other features that make it attractive, like for instance high power-to-weight ratio, high fuel energy density which facilitates carrying large amounts of fuel energy, low manufacturing cost and long durability with minimal maintenance.

There are two main types of internal combustion engines: the spark ignition (SI) engine and the compression ignition (CI) engine. They are also known as the Otto engine and Diesel engine, respectively, named after the inventors. The fuel usually used in SI engines is gasoline but it is also possible to use other fuels such as natural gas and alcohol. The Diesel engine utilizes, as the name implies, diesel as fuel.

2.1 SI engine and CI engine fundamental operating principel

Both SI and CI engines can be divided into subgroups defined by the number of strokes that occur during one working cycle. Two-stroke cycles are mainly used in SI engines for very light low-cost applications such as chain saws and lawnmowers, however heavy applications such as locomotives and ships use two-stroke Diesel engines. The majority of other engine-based applications use the four-stroke cycle. The four-stroke operating cycle can be explained with references to Figure 1:

a) *Intake stroke.* The inlet valve is open and fresh air/fuel-mixture is drawn into the cylinder as the piston travels towards bottom dead center (BDC). In the case of CI engines, only air is drawn into the cylinder during the intake stroke.

b) *Compression stroke.* Both valves are now closed. As the piston is traveling towards top dead center (TDC) the air/fuel charge is compressed, and as the piston approaches TDC, the charge is ignited by a sparkplug and the combustion is initiated. In the case of CI engines, the fuel is injected towards the end of the compression stroke and the fuel self-ignites due to the high cylinder temperature.

c) *Expansion stroke or Power stroke.* As a result of the combustion, the temperature and pressure in the cylinder is raised. The hot and pressurized in-cylinder gases perform useful work as they expand and push the piston down towards BDC.

d) *Exhaust stroke.* The exhaust valve opens shortly before the end of the expansion stroke and remains open during the entire exhaust stroke. As the piston travels towards TDC the burned gases are swept out past the exhaust valve.
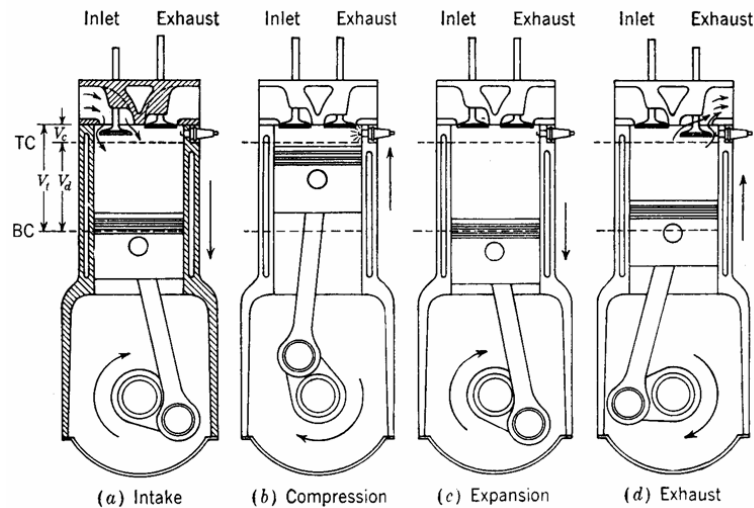
Figure 1 The four strokes of a SI engine [11].

The four-stroke cycle produces one power stroke every second crankshaft revolution. Over the years, ever since the introduction of the first four-stroke engine, researchers and inventors have believed that a power stroke could be generated with each crankshaft revolution. These beliefs lead to the development of the two-stroke engine. The two-stroke operating cycle can be explained with references to Figure 2:
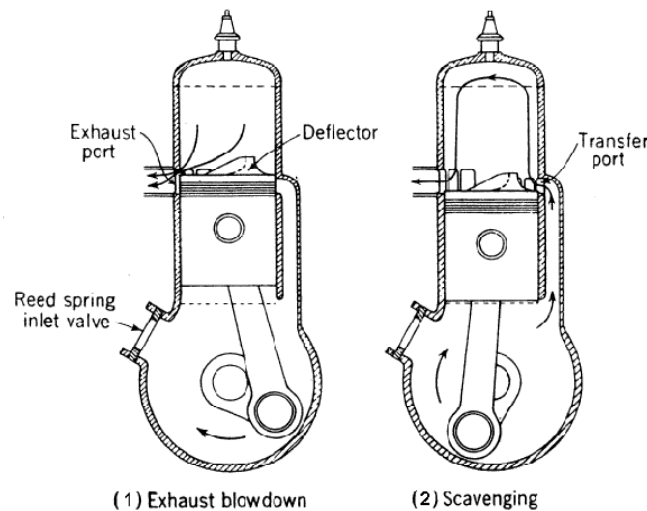
Figure 2 The two-stroke cycle illustrated for a crankcase-scavenged engine [11].

a) *Compression Stroke*. The inlet and exhaust ports are closed during the compression stroke. As the piston is traveling towards TDC the trapped charge is compressed, while the underside of the piston draws in fresh charge into the crankcase through a Reed spring inlet valve. The fuel can either be premixed or injected towards the end of the compression stroke. Ignition of the charge occurs as the piston approaches TDC.

b) *Expansion or Power stroke*. As the combustion propagates throughout the combustion chamber, the temperature and pressure increase and forces the piston down. During the downward movement of the piston, the charge in the

crankcase is compressed. The gas exchange process starts as the piston approaches BDC and uncovers the exhaust port. This starts the blowdown of exhaust gases through the exhaust port. When the piston reaches BDC the transfer port is also uncovered, and the compressed charge in the crankcase expands into the cylinder and pushes the remaining exhaust gases out through the exhaust port.

The advantage with the two-stroke engine is that it is simple to manufacture (few moving parts) and it is more powerful than the four-stroke engine since the two-stroke engine generates a power stroke on every crankshaft revolution. The problem with two-stroke engines is that it is difficult to achieve an efficient scavenging process and a portion of the fresh charge flows directly out of the cylinder during the scavenging process.

2.2 The Homogeneous Charge Compression Ignition (HCCI) Engine

Even though the ICE has evolved significantly over the last 100 years it is not all roses. The SI engine suffers from low efficiency at low loads and the CI engine suffers from high emissions of Nitrogen Oxides (NO_x) and Particulate Matter (PM). The Homogeneous Charge Compression Ignition (HCCI) engine is a hybrid of the SI engine and the CI engine processes. HCCI combines the high efficiency of the CI engine with the low NO_x and PM emissions of a SI engine. In a HCCI engine, the fuel and air are mixed prior to combustion just like in SI engines and compression of this mixture causes auto-ignition like in the CI engine. The conceptual differences between the combustion in SI, CI and HCCI engines are illustrated in Figure 3.
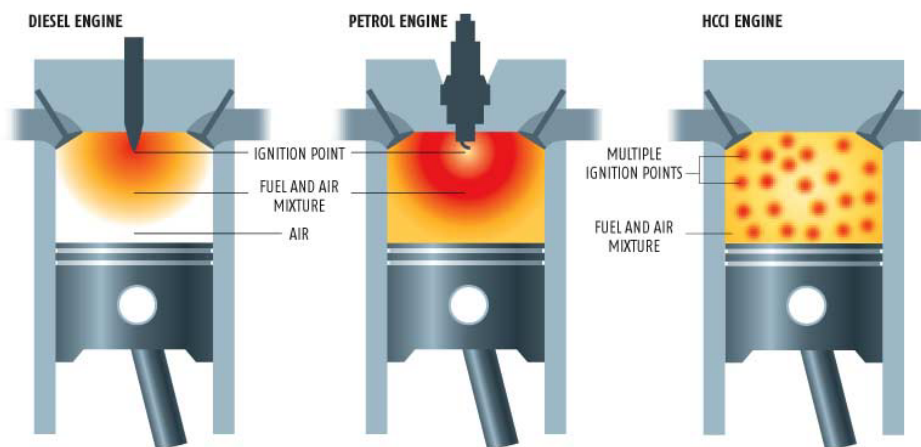
Figure 3 Illustration of the combustion process in a SI, CI and HCCI engine [12].

The defining characteristics of HCCI are that ignition of the air/fuel-mixture starts simultaneously at several locations, making the combustion occur almost simultaneously throughout the entire combustion chamber which in turn contributes to a very fast combustion rate. The high combustion rate leads to high pressure rise rates and noise levels. In order to avoid this and prevent engine failure, the air/fuel-mixture has to be diluted. The diluents can be air, recirculated exhaust gas (EGR) or trapped residuals. By diluting the mixture and making it lean, the combustion temperature will

be low which results in very low NO_x emissions and almost no PM, while HC and CO emissions increase due to lower combustion efficiency.

Due to the nature of HCCI combustion, there is no actuating mechanism directly controlling start of combustion making the control of combustion difficult. The HCCI combustion initiation process depends highly on chemical kinetics of the air/fuel mixture and thus the time history of pressure and temperature in the cylinder. There are various methods for controlling the HCCI ignition timing through these parameters. Possible methods are control of the inlet air temperature [13], variable compression ratio [14], dual fuel injection [15], variable valve timing [16] and exhaust gas recirculation [17], just to mention a few.

3 Conventional Valve Actuation

Since the beginning of the ICE history, almost all engines have had some sort of valve design for the gas exchange process. The purpose of the gas exchange process is to remove the burnt gases from the combustion chamber and admit a fresh charge for the next cycle.

3.1 Valve design

The most commonly used valve design in four-stroke internal combustion engines is the camshaft driven poppet valve. The main advantages of poppet valves are that they are cheap to manufacture, good flow characteristics and sealing properties, easy lubrication and good heat transfer to the cylinder head.

The poppet valve is most often a flat disk of metal with a long rod known as the valve stem. A somewhat typical valvetrain is illustrated in Figure 4.
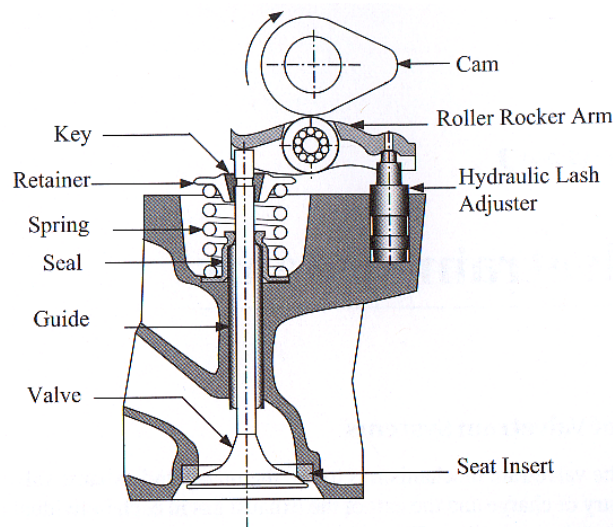
Figure 4. Schematic of a valvetrain [18].

The engine normally operates the valves by pushing on the stems with cams and cam followers. The valve spring keeps the valve closed tightly against its seat until the valve is opened by the cam. As the cam pushes the stem down and the valve opens, the valve spring is pressed together. The compressed valve spring pushes the valve against the cam lobe and the contact remains throughout the whole valve movement.

3.2 Valvetrain operating systems

The placement of camshafts, valves and possible transfer mechanisms between camshaft and valve can be done in several ways. In the overhead valve (OHV) setup the camshaft is mounted in the cylinder block and the valves are operated from the camshaft via cam followers, push rods and rocker arms. An example of this kind of valvetrain arrangement is illustrated in Figure 5. The disadvantage with this kind of systems is that, due to higher inertia caused by larger amount of valvetrain components it is difficult to accurately control the valve timing at high rpm. One way to solve this is to decrease the

inertia by minimizing the amount of moving parts, and the solution is the overhead camshaft (OHC) setup in which the camshaft is mounted either directly over the valve stems or it can be offset, which means that the valves are operated by rockers. In Figure 6, a double overhead camshaft (DOHC) valvetrain without offset can be seen. In this setup, the cam lobe acts directly on the cam follower. The disadvantage with this kind of system is mainly that it is a more complex and expensive design compared to the OHV setup.
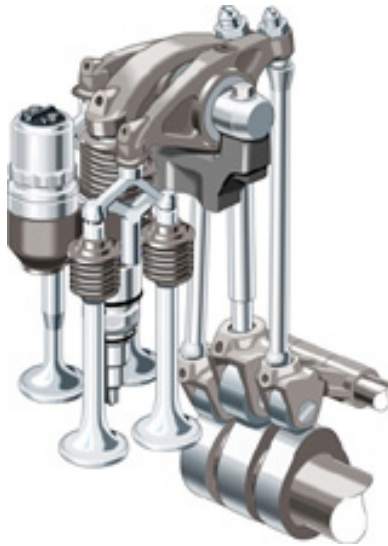
Figure 5. Valvetrain mechanism for a Scania 12 liter Diesel engine [20].
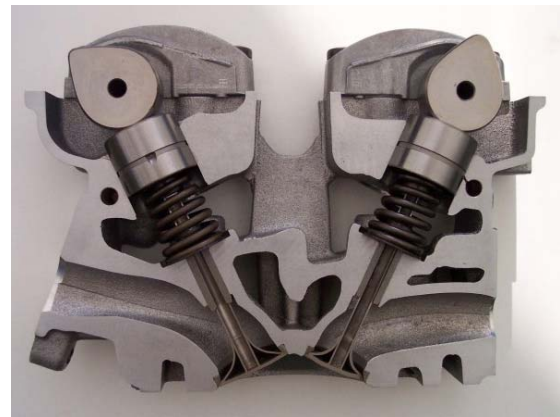
Figure 6. Double overhead camshaft (DOHC) valve arrangement [19].

3.3 Valve Actuation

The term *valve actuation* refers to the valve lift event and includes valve timing, valve lift height and duration. The valve lift height and duration are defined by the geometry of the cam, while valve timing is controlled by both cam shape and the position of each cam relative to each other. The valve actuation is responsible for controlling the communication between the cylinder and the intake- and exhaust system, and it is a very important factor in engine design since it affects engine performance, fuel economy and emissions.

3.3.1 Valve Lift

It is highly desirable to achieve a maximum valve lift as soon as possible after the initiation of valve opening. The reason is that with a fast valve opening sequence, the flow over the valve will be less restricted during a greater part of the valve lift duration and result in higher volumetric efficiency. Figure 7 illustrates an optimal valve lift profile with an infinitely fast valve opening and valve closing. However, such a valve lift profile would be impossible to implement in reality, since an instantaneous valve opening and

closing would mean infinite acceleration of the valve which would be much too severe for any valvetrain to endure. Also, the valve has to slow down as it approaches the seat in order to prevent the valve from hitting the seat with loud noises, and worn and broken parts as a result.
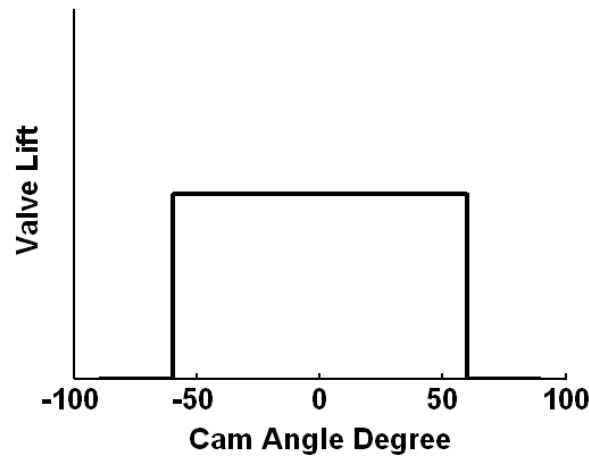
Figure 7 Ideal valve lift profile.

3.3.2 Valve Timing

Figure 8 illustrates the regular valve timings for a four-stroke engine.
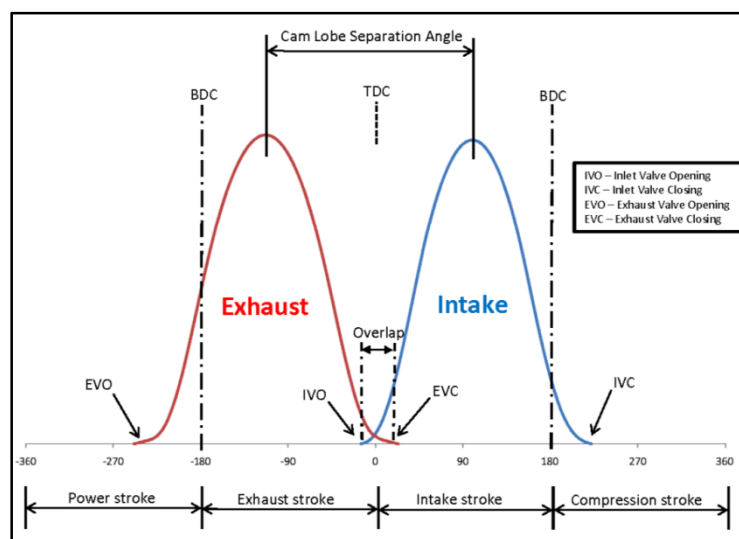
Figure 8 Regular valve timing diagram for a four-stroke engine.

At the end of the power stroke, as the piston approaches BDC, the exhaust valve starts to open. It remains open during the whole exhaust stroke and closes shortly after the start of the intake stroke. The reason why the exhaust valve opens before BDC and closes after TDC is that this behavior increases the average valve lift and thus minimizes the flow resistance in the exhaust port. At the end of the exhaust stroke the inlet valve starts

to open. This means that there is a short period of time when both the exhaust and inlet valves are open. This period is referred to as the *valve overlap* and it is designed to promote induction of fresh charge into the cylinder by using the vacuum created by the outgoing exhaust gases. The inlet valve remains open during the entire intake stroke and closes shortly after the start of the compression stroke.

4   Variable Valve Actuation

The disadvantage with conventional valve actuation in combustion engines is that once the camshaft has been configured and produced, its characteristics can never be changed. Since optimal timing and lift settings are different at high and low engine speeds, the fixed valve timing in conventional engines has to be a compromise between these two. For instance, a mid-size car with engine speeds hardly exceeding 3000 rpm uses a small valve overlap. Small valve overlap gives the engine a smooth idle and good slow speed torque. High rpm race cars, on the other hand, use a large valve overlap. A large valve overlap allows good engine breathing at high engine speeds but causes a rough idle and poor performance at low rpm. It is evident that in order to design an engine with good performance at both low and high engine speeds, the valve timings cannot be fixed and thus *variable valve actuation* (VVA) is needed. Variable valve actuation is a generalized term used to describe the altering of the valve lift event by means of variable valve timing, lift and duration. Since there are many ways in which this can be achieved, only the most common systems will be briefly described.

4.1   Camshaft-based VVA mechanism

The most widely used mechanism for VVA utilizes a specially designed camshaft as main component. In this kind of VVA systems the camshaft has some extra features for changing the valve timing or valve lift, or a combination of both. Some of the various systems will be described below.

4.1.1   Variable valve timing by camshaft phasing

In a cam phasing system, the camshaft can be rotated with respect to the crankshaft and thereby the valve timing can be changed while the valve duration and lift stays unaffected. Simpler systems only offer shifting between two fixed positions while more complex systems feature continuously variable valve timing within a defined crank angle range.
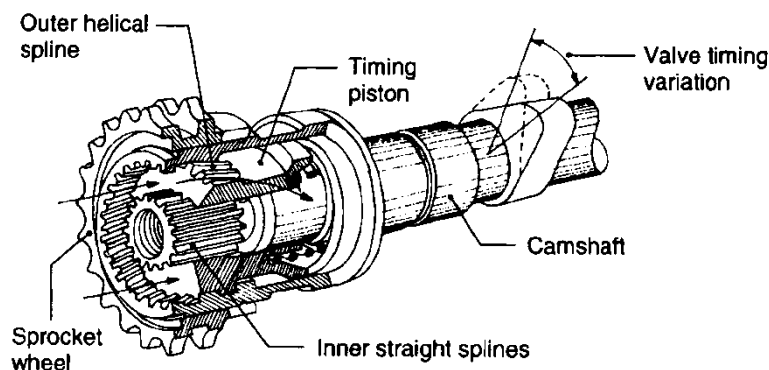
Figure 9 Alfa Romeo cam phasing mechanism using helical and straight splines [23].

Alfa Romeo was the first manufacturer to use a variable valve timing system in production cars. The patent for the system was filed 1979 in the USA [21] and models starting from 1984 used a phasing of the intake cam relative to the crankshaft [22]. The system is illustrated in Figure 9. What characterizes this system is that the intake valve duration remains constant while IVO and IVC are moved equally, see Figure 10.
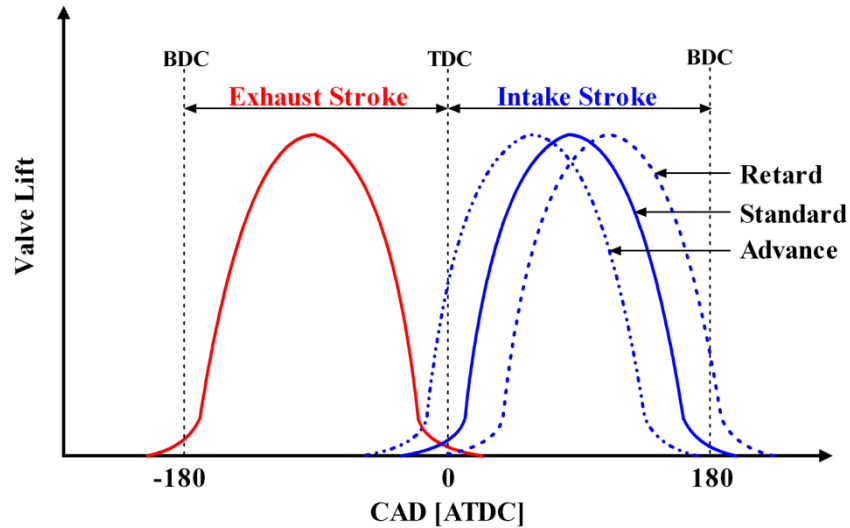
Figure 10 Illustration of inlet valve cam phasing.

At light loads and low engine speeds it is beneficial to retard the intake valve event, since the reduced valve overlap results in improved combustion (no blow back of exhaust gases to the intake side) and a delayed IVC reduces throttling losses. In low to medium speed range, the intake valve event is advanced and thereby the valve overlap is increased. The earlier IVC prevents the already inducted air from being expelled, thus increasing the power output. At high engine speeds it is favorable with late IVC in order to take advantage of the intake system ram effect and since the reduced valve overlap contributes to a lower residual gas fraction, the mass of the inducted air/fuel mixture is
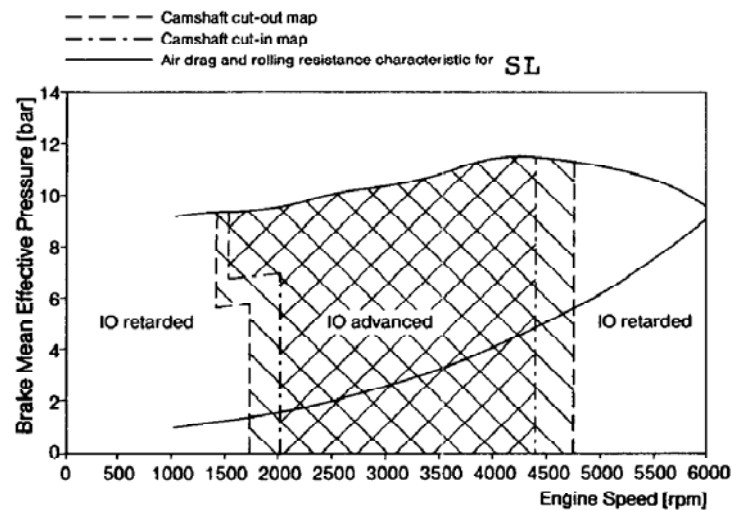
Figure 11 Variable valve timing map for a Mercedes-Benz 500 SL [24].

maximized with a higher engine power output as a result. Figure 11 shows the cam phasing strategy throughout the whole engine speed range for a Mercedes-Benz 500 SL. Toyota introduced a continuously controlled cam phasing system in 1996. It is known as the VVT-I system and it gives continuously variable intake cam phasing by up to 60 crank angle degrees (CAD). The VVT-I system showed improvements in fuel economy by 6%, compared to a similar engine using a conventional camshaft [25].

4.1.2 Variable valve lift by cam profile switching

A drawback with cam phasing is that the valve event duration and valve lift height are unaffected. Unaffected valve duration means that if IVO is retarded, then IVC is also retarded by the same amount, which in some cases leads to reduced amount of charge entering the engine. This could be avoided with a system that allows altering of the valve event duration. In this way, IVC can be adjusted for maximum volumetric efficiency at higher engine speeds and larger valve overlap.

The valve lift is also an important factor affecting engine performance. At low engine speeds, a lower valve lift is preferable, since it promotes more turbulence. At high engine speeds the valve lift height is set to a maximum in order to achieve efficient breathing. Figure 12 illustrates typical valve timing and valve lift height for a two-step cam profile switching system.
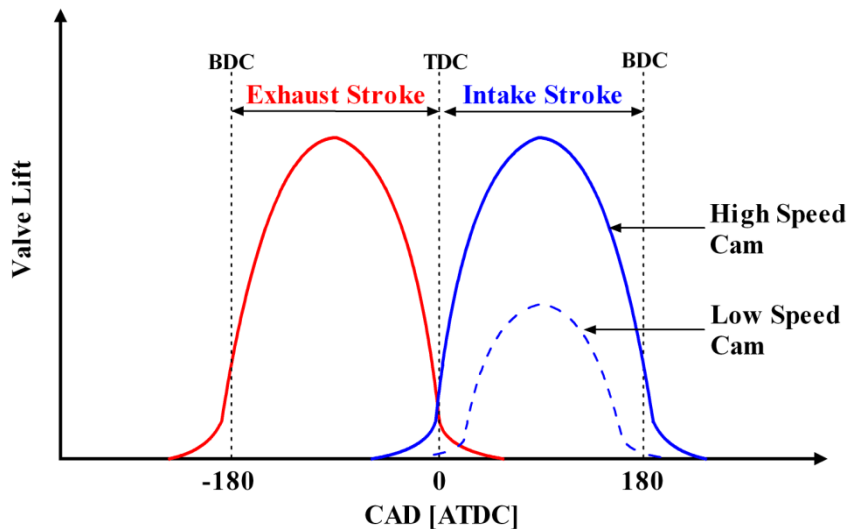
Figure 12 Illustration of two-step cam profile swithching.

Honda has developed a system called VTEC (Variable valve Timing and lift Electronic Control) which allows switching between two different cam profiles [26]. The engine has two low-speed cam lobes and one high-speed cam lobe, see Figure 13. As the engine moves into different rpm ranges, the engine controller can activate different lobes on the camshaft and change the cam timing. In this way, the engine gets the best features of low-speed and high-speed camshafts in the same engine.

Mitsubishi has developed a system similar to Honda´s VTEC which is known as MIVEC (Mitsubishi Innovative Valve Timing and Lift Electronic Control) [27]. The advantage

with this system compared to the VTEC system, is that when the high engine speed cam lobe is used, only the corresponding rocker arm is active, while VTEC activates all three rocker arms at the high engine speed setting. This reduces the total moving mass of the valvetrain and thus more aggressive valve acceleration is possible. Another advantage is that MIVEC offers valve deactivation and thus cylinder deactivation with lower fuel consumption as a result. The valve mechanism of the MIVEC system is illustrated in Figure 14.
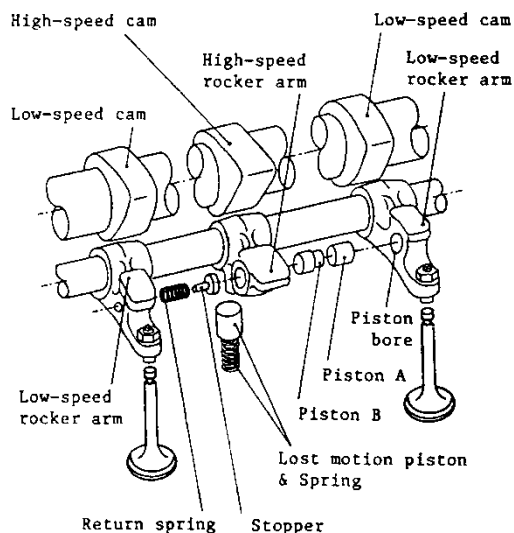
Figure 13 Honda VTEC variable valve actuation mechanism [26].
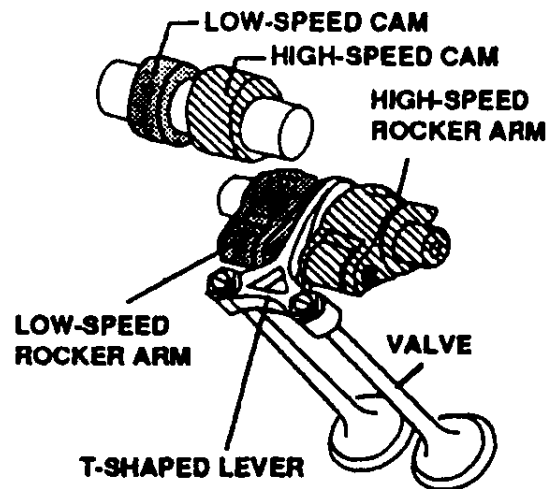
Figure 14 Valve mechanism of Mitsubishi's MIVEC system [27].

4.1.3 Variable valve lift by combining cam phasing and profile changing

A cam phasing system gives the ability to change the valve timing while a cam profile changing system introduces the possibility to change the valve lift. Both systems have benefits compared to a conventional camshaft. However, a combination of both systems would offer even better engine characteristics with lower fuel consumption and higher engine output. Both Toyota and Porsche have demonstrated such systems.

In 1998, Porsche showed their system called VarioCam Plus, which combines the best features of cam phasing and profile changing [28]. Three cam profiles are used for each valve, one low lifting and two high lifting, see Figure 15.

The system offers a total of 4 valve-lift and camshaft adjustment combinations, as can be seen in Figure 16. At part-load operation and engine speeds of less than 3700 rpm, the low-lifting cam is chosen together with retarded cam phasing, in order to ensure optimum combustion stability. At full-load operation with engine speeds exceeding 1200 rpm, the high-lifting valve profile is used together with advanced cam phasing [29].
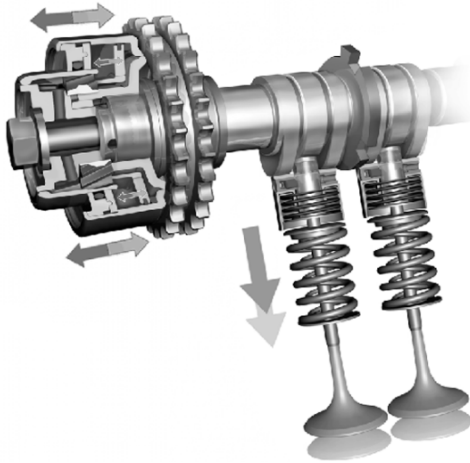
Figure 15 Porsche VarioCam Plus system [29].
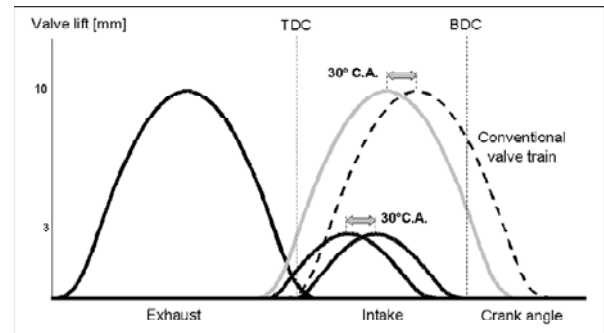
Figure 16 VarioCam Plus valve lift curves [29].

With variable valve lift and cam phasing, Porsche has lowered fuel consumption of the 2000 Porsche 911 by 18% compared to previous 911 models, while torque has increased by 40% (160 Nm). The exhaust emissions have also been reduced and the car fulfills the D4 and U.S. LEV emissions standards [30].

In 2000, Toyota presented their system called VVTL-i. The system is a combination of their previously developed cam phasing system, VVT-i, and cam profile switching [31]. The valve timing and lift for this system is shown in Table 1. The switch from low- to high setting occurs as late as at 6000 rpm. Results obtained by Shikida et al. [31] showed an increase in maximum power by about 26% for an engine equipped with VVTL-I.

Table 1 Valve timing and lift for the VVTL-i system [31].

	Exhaust			Intake		
	Open BBDC (CA)	Close ATDC (CA)	Lift (mm)	Open BTDC (CA)	Close ABDC (CA)	Lift (mm)
Low	34	14	7.6	-10 to 33	58 to 15	7.6
High	56	40	10.0	15 to 58	97 to 54	11.2

4.1.4 Fully variable valve actuation with camshaft

A valve actuating system that permits continuous variation of valve lift as well as valve timing is known as a fully variable valve actuation (FVVA) system. A lot of mechanical systems which offers FVVA have been proposed. One of them is the Valvetronic system developed by BMW. It is based on the technology of the BMW Double-Vanos system, which is a VVT system utilizing cam phasing, together with an additional possibility to shift the valve lift continuously [32]. The Valvetronic system has a conventional intake cam, but it also uses a secondary eccentric shaft with a series of levers and roller followers activated by an electric motor, see Figure 17.

Figure 17 Illustration of BMW's Valvetronic mechanism [33].
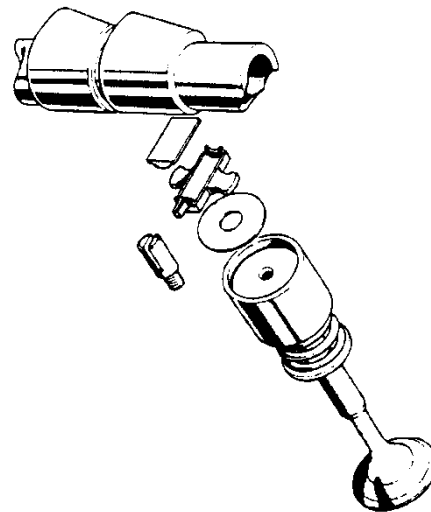
Figure 18 Fiat variable mechanism by Ferrari in a V8 engine [34].

Fiat presented a Ferrari V8 engine equipped with their FVVT system in 1991 [34]. The system uses a camshaft with multi-dimensional cam lobes. The change of valve lift curve is done by axial movement of the camshaft, see Figure 18. The linear contact between the cam lobe and the cam follower is maintained with a tilting pad in between. If combined with a cam phasing mechanism, Fiat's system would offer the possibility to change valve lift height, duration and timing.

4.2 Camless VVA mechanism

As stated before, the gas exchange in an engine with conventional camshaft based valve actuation is a compromise since the optimal valve timing at light loads and low engine speeds is not the same as the optimal valve timing at high engine speeds. Even though there are many camshaft-based mechanical VVA systems, they are all limited in their flexibility of individual valve and cylinder control. One way to solve this is to get rid of the camshaft. Instead the valves are actuated by some other mechanism, such as electrical, hydraulic or pneumatic. The valve timing and lift are electronically controlled by a computer. The computer receives information about the current state of the engine and depending on what is desired at the moment, the control program determines the most optimal valve timings. The valve timing can in this way easily be changed from cycle to cycle, which is a big advantage for combustion control.

The major advantage of camless VVA systems is the flexibility and the almost total control of the valve event. The disadvantage is that such systems are complex and expensive, and therefore used mainly by researchers in laboratories.

4.2.1 Electromagnetic Valve Actuation

Electromagnetic valve actuation (EMVA) offers great flexibility of valve timing, duration and lift. The valve actuation in this kind of systems is usually realized by different

combinations of solenoids and mechanical springs. Figure 19 shows a cross-section of GM's electro-mechanical valve actuator.
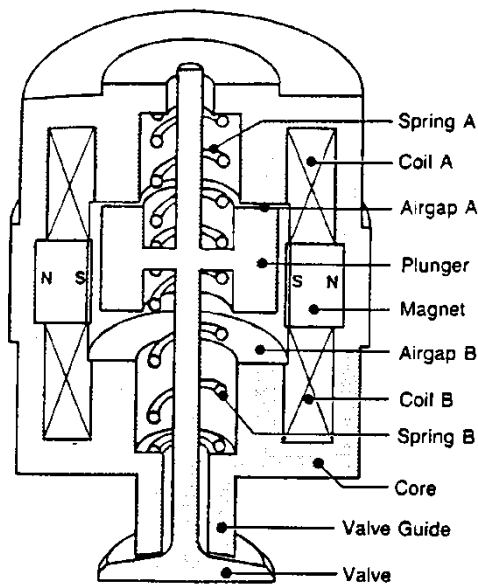
Figure 19 Cross-section of GM's electromechanical valve actuator [35].
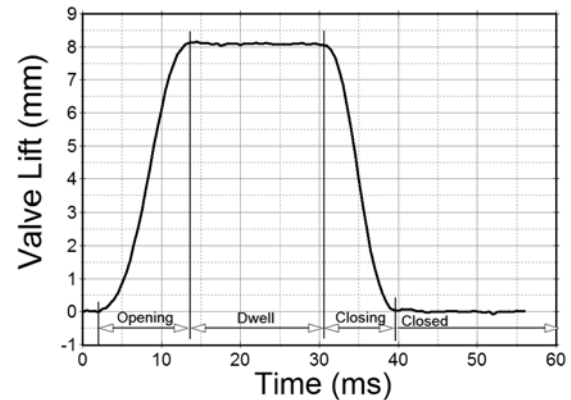
Figure 20 A typical valve lift profile for an electromagnetic valve train [37].

The valve is equipped with a plunger and placed inside a housing containing a permanent magnet and an electromagnet. When the valve is in its closed position, Spring A is compressed and the valve is held in place by the permanent magnet. To open the valve, coil A has to be activated and cancel the magnetic field of the permanent magnetic pole. This allows the spring force exerted by Spring A to accelerate the valve. As the valve moves towards its lower position, the plunger is attracted by the other permanent magnetic pole and spring B is compressed. The valve closing event is done in a reversed procedure compared to the valve opening event [36].

Figure 20 shows a typical valve lift profile achieved with an electromagnetic valve actuating system. Compared to a conventional valve lift, the electromagnetic valve lift profile has a much steeper valve-opening ramp which promotes better cylinder filling at low and medium engine speeds.

Theobald et al. [35] state that GM's electromagnetic system has lower energy consumption than a standard camshaft driven valve train at the same speed. A disadvantage with GM's system is that the valve seating velocity is unacceptably high with high noise levels as result. A solution to such valve seating problems has been proposed by Mianzo et al. [38] where the valve is slowed down by resistance induced by the valve stem entering a fluid-filled cavity. Because of the increased resistance, a soft seating of the valve head is achieved.

4.2.2 Electrohydraulic Valve Actuation

Another way to achieve camless valve operation is by electrohydraulic valve actuation (EHVA). Electrohydraulic valve actuators convert fluid pressure into motion in response to a signal. Schechter et al. [39] describes an EHVA system for variable control of engine valve timing, lift and velocity. The system does not use cams or springs, instead the

valves are both opened and closed by hydraulic force. Throughout the valve acceleration, the potential energy of the compressed fluid is transformed into kinetic energy of the valve. During deceleration the energy of the valve motion is returned to the fluid. Figure 21 illustrates Ford´s electrohydraulic valve train actuation concept and Figure 22 shows the lift profile for the system in question.
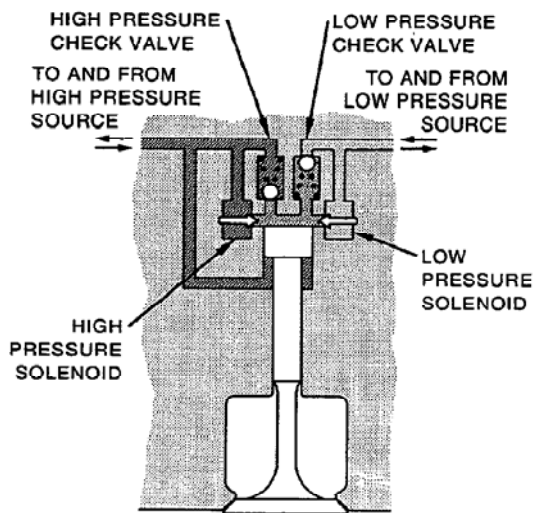
Figure 21 Illustration of Ford's electrohydraulic camless valve train [39].
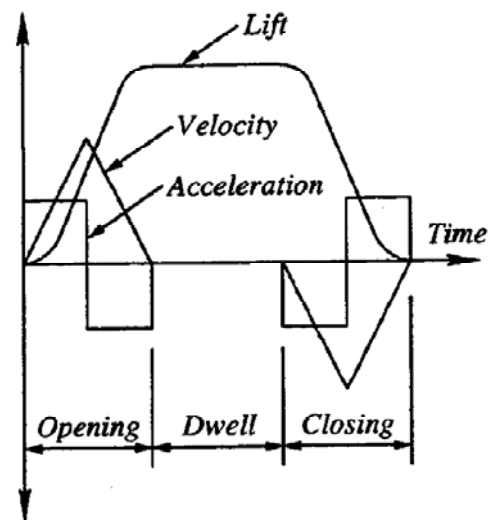
Figure 22 The lift profile of the electrohydraulic valve train presented by Schechter et al. [39].

While the valve is in its closed position, the high-pressure solenoid is opened and the high-pressure fluid is allowed to enter the volume above the valve. The pressure above and under the valve piston is equal but since the area on the upside of the valve piston is larger, the net hydraulic force is directed downward and therefore the valve opens. As the valve moves towards its lower position, the high pressure solenoid closes which results in a cut-off of the high pressure supply. Even though the pressure above the valve piston decreases, the valve keeps on going due to its momentum. As the valve moves towards its end position the low pressure check valve opens and low pressure fluid enters the volume in such way that the valve decelerates until it stops at the desired valve lift. During the dwell-period, both solenoids and check valves are closed, thus the valve is prevented from returning since hydraulic pressure acts on both sides of the valve piston. The valve closing event is initiated by the activation of the low pressure solenoid. The valve pushes the fluid back to the low pressure source while returning to its closed position. As the valve approaches its closed position, the high pressure check valve opens and the valve starts to slow down.

Lotus has been developing an electrohydraulic valve actuation system since the early 1990´s. The system is known as Lotus *active valve train* (AVT). It consists of a hydraulic piston attached to the engine valve which moves inside a hydraulic cylinder. The movement of the valve is controlled via fluid flow either above or below the actuator piston, and the fluid flow is in turn controlled by the high-speed servo valve [40]. Figure 23 shows a Lotus AVT system mounted on a cylinder head.
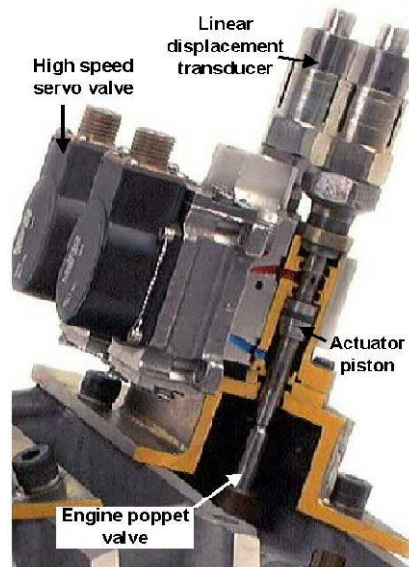
Figure 23 Lotus research AVT system [40].

Figure 24 illustrates the hydraulic circuit of the research AVT system. The valve profile is continuously monitored by a linear displacement transducer (LDT), which makes valve profile correction from cycle-to-cycle possible. The AVT system has fully flexible control of the entire valve event. The desired valve profile is entered in a control program and with the help of the LDT the valve is operated according to the desired valve lift profile. The system permits individual valve control and can operate different valve lift profiles on different valves. In addition to this, the system is capable of opening a valve more than once during an engine cycle [40, 41]. Valve profiles of varying shapes, such as polynomial, triangular or trapezoidal, are easily generated by an engine valve lift profile generator capable of storing up to 256 individual valve lift profiles [42].
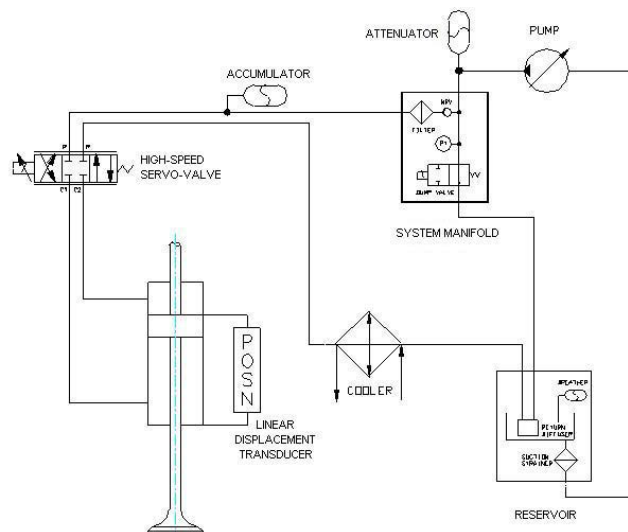
Figure 24 Schematic of the hydraulic circuit used in the research AVT system [40].

The aforementioned system is only intended for research purposes and it is not at all suitable for mass-produced engines. The reason is that the technology used is extremely expensive and the high-speed servo-valve does not allow controlled valve velocities with

sufficient accuracy above engine speeds of 4000 rpm [42]. Lotus and Eaton are collaborating to develop a production ready version of AVT and they expect to market the product in the 2008-9 timeframe [43].

4.2.3 Electro Pneumatic Valve Actuation

Although the previously described systems (EMVA and EHVA) show good results when used in research environments, they both suffer from various problems, making them a less attractive choice for production engines. The EMVA system suffers from fundamental problems like high levels of noise and packaging issues, while the EHVA system is very expensive and has issues regarding temperature variations. Electro pneumatic valve actuation (EPVA) seems to be a promising alternative to EMVA and EHVA, with characteristics such as full VVA flexibility, low energy consumption and low valve seating velocity (low noise levels) [4]. The EPVA system can be made more robust since air is not as sensitive as hydraulic fluids to temperature variations, at least not at the temperatures found in ICE applications. Also, air leaks are less severe than oil leaks and the need of high precision is therefore lower compared to hydraulic systems.

Cargine engineering AB has developed an EPVA system that offers fully variable valve control. The system has been evaluated in the work presented in this thesis and a dynamic model of the system has been developed and implemented in *Simulink/Matlab™* by Ma et al. [44]. An illustration of Cargine's pneumatic valve actuator can be seen in Figure 25.
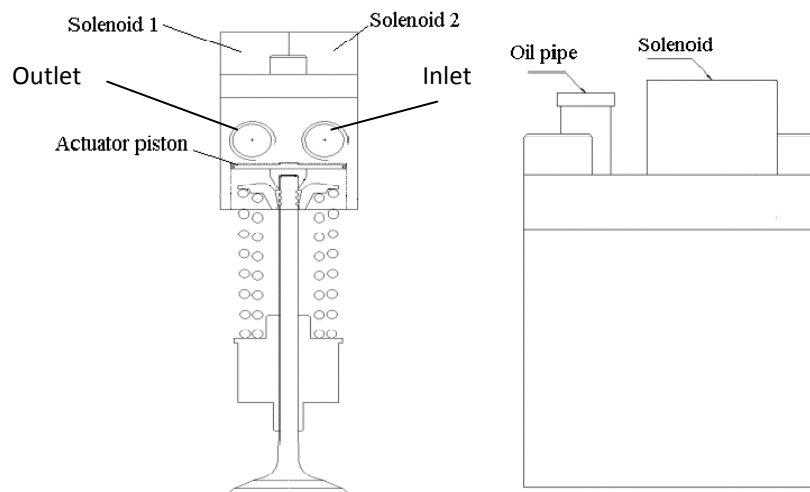
Figure 25 Illustration of Cargine's pneumatic valve actuator.

The pneumatic valve actuator consists of the actuator housing, two solenoids, two spool valves, two port valves, an actuator piston, a hydraulic latch/damper system and air flow channels inside the housing. Valve lift information is provided by optical sensors mounted inside the actuator.

Figure 26 shows an EPVA valve lift profile together with the corresponding solenoid voltage pulses. From Figure 26, it can be seen that the valve event consists of 3 sections,

namely the opening period, dwell period and closing period. The opening period starts with the activation of solenoid 1, S1, which in turn pushes the corresponding spool valve. The new position of the spool valve now permits pressurized air to enter the actuator cylinder. The pressurized air pushes the actuator piston and since the valve is in direct contact with the actuator piston, it starts to open. Solenoid 2, S2, is activated in order to stop the air charging of the cylinder and the time difference between activation of S1 and activation of S2, δ_1, therefore determines the valve lift. The pressurized air expands inside the actuator cylinder until it balances with the valve spring force. At the end of the opening period, the hydraulic latch is activated and the valve is prevented from returning. The hydraulic latch is active during the whole dwell period. When S1 is deactivated, the latch is disabled which in turn starts the air discharge from the actuator cylinder and the valve starts its closing period. The time difference between the deactivation of S2 and S1, δ_2, must always be positive to prevent a second air filling of the actuator cylinder since this would trigger a second valve lift event. At the end of the closing period (about 3 mm before the end of valve lift) the hydraulic damper is activated, and starts to slow down the valve. In the interval 1.0 to 0.0 mm, the seating velocity is constant with a magnitude of approximately 0.5 m/s. Thereby the damper ensures a soft-seating with a low level of noise as a result.
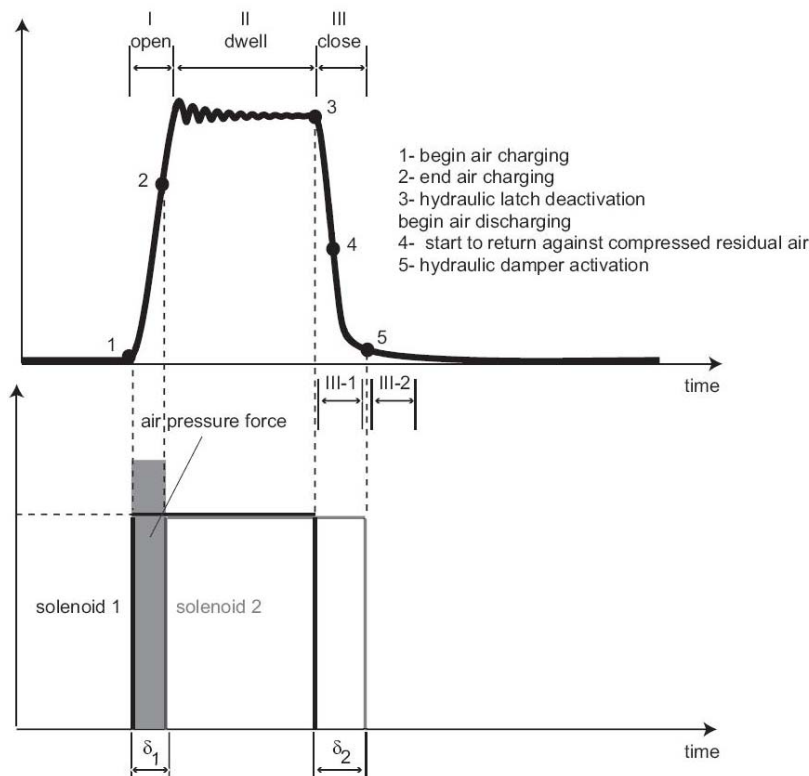
Figure 26 A typical valve lift profile achieved with Cargine's EPVA system. Below the valve lift curve, a solenoid action chart can be seen. Observe that the system delays are excluded from the solenoid chart [45].

Cargine is not alone in this field, however, it seems as their product is the one most likely to reach the market in a near future.

Johnson et al. [46] describes a free-piston engine using pneumatically operated valves. However, the valves in the engine described are not of the conventional type. Instead of poppet valves, the engine uses spool valves. As the piston approaches the end of its stroke, the pressure is built up in the cylinder and pressurized gas is conducted to the valves through fluid lines, making the spool valves move in the desired direction. The system does not admit any type of control over the valve event.

Richeson et al. [47] presents an electronically controlled pneumatically powered transducer for use as a valve actuator in an ICE. The transducer contains a piston which can easily be coupled to an engine valve. The piston is displaced by pressurized air controlled by permanent magnet control valves. At the start of the opening period, the permanent magnet is temporarily neutralized making the control valve open. This leads to a filling of the cylinder above the piston, thus pushing it to its opposite end position. When the piston reaches the end of its stroke, the control valve is closed by the permanent magnet and the pressurized air in the cylinder keeps the piston at its end position and the dwell period has been initiated. To start the closing period, the permanent magnet below the piston is neutralized which admits opening of the control valve and results in a subsequent charging of the cylinder from underneath the piston. The system is equipped with a soft-seating mechanism using air as cushion. The system can be described as a VVT system, since the valve timings can be controlled as desired, but the lack of valve lift control disquakifies it as an FVVA system. Gould et al. [48] tested the system described above, implemented in a test engine, with satisfying results considering that no optimization of the implementation has been done. Figure 27 shows the three EPVA valve lift profiles with constant valve lift duration at three different engine speeds.

In 2005, Watson et al. [49] showed results achieved from simulations of a pneumatic valve actuation system, however no prototype has been demonstrated so far.
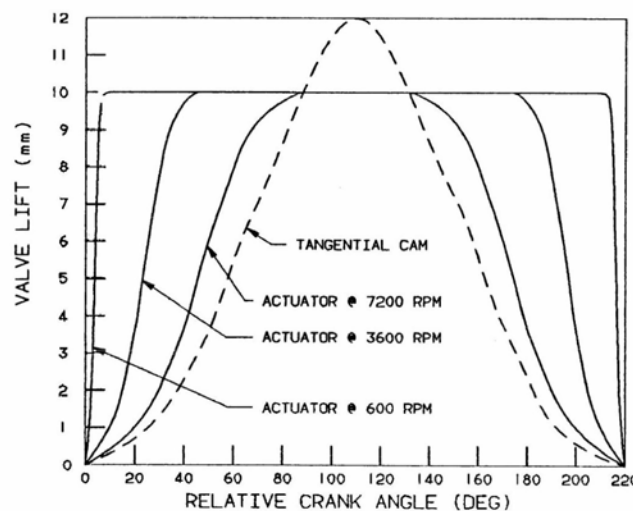
Figure 27 Valve lift profile comparison between cam driven and pneumatic actuator driven valves [48].

5 Valve Strategies enabled by Fully Variable Valve Actuation

With FVVA, unlimited possibilities to investigate effects of various valve timings arise. For instance, by closing the inlet valve late (a number of degrees ABDC) the effective compression ratio is changed, with a second opening of the exhaust valve ATDC "internal" EGR is achieved, deactivation of valves in order to alter the in-cylinder flow etc. Some of the most common valve strategies enabled by FVVA will be discussed in the forthcoming sections.

5.1 Negative Valve Overlap

For a very long time EGR has been used in order to reduce the NO_x exhaust emissions. The exhaust gases recirculated to the intake manifold dilutes the air/fuel charge which results in a reduced peak combustion temperature and thereby the temperature-dependent NO_x emissions will be lowered. However in an engine utilizing HCCI combustion, the residual gases are used for a completely different reason. Since HCCI is a combustion concept where the air/fuel-mixture self-ignites, it depends to a great extent on the charge temperature. One way to increase the charge temperature is to dilute it with hot burned residual gases. This can be achieved with a valve strategy known as *negative valve overlap* (NVO).
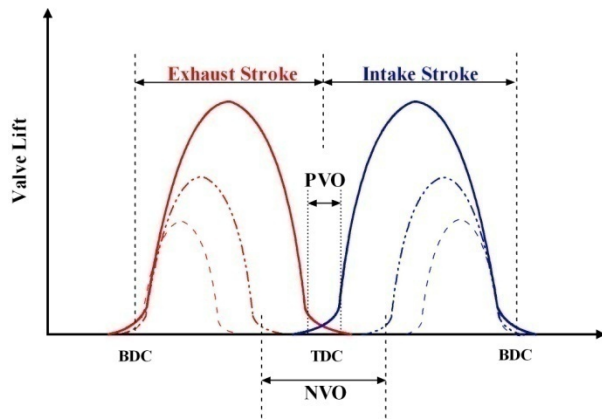
Figure 28 Illustration of valve profiles for standard engines (solid lines) and for engines utilizing different degrees of NVO (dashed lines).
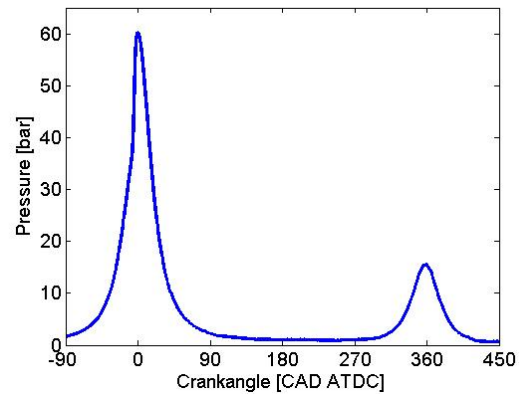
Figure 29 Pressure trace from a engine running with HCCI combustion and a NVO of 100 CAD.

With NVO, the exhaust valve closes somewhere before TDC and a large amount of hot residual gases are then trapped in the cylinder. The residuals are then compressed during the rest of the exhaust stroke and then expanded during the intake stroke until they reach ambient conditions when the inlet valve opens. It is important to open the inlet valve at the right moment, since an early IVO leads to a blowdown of residuals through the inlet port, with unnecessary pumping losses. On the other hand, late IVO means that the residuals will be expanded beyond ambient conditions and vacuum is created which costs work. Ideally, exhaust valve closing (EVC) and IVO should be

mirrored with respect to TDC, i.e. the period from TDC when the intake and exhaust valves are closed during gas exchange should be almost equal. Figure 28 shows the valve profile for an engine with conventional valve timing together with valve lift profiles for two different degrees of NVO. Figure 29 show the in-cylinder pressure from an engine run with NVO HCCI.

Numerous researchers have shown results involving NVO in their studies over the past 10 years. The NVO strategy was first published by Willand et al. [50] in 1998, however no results were presented. Among the first to show results of NVO HCCI was Kontarakis et al. [51] in 2000.

5.2 Rebreathe Strategy

Another way to retain residuals in the cylinder is by exhaust rebreathing. Instead of trapping the residuals in the cylinder and then compressing them, the exhaust gases are expelled through the exhaust or inlet port, after which they are brought back into the cylinder during a part of the intake stroke. A rebreathing strategy can be achieved in a number of ways and four of them will be explained with references to Figure 30.
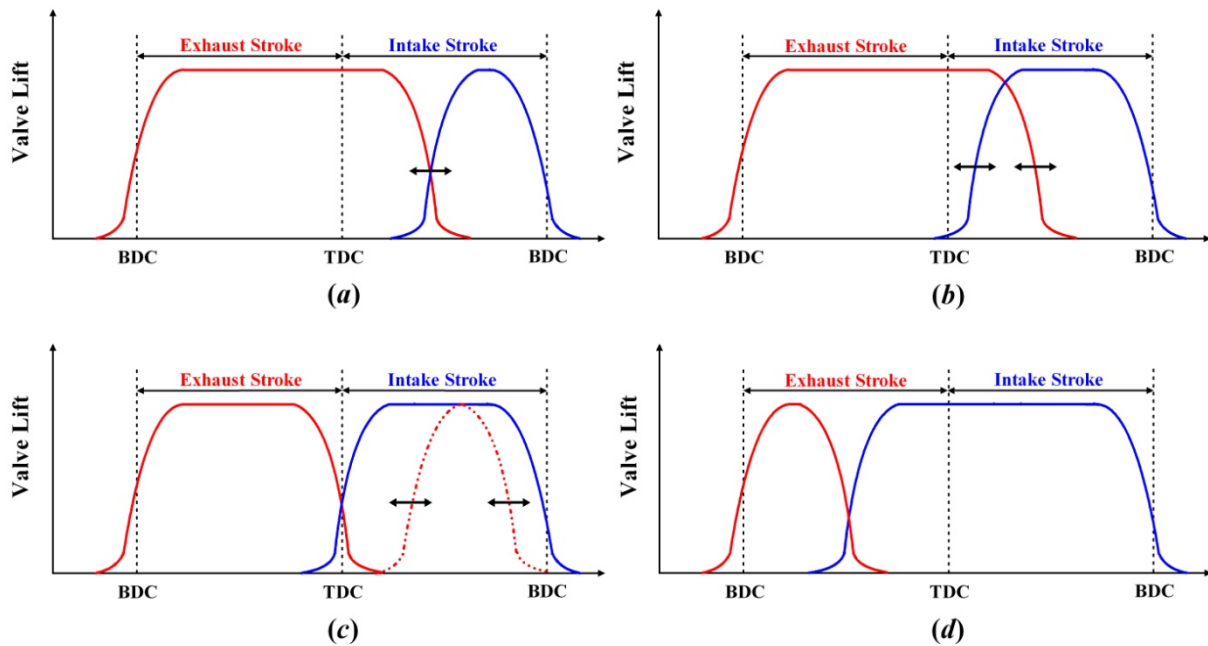
Figure 30 Illustration of exhaust rebreathing achieved by different valve timing strategies: (*a*) exhaust port recirculation; (*b*) inlet and exhaust port recirculation; (*c*) exhaust port recirculation with a second exhaust valve lift; (*d*) intake port recirculation.

Figure 30s shows the valve timings for exhaust port recirculation. In this type of strategy, the exhaust valve remains open during the whole exhaust stroke and closes during the intake stroke. In this way exhausts are first expelled through the exhaust port, after which they are brought back to the cylinder. The inlet valve opens first after the exhaust valve closes in order to prevent mixing between the reinducted exhausts and the fresh charge, and thereby secure a stratified charge mixture [52]. Results achieved by engines running with this kind of rebreathing strategy have been shown by, amongst others, Kaahaaina et al. [53].

In Figure 30b a second type of rebreathing strategy can be seen. This strategy is achieved by having a *positive valve overlap* (PVO) between EVC and IVO during the intake stroke. With this kind of valve timings, the exhausts will be reinducted together with the fresh charge during the intake stroke, with a less stratified mixture as a result [52, 53].

A third rebreathing strategy is illustrated in Figure 30c. Here, the rebreathing is achieved by a second exhaust valve lift event. This strategy is mainly used in engines where valve-to-piston contact around TDC is possible. The exhaust valve is open during the entire exhaust stroke and closes around TDC. During the intake stroke, both inlet and exhaust valves are opened simultaneously and the exhausts are reinducted together with fresh charge [54].

The last rebreathing strategy can be seen in Figure 30d. The exhaust valve closes early during the exhaust stroke, shortening the conventional exhaust process. Instead, the inlet valve opens immediately after that the exhaust valve has closed, and the exhaust gases are expelled through the inlet port. The inlet valve remains open until the end of the intake stroke. This strategy gives a minimized stratification of fresh charge and exhausts, due to the mixing of gases in the intake. Since the hot exhausts are pushed into a cold intake system, the charge temperature will be lower compared to the other strategies, with a reduced possibility to reach auto ignition temperature, as a result [52].

5.3 Atkinson/Miller Cycle

The Atkinson cycle was invented in the 1880s by a British engineer named James Atkinson. The main feature of the Atkinson cycle is that the expansion stroke is longer than the compression stroke, thus converting a greater portion of the energy from heat to useful mechanical energy with a greater efficiency as a result. In 1886 Atkinson presented the "cycle engine" which utilized the Atkinson cycle. The disadvantage with the cycle engine, however, was that the mechanisms for having different stroke lengths were complex, with an increased risk of failure and increased friction losses, as a result. Because of this, in combination with expiration of Nicolaus Otto's patent on the four-stroke cycle in 1890, the cycle engine did not survive for very long [55].

In 1954, Ralph Miller, patented the so called "Miller cycle" which is a modified version of the Atkinson design [56]. The main idea with the Miller cycle is that the difference between compression ratio and expansion ratio is achieved by closing the inlet valve past the end of the intake stroke, rather than being a geometrical difference between compression and exhaust stroke. In this way a part of the charge inhaled during the intake stroke is expelled through the inlet port until the inlet valve closes, whereupon the compression starts. However, the decreased amount of charge leads to a lower maximum power. This can be compensated by the use of a supercharger. The Miller strategy can also be achieved by closing the inlet valve before the end of the intake stroke. Thermodynamically there are no differences between late IVC and early IVC.

Luria et al. [57] presented in 1982 a concept called the Otto-Atkinson engine which operates as a hybrid cycle between the conventional Otto cycle and the Atkinson cycle. Even though "Atkinson" is referred to in the name of the concept, it utilizes the late IVC

as described by Miller. Toyota utilizes the Otto-Atkinson concept in their hybrid vehicle named Prius [58].

If the Miller strategy is combined with a FVVA system the effective compression ratio of the engine can easily be changed which makes the Miller cycle a promising aid in the control of HCCI combustion.

6 Vehicle Hybridization

Growing environmental concerns, together with higher fuel prices, has created a need for cleaner and more efficient alternatives to the propulsion systems of today. Currently vehicles are equipped with engines having a maximum thermal efficiency of 30-40 %. The average efficiency is much lower, especially during city driving since it involves frequent starts and stops. According to Figure 31, the idling losses are as high as 17.2%.
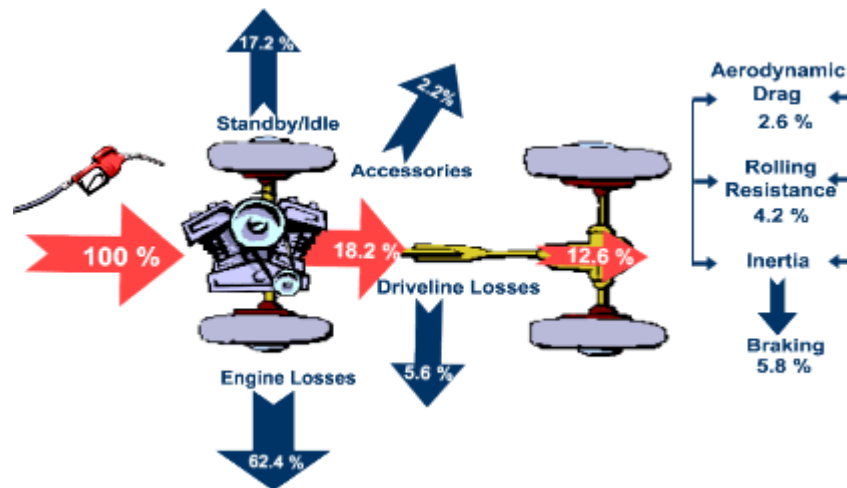
Figure 31 Illustration of the different losses in a conventional vehicle [59].

All this has turned the attention towards hybrid vehicles. They have proven to have significant potential to improve fuel economy and reduce exhaust emissions which, together with tax incentives in some countries and other similar benefits only offered to owners of hybrid vehicles, have contributed to an amazing increase in sales over the past couple of years, see Figure 32.
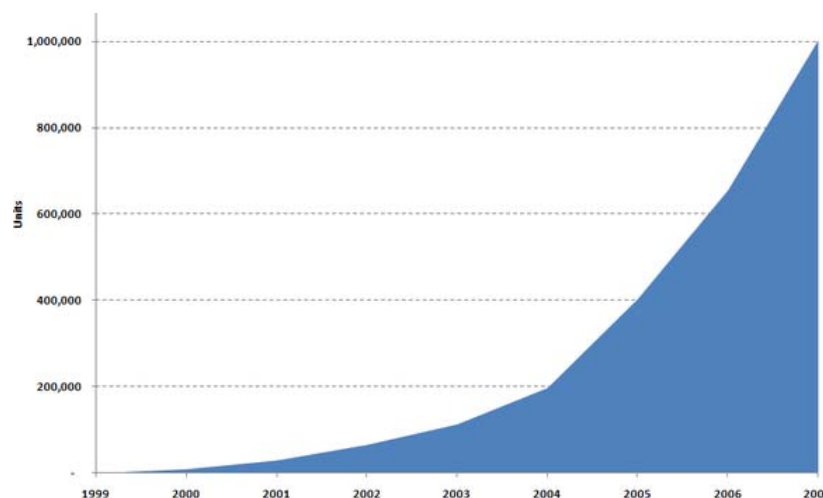
Figure 32 Cumulative reported US sales of hybrid vehicles during the period 1999-2007 [64].

6.1 Introduction

The classical definition of a hybrid vehicle is that it is a vehicle that has more than one source of propulsion power. The definition of a hybrid vehicle stated by UN in 2003 [60], also includes two different energy storage systems. Vehicle hybridization can be done in various ways. The perhaps most uncomplicated example of vehicle hybridization is the power-assisted bicycle, where power is delivered both via an electric motor or ICE and the driver himself. Hybridization of very large transportation vehicles, such as trains, is also possible. In 2007, the Sydney Morning Herald reported that Japan was about to launch the first hybrid train, named the Kiha E200. It was equipped with a diesel engine and two electric motors under each of its cars, and the recovered energy is stored in lithium ion batteries placed on the roof [61]. In the following sections, a more detailed description of the electric hybrid and the pneumatic hybrid will be given.

6.2 Electric Hybrid

The most common combination of propulsion sources for hybrid vehicles is that of an electric motor and an ICE, known as the *hybrid electric vehicle* (HEV). It combines the range advantage of a conventional vehicle with the environmental benefits of an electric vehicle. The HEV can either alter propulsion sources or combine them. The power supply to the electric motor comes from a large onboard battery. The battery can either be charged by the ICE or by capturing the kinetic energy from the vehicle during deceleration and convert it into electrical energy.

In conventional vehicles the ICE is run at different load points, depending on the current power demand. Switching between different load points will lead to a relatively low average efficiency, since far from all load points offer maximum efficiency. For instance, low load operation suffers from low efficiency due to very high throttling losses. The switching between different load points also has a negative effect on exhaust emissions. For instance, results shown by Samulski et al. [62] indicate a considerable increase in emissions during transient operation.

In a HEV the ICE cooperates with an electric motor, which leads to the possibility of a more optimal use of the ICE. Usually, HEVs use a downsized ICE with reduced size and power. For instance the Toyota Prius has a 1.5 l engine producing 57 kW (76 hp) of power [63]. The reason is that by downsizing an engine, its power density increases. The engine will be run at a higher average load during a driving cycle which means that the average intake pressure will be higher with lower throttling losses as a result. The reduced peak power of the ICE can be compensated by added power from the electric motor.

Another benefit with the HEV is the possibility of utilizing regenerative braking. Basically, this means that the electric machine can be used as a generator and the energy, otherwise lost during braking, can be stored into the battery for use at a subsequent acceleration of the vehicle.

City driving involves frequent stops and starts of the vehicle. During idling, the ICE consumes fuel without producing any useful work thus contributing to higher fuel consumption and unnecessary exhaust emissions. The HEV solves this by shutting off

the ICE during a full stop. In this way no fuel will be consumed during idling with no exhaust emissions during this period.

Even though HEVs has many benefits compared to a conventional vehicle, there are some drawbacks making HEVs less appealing in the eyes of the customers. The main disadvantages with electric hybrids are that they require an extra propulsion system and large heavy batteries with a limited life-cycle. This introduces extra manufacturing costs which are compensated by a higher end-product price comparable to the price of high end vehicles. The limited life-cycle of the batteries also contributes to a higher life-cycle cost of HEVs.

The power sources found in a HEV can be combined in numerous ways. However, the most common drive train configurations are the series and parallel HEV. A *series hybrid* is a configuration in which only one energy converter can provide propulsion power. The ICE, which is operated in the most optimal regime, drives an electric generator and thus mechanical energy is converted to electrical energy which then is stored in the battery. The propulsion power is provided solely by the electric motor, see Figure 33. The addition of an ICE to the configuration extends the driving range considerably compared to an electric vehicle.
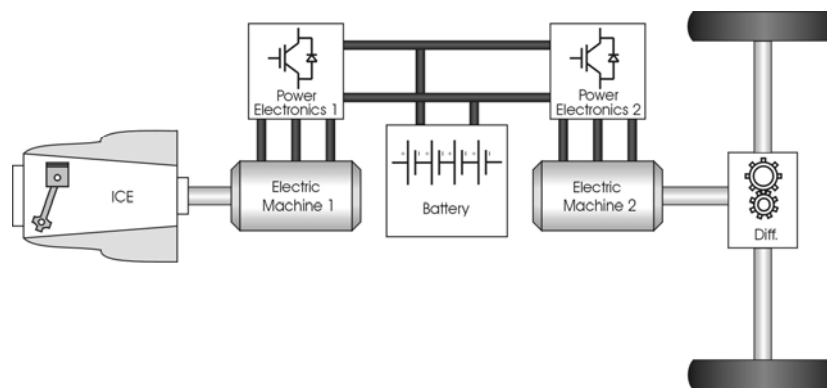
Figure 33 Illustraion of the series hybrid drivetrain [65].

In a *parallel hybrid,* the ICE and the electric motor are connected to the driveshaft through separate clutches. In this configuration the propulsion power can be supplied by the ICE, by the electrical motor, or by a combination of both, see Figure 34. The cooperation between the ICE and the electric machine can be chosen is such way that the current demand for power can be met. When using only the ICE, the electric machine can function as a generator and charge the battery. The electric machine can also be used during vehicle deceleration to charge the battery. The major advantage of the parallel hybrid compared to the series hybrid is that the possibility of using the ICE as propulsion source leads to fewer energy conversions with less energy conversion losses as a result. One of the drawbacks with this strategy, is that during city driving involving long periods of slow driving, the battery can be discharged, forcing the ICE engine to kick in and operate in a regime where it is less efficient.
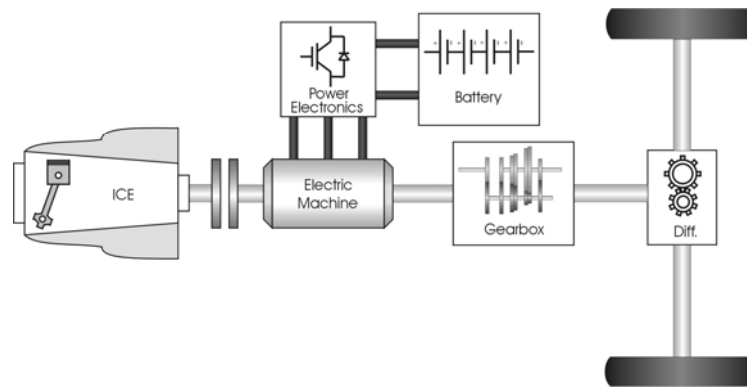
Figure 34 Illustration of the parallel hybrid drivetrain [65].

The series hybrid configuration can be combined with the parallel hybrid configuration, forming a configuration known as the *power split hybrid* configuration. In this configuration the ICE can either be utilized as a propulsion source or drive the generator and thus charge the battery. The Toyota Prius is an example of such a hybrid. The advantage with the power split hybrid is that it can adapt to the current conditions in a more efficient way compared to the other two systems. However, the disadvantage with such a system is the increased cost due to increased complexity.
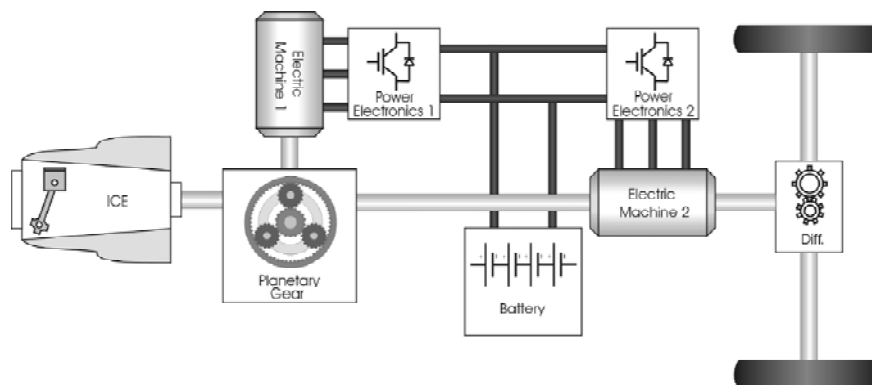
Figure 35 Illustration of the power-split hybrid drivetrain [65].

Although the modern electric hybrids only have been around for about ten years, the idea with electric hybridization of vehicles is not new. In 1896, a Belgian company named Pieper developed the first electric hybrid called "Auto-Mixte" and in 1901 the company had built two petrol-electric vehicles equipped with a 60 hp ICE and a 40 hp electric motor, giving the vehicle a total power of 100 hp. In 1902, H. Krieger developed a series hybrid vehicle and around the same time, hybrid vehicles were manufactured in Germany by Lohner-Porsche [66]. Even though a lot of effort was put into developing and bringing the hybrid vehicles to the market, they did not become as successful as expected. The early hybrids were mainly built in order to assist the weak ICEs of that time. However, due to rapid advances in ICE technology, with improvements in power density and efficiency, there were no longer any advantages with electric hybrids [67].

6.3 Pneumatic hybrid

As stated earlier, the main drawbacks with electric hybrids are that they require an additional propulsion system and large heavy batteries. All of this costs the manufacturers a lot of money, which is compensated by a higher end-product price. One way of keeping the extra cost as low as possible and thereby increase customer attractiveness, is the introduction of the *hybrid pneumatic vehicle* (HPV). In contrast to the HEV, the pneumatic hybrid is a relatively simple solution utilizing only an ICE as propulsion source. Instead of expensive batteries with a limited life-cycle, the pneumatic hybrid utilizes a relatively cheap pressure tank to store energy. In order to run the engine as a pneumatic hybrid, a pressure tank has to be connected to the cylinder head in some way. Tai et al. [2] describe an intake air switching system in which one inlet valve per cylinder is fed by either fresh intake air or compressed air from the pressure tank. Andersson et al. [3] describes a dual valve system where one of the intake ports has two valves, one of which is connected to the air tank. A third solution would be to add an extra port to the cylinder head, which would be connected to the air tank. Since these three solutions demand significant modifications to a standard engine a simpler solution, where one of the existing inlet valves is converted to a tank valve, has been chosen and used in this thesis. The drawback with this solution is that there will be a significant reduction in peak power, and reduced ability to generate and control swirl for good combustion. Another prerequisite for pneumatic hybridization is a fully variable valve actuation system to control the valves and thereby control the pressurized air flow to and from the tank.

Pneumatic hybrid operation introduces new operating modes in addition to conventional ICE operation. During deceleration of the vehicle, the engine is used as a compressor that converts the kinetic energy of the vehicle into potential energy in the form of compressed air which is stored in a pressure tank. This kind of operation is referred to as the *compressor mode* (CM). After a standstill, the engine is used as an air-motor that utilizes the pressurized air from the tank in order to accelerate the vehicle. This type of engine operation is known as the *air-motor mode* (AM). A third possible mode of operation is the air-power assist mode (APAM). During APAM the stored compressed air is used for supercharging the engine when there is a demand for higher torque, for instance during the turbo-lag[1] period. During periods when no energy is required from the engine, like idling and when the gas pedal is released, the ICE can be completely shut off. This means that during such periods there will be no fuel consumption and thus no exhaust emissions.

6.3.1 Modes of Operation

In *compressor mode*, the engine is used as a 2-stroke compressor in order to decelerate the vehicle. The kinetic energy of the moving vehicle is converted to potential energy in the form of compressed air. The operating cycle of CM can be explained with references to Figure 36 and Figure 37. The numbers in brackets refer to the numbers in the PV-diagram.

---

[1] Turbo-lag is the time it takes for the turbine to reach necessary speed from the moment the driver has pressed the gas pedal.

I. *Intake stroke.* During CM the inlet valve opens a number of CAD after TDC and brings fresh air to the cylinder (1). At the end of the intake stroke, as the piston reaches BDC, the inlet valve closes (2).

II. *Compression stroke.* The moving piston starts to compress the air trapped in the cylinder after BDC and the tank valve (the valve which controls the flow of air between the cylinder and the pressure tank) opens somewhere between BDC and TDC (3), depending on how much braking torque is needed. For instance a very early IVO means that there will be a blowdown of pressurized air into the cylinder, and the piston has to work against a much higher pressure, thus a higher braking torque is achieved. The pressure tank is charged with compressed air as long as the tank valve is open. The tank valve closes shortly after TDC (4). At this point the cylinder is filled with compressed air at the same pressure level as the air in the pressure tank. As the piston moves towards BDC, the compressed air expands and the intake valve opens (1) when ambient pressure is reached in the cylinder.
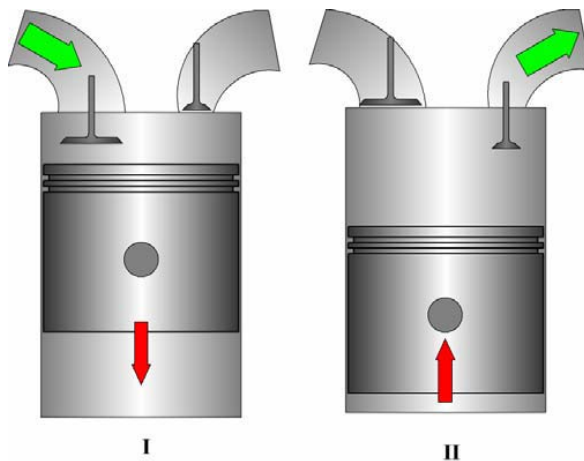
Figure 36 Illustration of CM. I) Intake of fresh air, II) Compression of air and pressure tank charging.
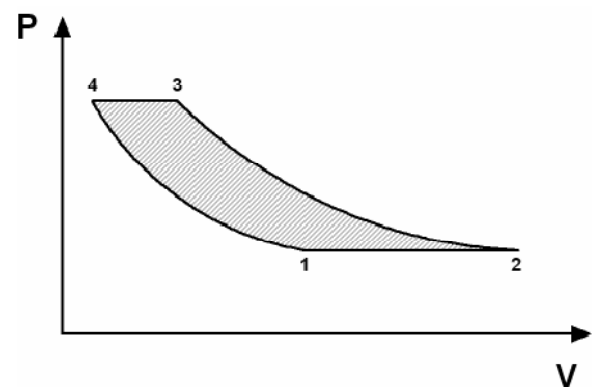
Figure 37 Illustration of the ideal PV-diagram of one CM cycle.

In *air-motor mode*, the engine is used as a 2-stroke air-motor that uses the compressed air from the pressure tank in order to accelerate the vehicle. The potential energy in the form of compressed air is converted to mechanical energy on the crankshaft which in the end is converted to kinetic energy. The operating cycle of CM can be explained with references to Figure 38 and Figure 39. The numbers in brackets refer to the numbers in the PV-diagram. Observe that the ideal PV-diagram for AM is the same as for CM, just reversed.

I. *Power stroke.* During AM the tank valve opens at TDC or shortly after (1) and the compressed air fills the cylinder to give the torque needed in order to accelerate the vehicle. Somewhere between TDC and BDC the tank valve closes (2), depending on how much torque the driver demands. Increasing the tank valve duration will increase the torque generated by the compressed air.

II. *Exhaust/compression stroke.* The inlet valve opens around BDC (3) in order to avoid compression of air as the piston travels towards TDC. Closing of the inlet

valve occurs somewhere between BDC and TDC (4), and is chosen in such a way that when the piston reaches TDC, the air trapped in the cylinder is compressed to the same level as the tank pressure level. If the inlet valve closes too late, the pressure in the cylinder at TDC will be below the tank pressure level, and as soon as the tank valve opens a blowdown of compressed air into the cylinder will occur. A rush of compressed air into the cylinder means that the pressure drop over the valve would increase which leads to a decrease in AM efficiency.
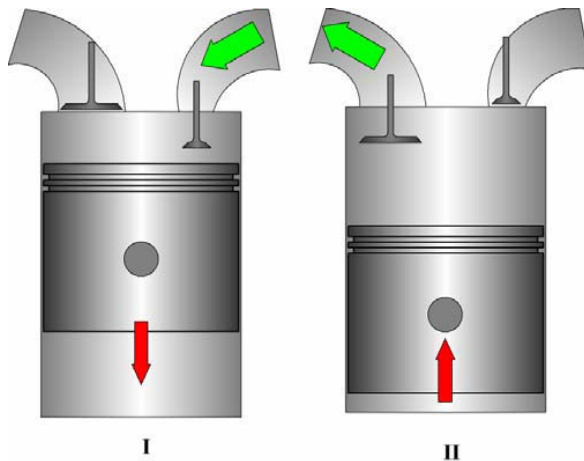
Figure 38 Illustration of AM. I) Intake of compressed air, II) Air venting.
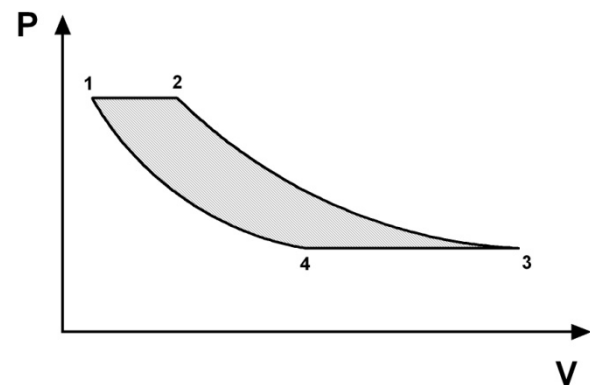
Figure 39 Illustration of the ideal PV-diagram of one AM cycle.

6.3.2 Short History

As with HEVs, the idea of hybrid pneumatic vehicles is far from new. In 1909, J.K. Broderick filed for a patent titled "*Combined internal combustion and compressed air engine*" [68]. He wrote in his application that his idea was to use compressed air together with an engine used for propelling a vehicle. The purpose of the compressed air is to assist the engine in starting when under heavy load, or when going uphill. The proposed configuration is also capable of generating compressed air which is stored in a tank. The compressed air can then be used for the purpose of illuminating the vehicle, for starting the ICE or to actuate the vehicle brakes. The compressed air is generated by two cylinders in a four-cylinder engine, and the remaining two cylinders operate in the usual manner. This can only be done while driving downhill or if the vehicle is at rest. He also mentions that the compressed air alone can be used for driving the vehicle.

In 1950, W.G Ochel et al. [69] came up with the idea of using a multicylinder engine to generate compressed air. The inventors stated that at that time, compressed air was normally generated by a compressor driven by an ICE, which lead to the requirement of increased space together with higher investment and maintenance cost. Their proposal was to use a multicylinder engine, where a number of cylinders operate in normal manner while the remaining cylinders compress air which then is stored in a pressure tank. This idea reminds a lot of the one patented by Broderick and the only difference seems to be that Broderick's invention was intended for use in a vehicle, while Ochel's invention was intended for stationary use where the compressed air would be used for actuating drill hammers, spray guns for painting, etc.

R. Brown describes, in a patent filed in 1972, an air engine powered by compressed air as an environmentally friendly alternative to the ICE which emits toxic exhaust gases [70]. In Brown's invention the compressed air is generated by a compressor driven by an electric motor.

In 1974, T. Ueno, filed for a patent which bore a great resemblance to Broderick's invention [71]. It involved compression of air by dedicated engine cylinders and utilization of compressed air in order to propel the vehicle. The main difference was that Ueno's invention was also capable of regenerative braking, which was not possible with Broderick's design.

With David Moyers invention, patented in 1996, the definition of the pneumatic hybrid as it is known today was complete. His idea was to add the supercharge mode, which meant that the intake pressure was raised beyond ambient pressure by the induction of compressed air stored in a pressure tank.

7 Experimental setup

During the project summarized in this thesis, three different test rigs have been used. The reason of switching between these test rigs was that the pneumatic hybrid project did not have a dedicated engine and the used test rigs had limited time slots available, which made moving between different test rigs inevitable.

7.1 The Scania D12 Diesel engine

All three test rigs used in the pneumatic hybrid project were equipped with engines originating from Scania D12 Diesel engines. However, each engine is modified in some way to fit the corresponding application. In following subsections, each engine will be described along with the necessary modifications.

7.1.1 Paper 1

The engine used in Paper 1 was an in-line six cylinder Scania D12 Diesel engine modified to operate as a single-cylinder engine. The standard version of this engine has 4 valves per cylinder and a camshaft with standard Diesel valve timings. A picture of the engine can be seen in Figure 40.

Figure 40 The Scania D12 Diesel engine used in Paper 1.
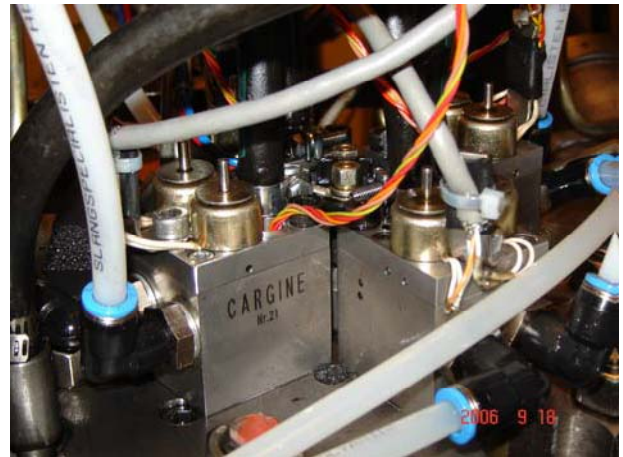
Figure 41 The pneumatic valve actuators mounted on the Scania cylinder head.

The standard Scania D12 engine uses a piston with a bowl in its crown. In the pneumatic hybrid project the standard piston has been exchanged for a flat piston in order to increase the piston clearance and thus avoid any valve-to-piston contact when using the pneumatic VVA system. The same flat piston has been used in all three papers presented in this thesis. Some engine specifications can be found in Table 2.

Table 2 Geometric properties of the Scania D12 diesel engine.

Displaced Volume	1966 cm3
Bore	127.5 mm
Stroke	154 mm
Connecting Rod Length	255 mm
Number of Valves	4
Compression Ratio	18:1
Piston type	Flat
Inlet valve diameter	45 mm
Exhaust valve diameter	41 mm
Valve Timing	Variable
Piston clearance	7.3 mm
Fuel injection	PFI
Fuel	Isooctane

The standard camshaft has been removed and the engine valves are actuated by the pneumatic VVA system described in Section 4.2.3. Figure 41 shows the pneumatic valve actuators mounted on the Scania cylinder head. The same setup has been used in all three papers presented in this thesis. In Table 3, some valve operating parameters are shown. The maximum valve lift height has been limited to 7 mm in order to avoid valve-to-piston contact. The standard valve springs have been exchanged for less stiff springs in order to reduce the energy required to operate the valves.

To be able to attach the actuators to the cylinder head a steel plate was designed and manufactured. The plate was designed in ProEngineer with the help of an engineering drawing of the Scania cylinder head. The plate and its dimensions can be found in Appendix A.

Table 3 Valve operating parameters.

Inlet valve supply pressure	3 bar
Exhaust valve supply pressure	3 bar
Hydraulic brake pressure	4 bar
Valve spring preloading	100 N
Maximum valve lift	7 mm

7.1.2 Paper 2

The engine used in Paper 2 was a single-cylinder engine originating from a six cylinder Scania D12 Diesel engine. A picture of the engine can be seen in Figure 42. Since the intent with this paper was to study pneumatic hybrid operation, a pressure tank has been added. The tank is an AGA 50 liter pressure tank suitable for pressures up to 200 bars. It is connected to the cylinder head by metal tubing suitable for pressures up to 60 bars and temperatures up to 500 °C. The size of the tank is selected based on availability rather than optimality. The engine has two separated inlet ports and therefore it was suitable to connect one of them to the tank since there will be no interference between

the intake air and the compressed air. One of the inlet valves was therefore converted to a tank valve.

The exhaust valves were deactivated throughout the whole study because no fuel was injected and thus there was no need for exhaust gas venting.
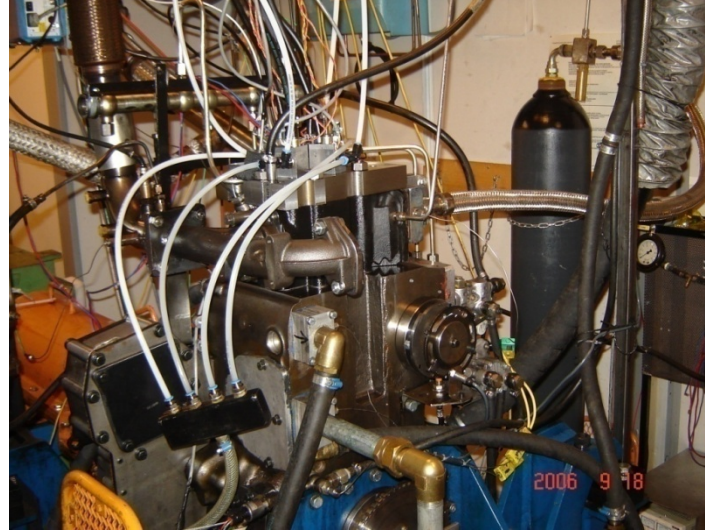
Figure 42 The single-cylinder Scania engine used in Paper 2.

The geometric properties of the engine have not been changed with the exception of one inlet valve which has been modified to work as tank valve, i.e. the valve that controls the air flow to and from the pressure tank, see Table 4. In order to open the tank valve at high in-cylinder pressures some modifications of the tank valve had to be introduced. The valve head diameter was decreased from 45 mm to 16 mm. Also the tank valve spring preloading had to be modified and was changed from 100 to 340 N in order to keep the tank valve completely closed for tank pressures up to 25 bars. Due to the increased valve spring preloading, the supply pressure to the tank valve has been increased in order to ensure proper valve operation.

Table 4 Valve geometric properties and operating parameters.

Inlet valve diameter	45 mm
Tank valve diameter	16 mm
Inlet valve supply pressure	4 bar
Tank valve supply pressure	6 bar
Hydraulic brake pressure	4 bar
Inlet valve spring preloading	100 N
Tank valve spring preloading	340 N
Maximum valve lift	7 mm

7.1.3   Paper 3

The engine used in Paper 3 was of same type as the engine used in Paper 1, i.e. an in-line six cylinder Scania D12 Diesel engine. In this setup one of the cylinders was modified for pneumatic hybrid operation, while the remaining cylinders were intact, see Figure 43.
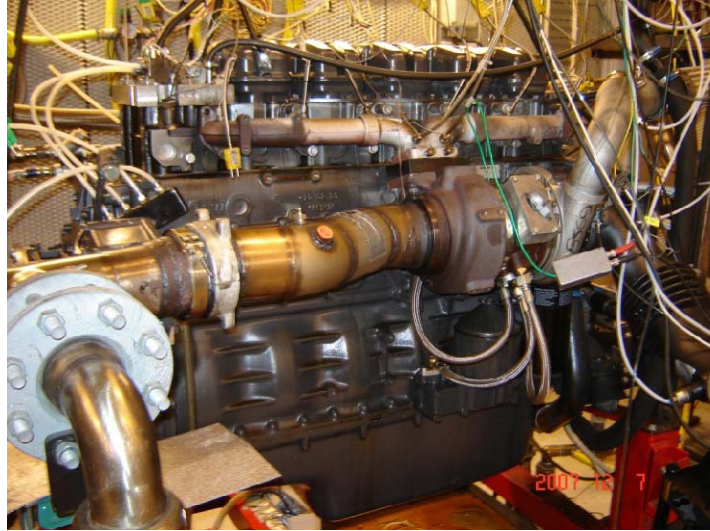
Figure 43 The modified Scania D12 Diesel engine. The operating cylinder is to the left in the picture.

Experiments performed in Paper 2 showed that the tank valve head diameter of 16 mm lead to considerable pressure losses over the valve. In order to avoid this, a pneumatic valve spring was designed and will be more thoroughly described in Section 7.2. The tank valve head diameter was therefore changed to 28 mm. Both tank valve geometries can be seen in Figure 44 and Table 5 shows some valve geometric properties and operating parameters. The original metal tubing which connects the pressure tank to the cylinder head, has an inner diameter of 25 mm which is smaller than the diameter of the new tank valve. Therefore, in order to eliminate the metal tubing as a potential bottleneck on account of air flow choking, the diameter of the tubing was doubled.

Table 5 Valve geometric properties and operating parameters.

Inlet valve diameter	45 mm
Tank valve diameter	16 and 28 mm
Inlet valve supply pressure	4 bar
Tank valve supply pressure	6 bar
Hydraulic brake pressure	4 bar
Inlet valve spring preloading	100 N
Maximum valve lift	7 mm

Figure 44 Picture illustrating the difference between the "small tank valve" (∅ = 16 mm) and the "large tank valve" (∅ = 28 mm).

7.2 Pressure compensated tank valve

In Paper 2, the tank valve head diameter was decreased from the original size of 41 mm to 16 mm in order to ensure proper valve operation at all time. Also the spring preloading was changed from 100 N to 340 N in order to keep the tank valve completely closed at tank pressures up to 25 bars. Both modifications lead to some complications. The reduced valve diameter increases the pressure losses over the tank valve and thus the regenerative efficiency will be reduced. The increased spring pre-loading will affect the pneumatic valve actuator energy consumption, however this is only of importance in a real vehicle where the actuators have to be feed with pressurized air from a compressor.

In an attempt to avoid the pressure losses over the tank valve, an in-house designed pneumatic valve spring has been developed and replaced the conventional tank valve spring. Figure 45 shows a simple cross section illustration of the pneumatic valve spring arrangement mounted on the cylinder head and the concept will be explained with references to Figure 45. The numbers in brackets refer to the ones displayed in Figure 45.

The pneumatic spring is constructed in such way, that it uses the tank pressure to keep the valve closed. A cylinder (1) is placed on the top of the cylinder head (4), with the tank valve (3) in the center of the cylinder. The cylinder is sealed at the bottom against the cylinder head and on the top the cylinder is sealed against the valve spring retainer (2). The space between the bottom sealing and the tank valve spring retainer is the pneumatic valve spring and it is connected to the tank valve port (6) and thus to the compressed air through 4 passages machined on the tank valve (5). The pressurized air enters the air passages on the valve and is guided up to the pneumatic valve spring, as indicated by the blue arrows. The passages are made in such a way, that the pneumatic spring will be connected to the tank valve port at all times and all possible valve lifts. Since the compressed air in the pneumatic spring works on the underside of the tank valve spring retainer and the compressed air in the tank valve port acts on the upside of the tank valve head, as indicated by the yellow arrows, the net force should be zero, and

thus the valve should be pressure compensated. This means that the tank will be kept closed without using any valve spring and the valve diameter can now be increased in order to reduce the pressure drop over the valve.
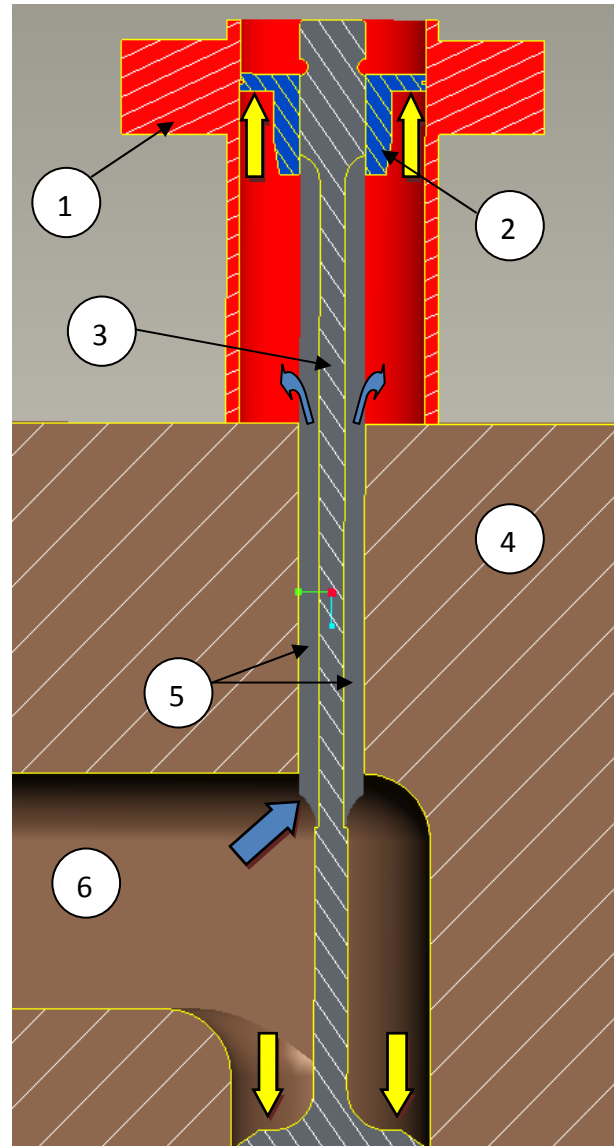
Figure 45 A simple cross section illustration of the pneumatic valve spring arrangement mounted on the cylinder head.

When the valve is open the force generated by the pressurized air acting on the upside of the tank valve head is canceled. This means that there now only exists a considerable force on the bottom surface of the valve spring retainer trying to close the tank valve. In order to overcome this problem, the tank valve actuator is fed with compressed air directly from the tank. This means that the pressure at a certain time is the same in the pneumatic valve spring as in the valve actuator. Since the actuator piston has a larger diameter than the tank valve spring retainer, the actuator will always have enough power to open the valve and maintain it open for as long as desired. Some geometrical properties of the pneumatic valve spring setup can be found in Table 6.

Table 6 Geometric properties of the pneumatic valve spring setup.

Pneumatic spring cylinder inner diameter	28 mm
Tank valve spring retainer diameter	28 mm
Tank valve poppet diameter	28 mm
Actuator piston diameter	32 mm
Compressed air guiding passage cross-section area	6 mm²

Since the pneumatic valve spring arrangement requires the actuator to be fed by compressed air from the tank, an extra pressurized air supply line had to be added. A problem with the actuator being fed with tank pressure is that there is a pressure threshold below which the pneumatic valve actuator will not work as expected. This means that the actuator has to be fed with compressed air from an external source. This adds thereby the need of having a pressure source switch. The switching system used in this study is built up by two check-valves which are arranged in such way that the source feeding the valve actuator will always be the source with the highest pressure. For instance if the external source of compressed air is set to 6 bars it will be the main feeding source until the pressure in the pressure tank exceeds 6 bars. A picture of the pressure source switching system is shown in Figure 46

Figure 46 Pressurized air switching system built up by two check-valves.

7.2.1 Modifications to the pneumatic spring

After some initial testing, some issues have been observed with the pneumatic valve spring. The issue of greatest importance is that the tank valve self-opens at certain running conditions during testing. The reason behind this behavior of the valve is high pressure oscillations in the tank valve port which have not been taken into consideration. When a high pressure pulse arrives to the tank valve, the force acting on the tank valve head will be increased. The tank valve will no longer be pressure compensated and the net force acting on the valve will not be zero, and as a result of this the valve will self-open. In order to eliminate this problem a valve spring with 220 N preloading has been added to the tank valve, which means that there will always be a net force acting to keep the tank valve closed.

7.3 The engine control system

The engine control system consists of a purpose built program, a standard PC, FPGA (Field Programmable Gate Array), A/D-converters and sensors. The engine control program has been built in *LabVIEW*, which is an entirely graphical programming language. The Graphical User Interface (GUI) is the link between the control program and the user, see Figure 47. From here the user can for instance set desired valve lift, valve opening and closing, etc. The GUI also contains some important graphs such as cylinder pressure, tank pressure, valve lift, PV-diagram. The graphs are useful since they show the current status of the system in a very descriptive way. The switch between different modes of engine operation such as CM and AM can easily be done by simply pushing the button for each engine mode respectively. The control program has been used for both steady state measurement, where most of the control parameters are set manually, and for continuously open-loop controlled operation, where all the control parameters are read from predefined look-up tables.
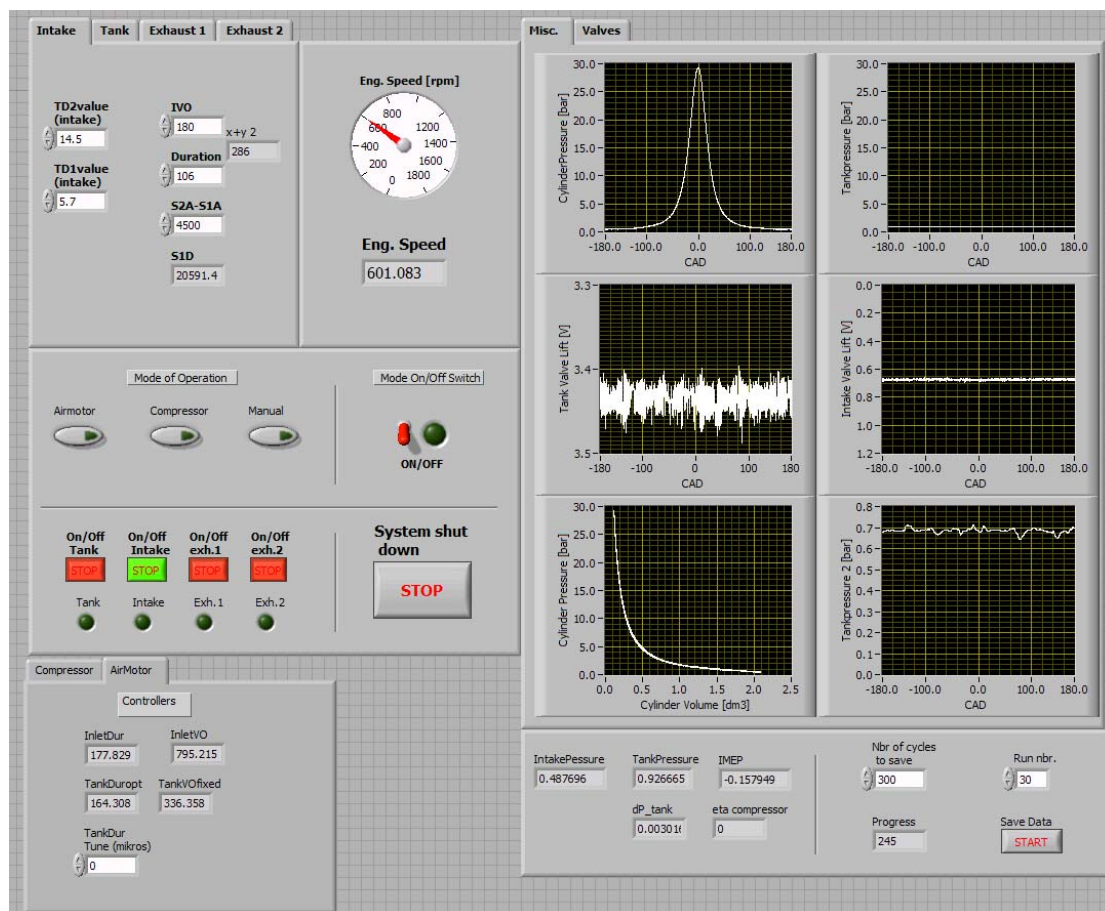
Figure 47 The GUI of the program controlling the VVA system during pneumatic hybrid operation.

The communication between the control program and the VVA system goes through an FPGA device of type *NI PCI-7831R*. The FPGA offers benefits such as precise timing, rapid decision making with loop rates up to 40 MHz and simultaneous execution of parallel tasks. All these benefits make the FPGA device a good tool for control of something so

time crucial as valve actuation. The NI PCI-7831R has 8 analog inputs, 8 analog outputs and 96 digital I/O.

For data acquisition a *NI PCI-6259* multifunction data acquisition (DAQ) device was used. It has 32 analog inputs, 4 analog outputs and 48 digital I/O. With this system it is possible to simultaneously collect data in 32 channels at 1.25 MS/s.

There are several sensors measuring the engine running status. The pressure is measured by pressure transducers of type *Kistler*® *7061B*. It is a piezoelectric pressure sensor which consists of a quartz crystal that is exposed to the gases through a diaphragm. When exposed to pressure, the crystal deforms and produces an electrical charge proportional to the pressure change in the cylinder. The electrical charge is converted in a charge amplifier to an analog voltage signal. The charge amplifier used in this thesis was of type *Kistler*® 5011. The pressure transducer is water-cooled in order to resist the tough environment inside the combustion chamber.

To be able to measure the temperature of the compressed air right after the tank valve and in the pressure tank, temperature sensors from Pentronic of type K have been utilized. They are mounted on the reconfigured intake port and on the pressure tank wall.

The pressure transmitter used for measuring changes in the tank pressure is a piezoresistive transmitter of type 21 R from Keller. It is suitable for pressures from 1 to 100 bar and temperatures up to 100 °C. It is located near the tank and measures the pressure in the connecting tube.

8   Results

In this section a summary of the results from the published papers enclosed in this thesis is presented. The results in this section can basically be divided into two main parts. The first part presents results from Paper 1 which deals with evaluation of the pneumatic VVA system used throughout the whole project. The second part shows results from Paper 2 and Paper 3. Paper 2 deals with an introductory study of the pneumatic hybrid concept while in Paper 3 different valve geometries have been tested together with optimization of the different pneumatic hybrid modes of engine operation.

8.1   Evaluation of the electro pneumatic VVA system

Valve lift, timing and duration have fixed values for conventional valve trains. These fixed values are usually optimized for the engine speed range most frequently used. They depend on what purpose the engine is designed for and represent a compromise between stable idle running and high engine speed performance. The ideal solution is to fully control when and how the valves should open and close. Such degrees of freedom make it possible to optimize the gas exchange for all operating conditions. The ability to fully control the valve event in an engine is of great importance to researchers and is a powerful tool for investigating different ICE related phenomena.

The aim of the study in Paper 1 was to evaluate the novel electro pneumatic VVA system from Cargine Engineering AB in order to establish whether the VVA system was stable and robust enough for further use in the laboratories belonging to the Division of Combustion Engines at the Lund University. The evaluation consists of two parts, where the first part was partly intended for testing the developed control program and partly to test the operational properties of the pneumatic VVA system. Observe that all data from the first part has been conducted during motored engine operation without combustion. In the second part, three different valve strategies for HCCI combustion control have been tested.

8.1.1   Testing program functionality and pneumatic VVA system performance

Precise valve timing is the most important factor when dealing with VVA systems. The engine performance depends to a great extent on precise valve timings and even an offset of a couple of CAD can change the characteristics of the combustion process. Precise valve timing is also crucial when operating the valves near TDC. In conventional engines, the valve closing period is designed in such a way that during closing the valve follows the piston motion towards TDC with a small distance between them, see Figure 48. A slight delay on the valve closing can lead to valve-to-piston contact with engine failure as a result. This is especially important with VVA systems operating with an almost quadratic valve lift profile, see Figure 49.
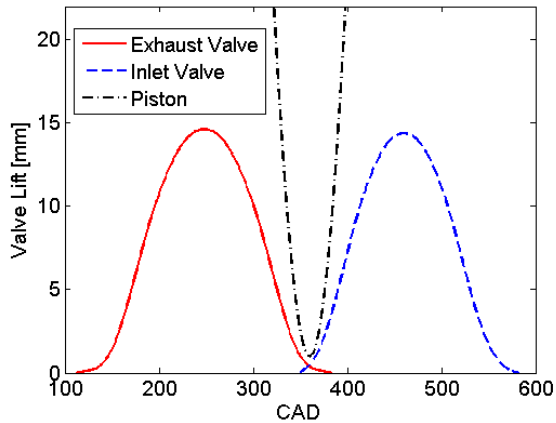
Figure 48 Exhaust and inlet valve lift profiles together with the piston position relative to TDC.
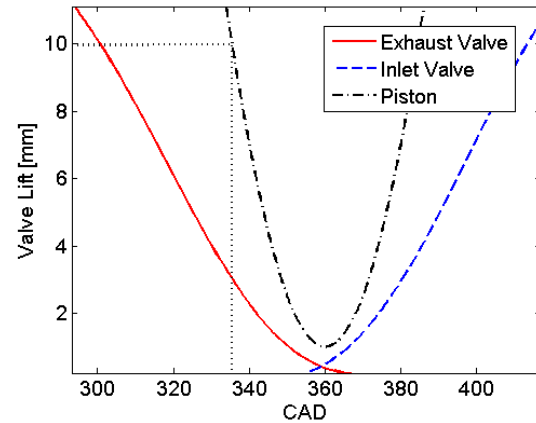
Figure 49 Close up of Figure 48. The dotted line illustrates the maximum allowed duration for a quadratic valve lift profile with a lift of 10 mm.

The figures above show that precise valve timing is crucial in order to avoid any complication. Therefore it is highly relevant to test the ability of the pneumatic VVA systems to perform desired valve timings. In the results that follow in this section, only the valve lift profile of one inlet valve will be shown, since the remaining valves show a similar pattern.
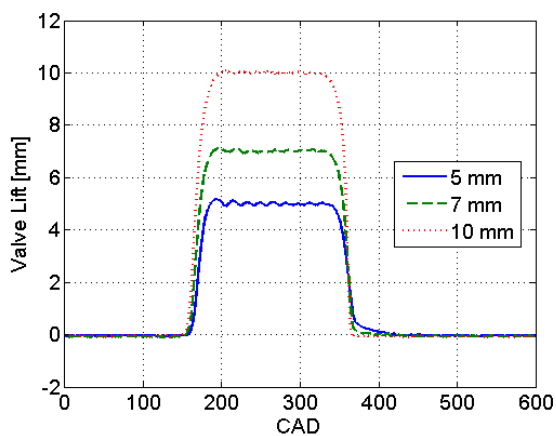
Figure 50 Variation of valve lift at constant valve lift duration of 200 CAD and an engine speed of 1000 rpm.
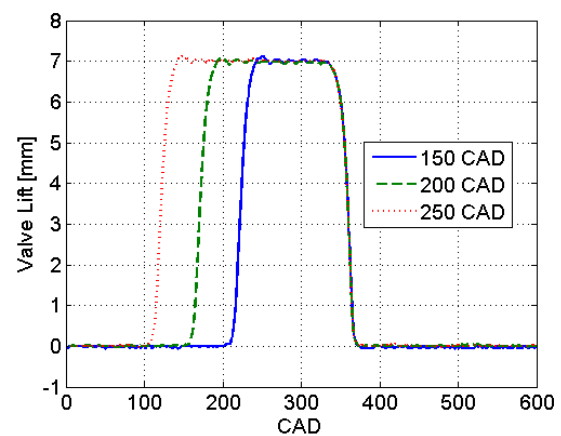
Figure 51 Variation of valve lift duration at a valve lift of 7 mm and an engine speed of 1000 rpm.

Figure 50 shows that the valve lift duration remains constant when the valve lift height is varied. In Figure 51, the valve lift duration has been varied while the valve lift height has been kept constant. It can clearly be seen that the change in duration does not affect the valve lift height or the other way around. This means that the valve lift height and duration are completely independent of each other which is a very important characteristic since it ensures proper valve timing and simplifies the control of the valve. If the valve-lift height would have been dependent on valve lift duration and vice versa, the control program would have to compensate for one parameter when the other is changed.
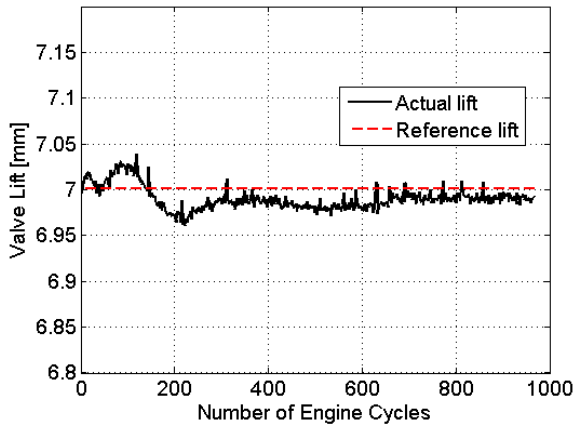
Figure 52 Cycle-to-cycle variations valve lift height at a valve lift duration of 200 CAD and an engine speed of 1000 rpm.
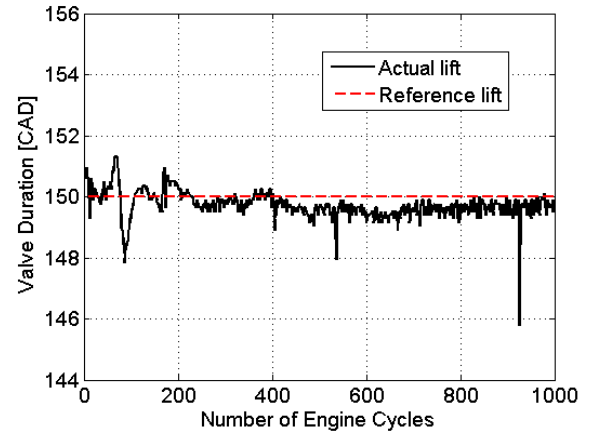
Figure 53 Cycle-to-cycle variations of valve lift duration at a valve lift height of 7 mm and an engine speed of 1000 rpm.

Repeatability is also an important factor in regards to valve operation. It is very important that the valve operates as desired in order to minimize cycle-to-cycle variations of combustion. The repeatability with regards to both valve lift height and valve lift duration of the pneumatic VVA system has been tested during open-loop controlled steady state operation. The results can be seen in Figure 52 and Figure 53. The responses show good repeatability at the chosen valve lift height and valve lift duration, respectively.

In order to be able to compare the results with each other the coefficient of variation (COV) can be used. COV is defined as:

$$COV = \frac{\sigma}{\mu} * 100 \tag{1}$$

where σ is the standard deviation and μ is the mean. The results, which can be seen in Table 7, show that there is a considerable difference between the repeatability of valve lift height and duration. However, both results have to be considered as good since their COV is quite small.

Table 7 COV for valve lift height and duration during steady state operation.

	COV (%)
Valve Lift Height	0.1805
Valve Lift Duration	0.3107

It is of great importance to explore the extreme operating limits of the pneumatic VVA system. Therefore, an investigation has been conducted in order to find the minimum valve lift height and the maximum engine speed in regards to valve stability. In the first part of the investigation, the engine speed range was tested. Since the maximum engine speed of the heavy duty Scania engine is about 2500 rpm, the upper engine speed limit during the test was set to 2500 rpm. Figure 54 shows that the valve lift remains stable at

the maximum allowed engine speed. The lower limit of the system is well below normal idle engine speed.
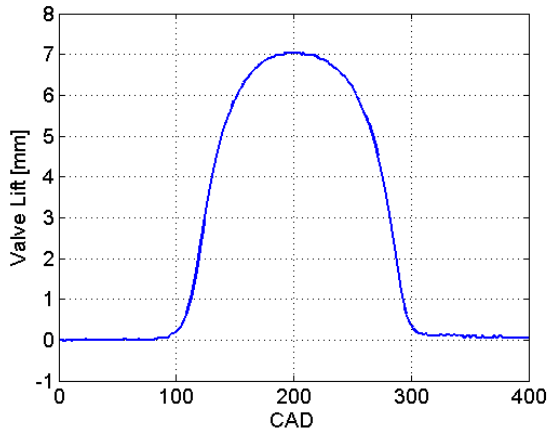
Figure 54 Valve lift of 7 mm at an valve duration of 200 CAD and an engine speed of 2500 rpm.
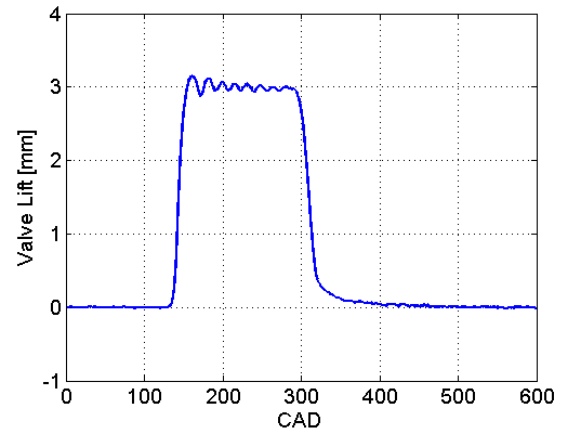
Figure 55 Valve lift of 3 mm at an engine speed of 1000 rpm and a valve lift duration of 200 CAD.

The second part of the investigation was to determine the lowest possible stable valve lift height. The results show that the valve lift remains stable all the way down to 3 mm throughout the whole duration and engine speed range during the test, see Figure 55. Below this height the valve behavior is quite unstable.

In a real vehicle, the energy consumption of the pneumatic VVA system is of great importance. However, in engine research laboratories, the energy consumption is less important since the researchers usually study different combustion related phenomena rather than economic aspects of the VVA system. Even though the tests perforned in this thesis are intended for evaluation of the pneumatic VVA for combustion research purposes, it can still be interesting to get an idea of the magnitude of the energy consumption associated with the pneumatic VVA system.

The energy consumption tests focused mainly on the pressurized air consumption and the energy consumption due to actuation of the solenoids is not included. It is assumed that the compressor uses 1 hp (736 W) to supply an air flow of 100 l_n/minute. This corresponds to a compressor efficiency of about 40%. The power consumption of the compressor is subsequently used to compute a mean effective pressure, ValveMEP, which simplifies comparison with other valvetrains. ValveMEP is defined as:

$$ValveMEP = \frac{2 \cdot P_{compressor}}{N \cdot V_d}$$

where N is the engine speed, V_d is the engine displacement volume and $P_{compressor}$ is calculated with the following equation:

$$P_{compressor} = \frac{Airflow}{100} \cdot 736 \, W$$
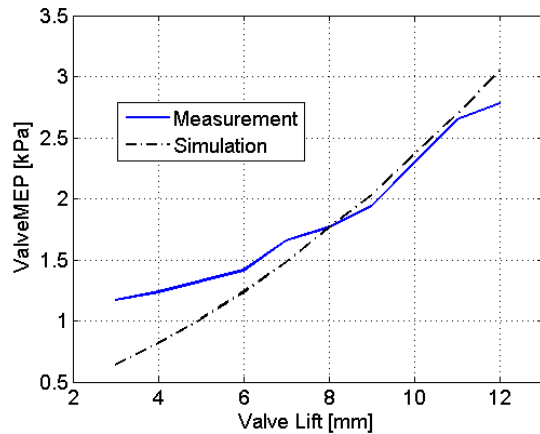
Figure 56 Valve mean effective pressure (single valve) as a function of valve lift at valve duration of 200 CAD and an engine speed of 1000 rpm.
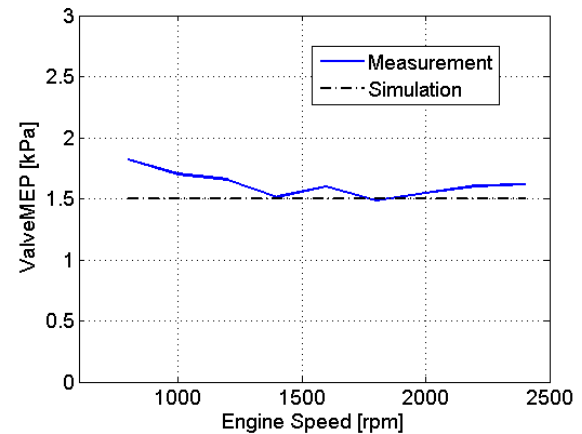
Figure 57 Valve mean effective pressure (single valve) as a function of engine speed at valve duration of 200 CAD and a valve lift of 7 mm.

Figure 56 shows how ValveMEP increases with increasing valve lift height at a constant opening duration and engine speed. This is quite logical, since an increase in valve lift height leads to a longer stroke executed by the actuator piston and thus a larger portion of air has to be inducted into the actuator cylinder. Figure 57 shows how ValveMEP varies with engine speed while valve lift is kept constant. It can be seen that ValveMEP remains almost constant with increasing engine speed which means that the amount of energy consumed during one engine cycle by the actuator does not depend on engine speed. However, this can be somewhat misleading since the pressurized air flow and thereby the energy consumption per time unit will increase with increasing engine speed, due to the higher frequency of valve actuation. Both figures also include simulated results of ValveMEP. The simulations have been done at the same conditions as the measured values in a program developed by Cargine Engineering AB.

8.1.2 Investigation of different valve strategies enabled by pneumatic VVA

The previous section has shown that the pneumatic VVA system offers great flexibility and stable function during motored engine operation. However, the system must also perform well during combustion operation. Therefore three different valve strategies for HCCI combustion control have been tested. The operation parameters for the tests can be seen in Table 8. Each valve strategy began with valve timings according to Table 9.

Table 8 Operating parameters.

Actuator intake pressure	3 bar
Hydraulic brake pressure	4 bar
Maximum valve lift	7 mm
Compression ratio	18:1
Engine speed	1200 rpm
Fuel	Isooctane
Fuel energy per cycle	0.75 kJ

Table 9 Initial valve timing.

IVO	0 CAD ATDC
IVC	180 CAD ATDC
EVO	0 CAD ABDC
EVC	180 CAD ABDC

The first strategy tested is *negative valve overlap* (NVO). With NVO, the amount of trapped residual gases can be varied. The basic idea is that the exhaust valve should close early while the intake valve should open late. A late EVC means that a higher portion of the exhaust gases will be trapped in the cylinder. With more residual gas the charge temperature increases and therefore the combustion will start progressively earlier. Figure 58 shows how EVC and IVO vary with NVO. It can also be seen that with increasing NVO the pressure during the gas exchange increases. Observe that the right valve lift profile belongs to the exhaust valve while the left valve profile belongs to the inlet valve.
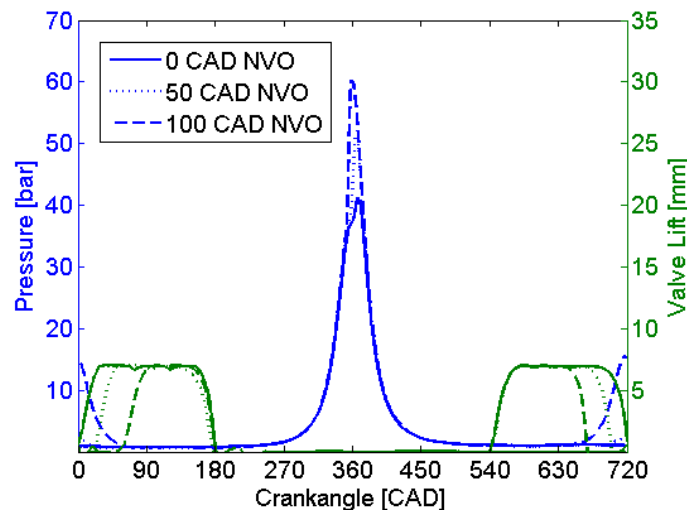
Figure 58 An illustration of the in-cylinder pressure and the valve lift profiles achieved with NVO strategy.

Figure 59 shows how CA50 varies with NVO. CA50 is the crank angle where 50% of the energy from the combustion has been released. An increase in NVO leads to an increase in charge temperature and since this leads to a higher peak temperature after compression the combustion will take place earlier and thus CA50 will advance. This can clearly be seen in Figure 59.
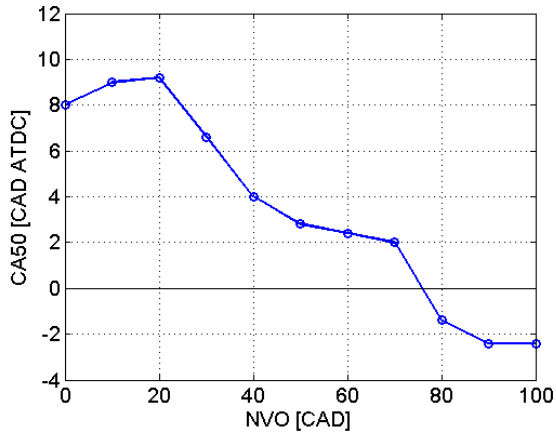
Figure 59 CA50 as a function of NVO
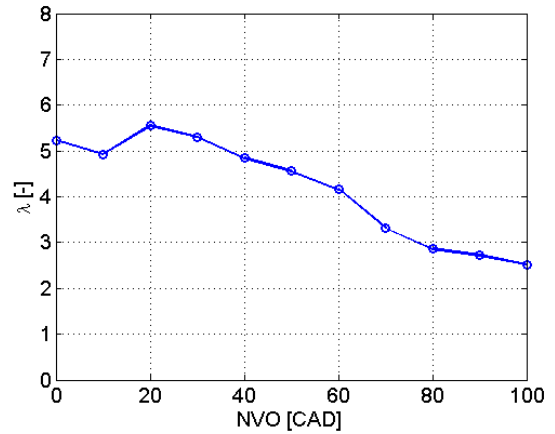
Figure 60 Lambda as a function of NVO

NVO displaces some of the air in the combustion chamber and thus the air/fuel ratio should decrease. Figure 60 shows exactly this behavior. An increase in NVO leads to a higher level of residual gas trapped in the cylinder. This means that when the inlet valve opens, a part of the cylinder volume will already be occupied by residual gas and therefore the amount of air inducted during the intake stroke will be lower and the air/fuel ratio will decrease.

The second strategy tested is *rebreathing*. The idea with the rebreathing strategy is to open the exhaust valve a second time a short while after it has closed the first time. It is a strategy very similar to the NVO strategy. The amount of rebreathed exhaust gas increases with
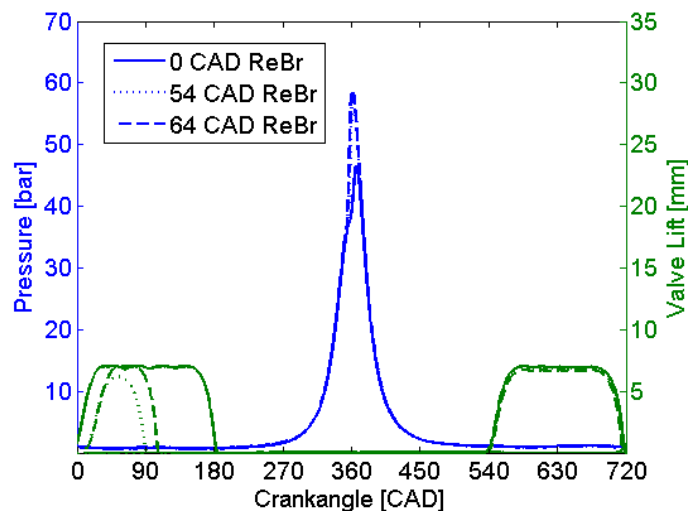
Figure 61 An illustration of the in-cylinder pressure and the valve lift profiles achieved with rebreathe strategy. The dashed and dotted valve profiles in the 0-90 CAD interval represent the rebreathe opening of the exhaust valve.

increasing duration of the rebreathe opening and the difference from NVO operation is that with the rebreathe strategy the burned gas is not compressed during the gas exchange. An illustration of the rebreathe strategy can be seen in Figure 61.

The behavior of CA50 in Figure 62 with respect to the rebreathe duration is as expected. An increase in rebreathe duration leads to an increase in amount of reinducted exhaust gas with a higher charge temperature as a result. The increased charge temperature will, as in the case with NVO, lead to an earlier start of combustion and therefore CA50 will advance. The minimum duration of the rebreathe opening was limited to 50 CAD. This corresponds to an NVO of 100 CAD. Comparing Figure 59 with Figure 62 shows a considerable difference in CA50 between NVO of 100 CAD and rebreathe duration of 50 CAD. There are two contributing reasons for this diference. One reason is that the charge temperature is higher with NVO than with the corresponding rebreathe duration, since with NVO the residuals are compressed after IVC. The other reason is that during the rebreathe opening, the flow of reinducted exhaust gas past the exhaust valve is somewhat restricted. This means that the amount of residual gas at rebreathe valve closing will be less compared to the amount of residual gas trapped in the cylinder with corresponding NVO timing and thus the temperature will be lower.
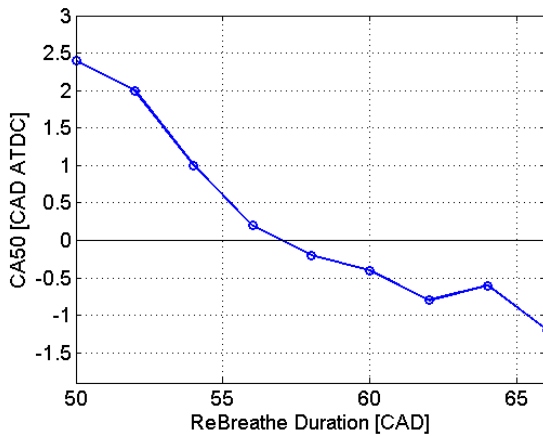
Figure 62 CA50 as a function of Rebreathe duration.
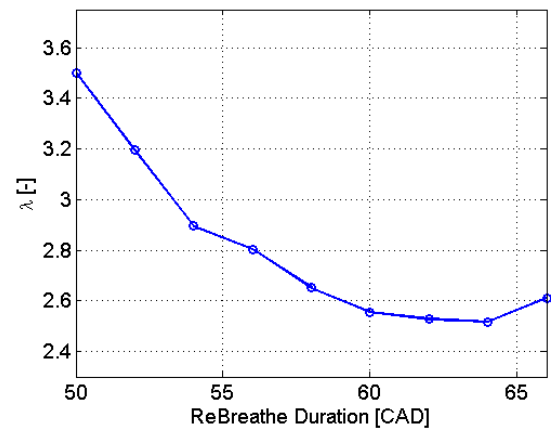
Figure 63 Lambda as a function of Rebreathe duration.

The second reason can also be confirmed by Figure 63. At rebreathe duration of 50 CAD, lambda is one unit higher compared to lambda at the corresponding NVO timing. This means that less air has been displaced by residuals which proofs that the amount of residuals has been restricted during the reinduction.

The last strategy tested is the *Miller cycle*. With this strategy, the effective compression ratio can be varied by either closing the inlet valve early or late. The decrease in compression ratio, and thus compression work, leads to a decrease in charge temperature after compression. Figure 64 shows how the Miller strategy affects the in-cylinder pressure.
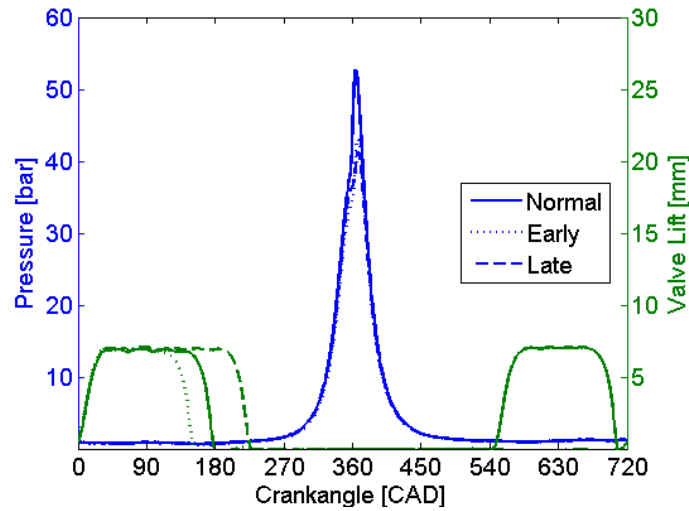
Figure 64 An illustration of the in-cylinder pressure and the valve lift profiles achieved with Miller strategy.

In Figure 65, the effect of late and early IVC on CA50 can be seen. The reason why CA50 is retarded between IVC 0-10 CAD ABDC is due to a combination of optimal volumetric efficiency and somewhat cooler charge. Due to tuning effects, the volumetric efficiency is at its maximum somewhere between 0-10 CAD ABDC and thus the highest possible amount of air will be inducted if IVC occurs during this interval. This can be verified by Figure 66, where the air/fuel ratio is at its maximum in the abovementioned interval. A late IVC also means that the total flow of air in and out of the cylinder will be higher compared with early IVC, and thus the in-cylinder temperature will decrease. These two effects combined lead to a retardation of CA50.

With early IVC the amount of air inducted during the intake stroke is limited. After IVC the air is expanded beyond ambient conditions and then compressed as the compression stroke begins. A smaller portion of inducted air means that there is less mass to heat up and thus the charge temperature will increase at a higher rate compared with late
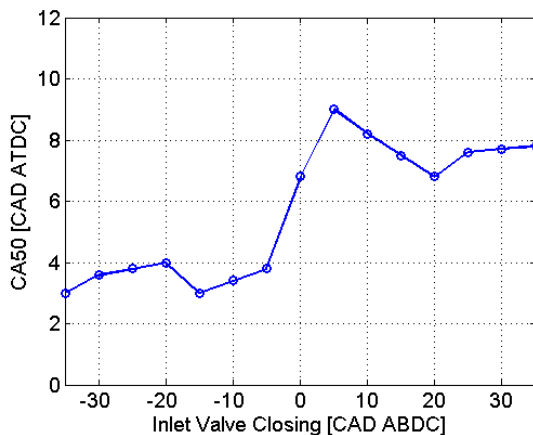
Figure 65 CA50 as a function of IVC.
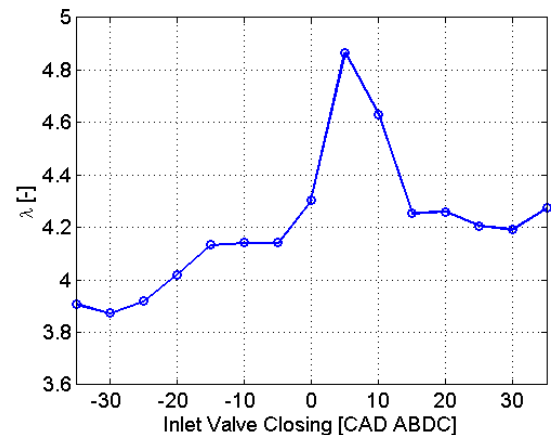
Figure 66 Lambda as a function of IVC.

IVC and thereby the end temperature after compression will be higher with an advance in CA50 as a result.

The results presented above are somewhat surprising since the Miller strategy leads to a lower compression ratio and thus a lower temperature at the end of compression should be expected with a delayed combustion as a result. However, the results shown in this thesis indicates the opposite of this behavior. The reason might be that during the IVC interval between -35 and 35 CAD ABDC, the rate of volume change is quite small. The volume change from TDC to 35 CAD ABDC is about 10% of the total volume even though the piston has travelled one fourth of the entire compression stroke. This mean that beyond 35 CAD ABDC the temperature will probably start to decrease drastically and the combustion will be delayed.

8.2   The pneumatic hybrid

Pneumatic hybrid operation introduces new operating modes in addition to conventional ICE operation. During compressor mode (CM) the engine is used as a compressor and the compressed air is stored in a pressure tank. During air-motor mode (AM) the engine is used as an air-motor utilizing pressurized air from the pressure tank. The focus of this thesis has been on testing and optimizing CM and AM in terms of valve geometry and valve timing.

8.2.1   Initial testing of Compressor Mode

The CM operation can mainly be done in three ways. The first way is to achieve as high compression efficiency as possible. This is done by the introduction of feedback or feedforward control of the tank valve. The tank valve is controlled in such a way that it opens when the in-cylinder pressure is equal to the tank pressure.

The second way is to achieve as much braking torque as possible. The maximum braking torque is achieved when the tank valve opens at or shortly after BDC. This strategy leads to a blowdown of pressurized air from the pressure tank into the cylinder and thus the cylinder will be charged with air at current tank pressure instead of atmospheric air.

Finally, the third way is actually a combination of the previous two and is the one that will be used in a real application. For instance, if the driver releases the gas pedal, the engine will be operating in CM at highest possible efficiency. When the driver presses the brake pedal, the CM operation will drift away from the highest efficiency towards highest braking torque.

This thesis focuses mainly on the first method, i.e. achieving as high CM efficiency as possible.

Table 10 shows the valve timings used in this part of the experiment. As can be seen, the tank valve is set to open when the cylinder pressure equals the tank pressure. The tank valve opening (TankVO) is controlled by an open-loop controller based on the polytropic compression law:

$$p_2 = p_1 \left(\frac{V_1}{V_2}\right)^k$$

where p_1 corresponds to the pressure at BDC and p_2 is the pressure at any point in the cycle. V_1 is the maximum volume in the cylinder and V_2 is the cylinder volume at cylinder pressure p_2. By setting p_2 equal to the tank pressure, the volume at the given pressure can be calculated and from that it is possible to calculate proper valve timing. The advantage with this strategy is that the valve timings are determined in a very simple way, however, the drawback is that the polytropic exponent, κ, depends on the heat losses and setting it to a constant value introduces some errors in the TankVO control algorithm.

Table 10 Valve timing strategy during CM operation

Tank valve opening	Cylinder pressure ≈ tank pressure
Tank valve closing	10 CAD ATDC
Inlet valve opening	35 CAD ATDC
Inlet valve closing	180 CAD ATDC

Figure 67 and Figure 68 show the PV-diagram of one CM cycle during real engine testing at two different tank pressures. Comparing both figures with Figure 37 (ideal PV-diagram of one CM cycle), clearly indicates the absence of the isobaric event (the step between point 3 and 4 in Figure 37) during real engine testing. The reason is that the chosen tank valve head diameter of 16 mm is quite small and the air flow over the valve becomes very restricted, also known as *choked flow*. This will therefore lead to an overshoot in cylinder pressure compared to ideal conditions. An attempt to lower this overshoot has been done and will be presented in Section 8.2.2. From Figure 67 and Figure 68 it can also be seen that the overshoot in cylinder pressure increases with
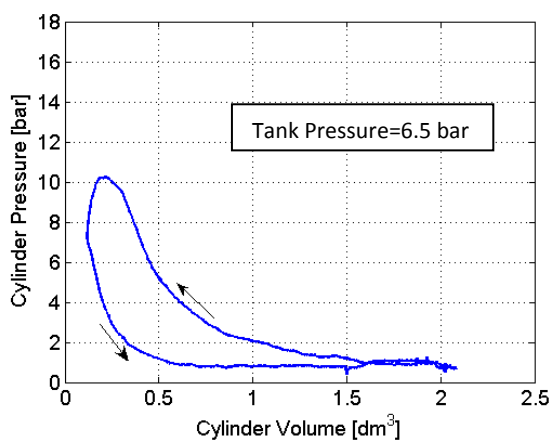

Figure 67 PV-diagram of one CM cycle at a tank pressure of 6.5 bars and an engine speed of 600 rpm.
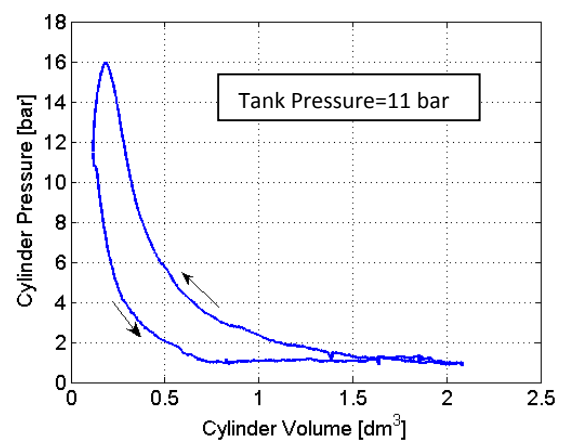
Figure 68 PV-diagram of one CM cycle at a tank pressure of 11 bars and an engine speed of 600 rpm.

increasing tank pressure. The reason is that with higher tank pressure the TankVO occurs later and thus the air trapped in the cylinder has to be evacuated in less time. Since the air flow is restricted, this will lead to an increase in overshoot.

The overshoot in pressure also increases with increasing engine speed. This is due to the fact that with increasing engine speed there is less time to vent the cylinder from compressed air. Figure 69 illustrates this at three different engine speeds.
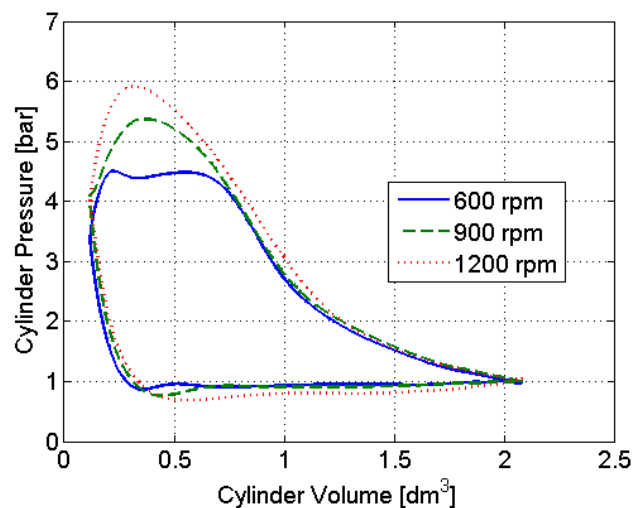
Figure 69 PV-diagram of one CM cycle for three different engine speeds at 4 bars of tank pressure.

Figure 70 shows the accumulated mean tank pressure during 800 consecutive cycles at three different engine speeds. It is noticeable that there is a difference between the tank pressures for different engine speeds. This can probably be explained with leakage of pressurized air from the pressure tank into the cylinder through the tank valve. Since leakage of compressed air through an orifice is constant in time at a constant pressure, the amount of air inducted into the cylinder per cycle due to leakage will decrease with increasing engine speed, and thus the end tank pressure should reach a higher level. At 1200 rpm, this explanation is not enough since the end tank pressure is even lower than at 600 rpm. The reason is probably that the control program by coincidence is better optimized at 600 and 900 rpm.

Figure 71 shows the IMEP generated during 800 consecutive engine cycles at three different engine speeds. The reason why IMEP decreases after approximately 400 cycles at 900 and 1200 rpm is that the valve closing (TankVC) is not open-loop controlled but set to a constant value. Constant TankVC will affect the negative IMEP at higher tank pressures because ideally TankVC should be retarded towards TDC with increasing tank pressure. The TankVC should always be set in such a way that the pressurized air trapped in the cylinder will be expanded to atmospheric pressure when the piston reaches BDC. At higher tank pressures, a late TankVC means that the in-cylinder pressure is higher than desired, and the excess pressure pushes the piston as it moves towards BDC and thereby contributes with positive IMEP which decreases the negative IMEP for the whole cycle. This phenomenon is engine speed dependent, since at higher

engine speeds the compressed air will have less time to evacuate the cylinder and a larger portion of compressed air will be trapped in the cylinder after TankVC.
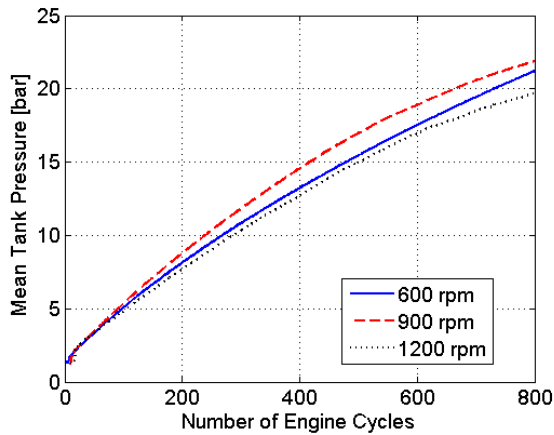
Figure 70 Mean tank pressure during CM as a function of engine cycle number at three different engine speeds.
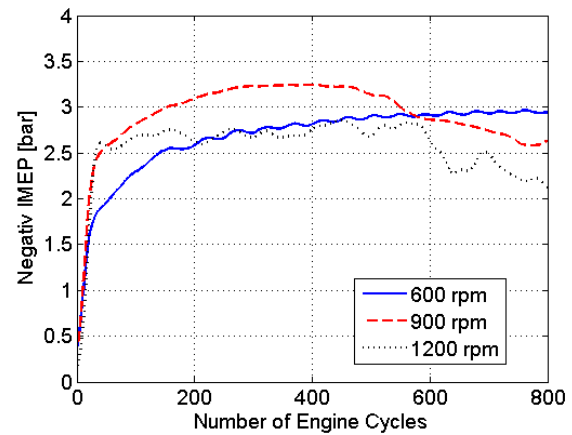
Figure 71 Negative IMEP during CM as a function of engine cycle number at three different engine speeds.

8.2.2 Optimizing the compressor mode

The optimization of the compressor mode has been done in terms of valve timing and valve geometry. Correct valve timing is the key to good pneumatic hybrid efficiency and proper valve geometry reduces unnecessary energy losses due to restricted flow.

In the previous section, it was stated that the open-loop control was based on the polytropic compression law. The disadvantage with this method is that it does not give an accurate valve timing. In order to avoid this error, a method for optimizing the CM has been developed. The main idea with this method is to find the most optimal valve timing at a given tank pressure and, in order to do that, the tank pressure needs to be constant throughout the whole testing interval. With the aid of a pressure relief valve it is possible to change the pressure level in the system. The pressure in the tank will become constant when the amount of air charged into the tank is equal to the amount of air released from the tank and by adjusting the pressure relief valve opening angle it is possible to set a desired steady-state tank pressure.

Figure 72 shows a TankVO optimization sweep for the small tank valve at various steady-state tank pressures. TankVC, IVO and IVC were set to a constant value at this optimization. It can clearly be seen how negative IMEP is affected by TankVO timing during optimization of CM. The figure shows that there is an optimal TankVO timing for every tank pressure when taking highest efficiency into consideration, highest efficiency corresponds to the minimum in each curve. This means that it takes less power to compress the inducted air at this point than at any other point on the curve at a given tank pressure. If higher braking torque is needed, the efficiency has to be sacrificed.

The reason why negative IMEP increases at early TankVO is that when the tank valve opens earlier than optimal, there will be a blowdown of compressed air into the cylinder due to the fact that the pressure level in the cylinder is lower than in the pressure tank.

At a certain premature TankVO, negative IMEP will dramatically increase with increasing tank pressure, due to a larger pressure level difference between the cylinder and the pressure tank.
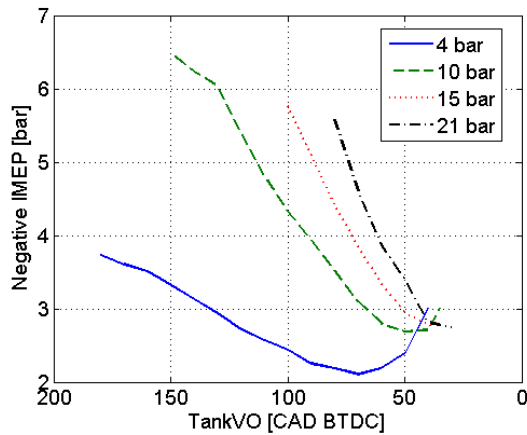
Figure 72 Negative IMEP obtained during steady-state CM as a function of TankVO during optimization of CM at various tank pressures and an engine speed of 600 rpm
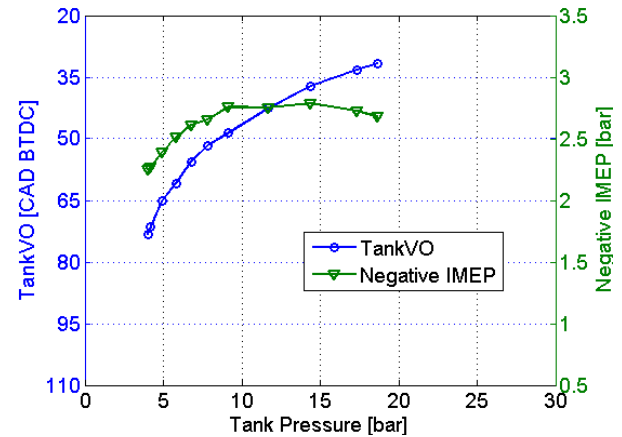
Figure 73 TankVO and negative IMEP during CM optimization as a function of tank pressure at an engine speed of 600 rpm

Figure 73 shows how optimal TankVO and corresponding negative IMEP varies with increasing tank pressure. The reason why the negative IMEP decreases after a tank pressure of approximately 14 bar, is that the optimization has been done with focus on TankVO while TankVC has been set to a constant value of 10 CAD ATDC.
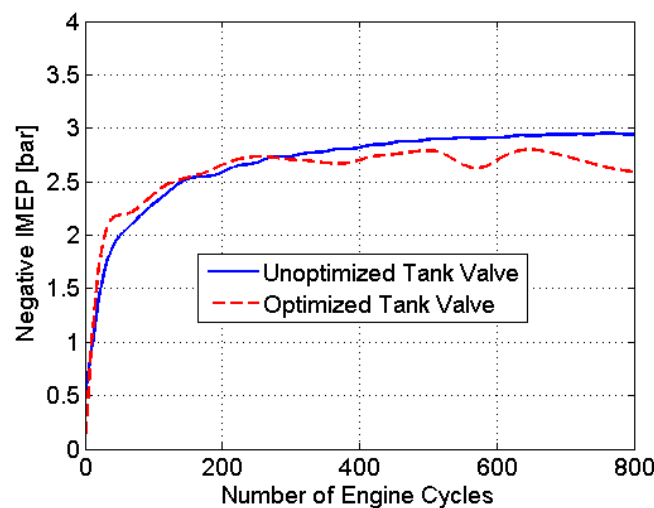
Figure 74 Comparison of negative IMEP for unoptimized and optimized TankVO as a function of engine cycle number during CM operation. End tank pressure is about 21 bar in both cases.

CM operation testing has been done both with unoptimized tank valve operation, and with the optimal TankVO timings seen in Figure 73. The result can be seen in Figure 74 where negative IMEP for both unoptimized and optimized TankVO is shown. Initially, negative IMEP for unoptimized TankVO is similar to negative IMEP for optimized TankVO, but after about 300 engine cycles negative IMEP for the optimized tank valve

remains reasonably constant while negative IMEP for the unoptimized tank valve continues to increase throughout the rest of the test.

The initial testing of CM showed that the chosen valve design leads to a very restricted air flow through the valve. In an attempt to minimize the restriction of air flow, the old setup with a valve head diameter of 16 mm has been replaced with a valve that has a valve head diameter of 28 mm in combination with the previously described pneumatic valve spring arrangement.

From now on the tank valve with a valve head diameter of 16 mm will be referred to as the "small tank valve" and the pressure compensated valve with a valve diameter of 28 mm will be referred to as the "large tank valve".

Figure 75 and Figure 76 illustrates the pressure drop over the small and large tank valves, respectively, obtained at three different engine speeds during CM. The hump-like behavior between 100 and 200 engine cycles at both 900 and 1200 rpm in Figure 76 occurs due to the pressurized air source switching system described earlier. As the tank pressure is reaching a pressure level close to the switching pressure level, the tank valve lift height is decreasing, see Figure 77. The tank valve lift has decreased by almost 1 mm at engine cycle 150 compared to cycle 100. At cycle 200 the tank valve lift height has nearly returned to a maximum. The reason for this behavior is thought to be bad interaction between the check-valves due to pressure oscillations in the pressurized air supply line. During normal running
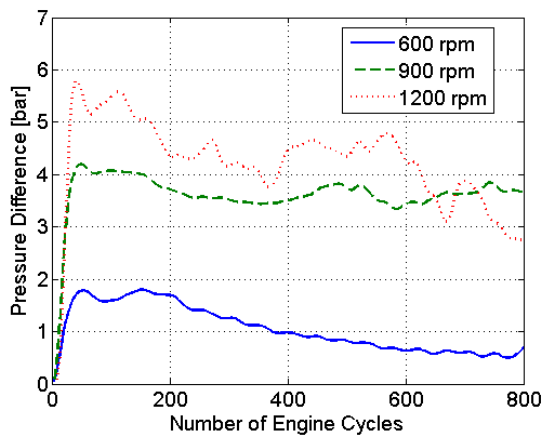
Figure 75 Pressure difference between in-cylinder pressure and maximum pressure after the tank valve (port pressure) as a function of engine cycle number at various speeds. Small tank valve setup.
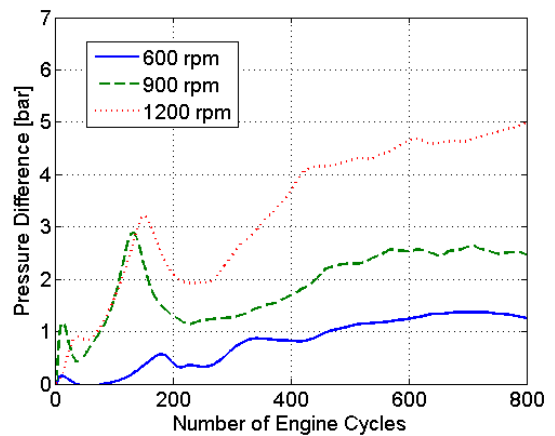
Figure 76 Pressure difference between in-cylinder pressure and maximum pressure after the tank valve (port pressure) as a function of engine cycle number at various speeds. Large tank valve setup.

conditions one of the check-valves will be completely open, but during the transition period, both check-valves will open and close frequently due to the pressure oscillations, which leads to a deficit in pressure and thus the valve lift will decrease.
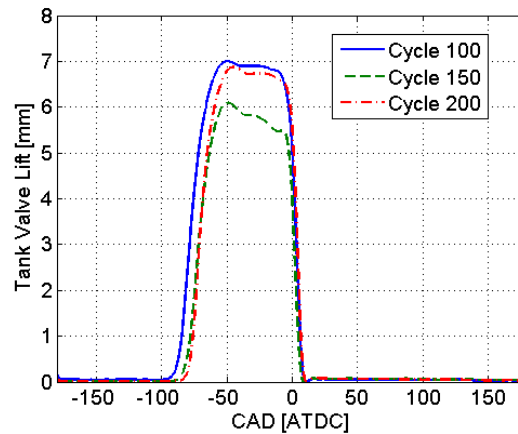
Figure 77 Tank valve lift at three different engine cycles and at an engine speed of 1200 rpm.

Figure 78 shows a TankVO optimization sweep for the large tank valve at various steady-state tank pressures, similar to the TankVO sweep in Figure 72. With the larger valve, the negative IMEP at a tank pressure of 4 bar and at optimal TankVO for both 600 and 900 rpm is lower compared to the negative IMEP in Figure 72 at the same tank pressure. This is because the pressure drop is decreased due to the larger tank valve head diameter. At 10 and 15 bar, there is hardly any difference between negative IMEP for the large tank valve compared to the small tank valve. The only difference is that the optimal TankVO for the large tank valve is advanced a number of CAD compared to TankVO for the small valve. One of the reasons for this behavior is most likely that there is a blowdown of pressurized air into the cylinder through the tank valve. It seems as the tank valve is not completely pressure compensated as expected and thus there is a net force acting to open the tank valve. Another reason is that there is some pressure losses in the pressurized air supply line between the tank and the pneumatic valve actuator, which means that the pressurized air fed to the valve actuator at a certain time is not the

Figure 78 Negative IMEP obtained during steady-state CM as a function of TankVO for the large tank valve setup at various tank pressures and engine speeds.
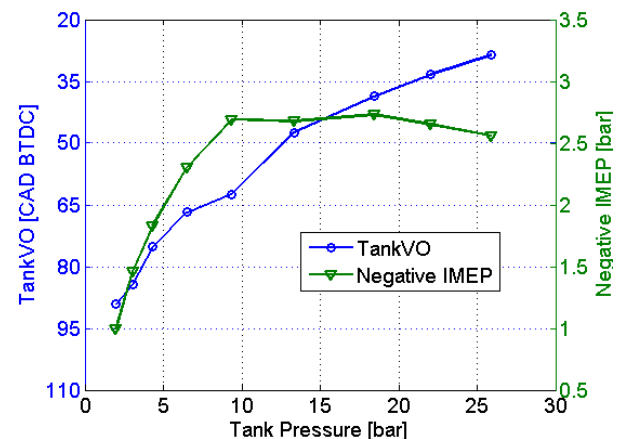
Figure 79 TankVO timing and corresponding negative IMEP during CM optimization as a function of tank pressure for the large tank valve setup at an engine speed of 600 rpm.

same as the mean tank pressure at the corresponding time and therefore the ability to open the tank valve at optimal timing is lost and has to be advanced. An advance in TankVO compared to optimal timing means that there will be a blowdown of pressurized air into the cylinder and thus negative IMEP will increase. The reason why negative IMEP for the large tank valve is considerably lower than for the small tank valve at 4 bar of tank pressure is that at this tank pressure level, the actuator is fed with 6 bar of compressed air from an external source. This means that, at this point there is a surplus of 2 bars feeding the valve actuator and thus the optimal TankVO timing can be achieved.

Figure 79 shows how optimal TankVO and corresponding negative IMEP varies with increasing tank pressure for the large tank valve setup. Comparing negative IMEP from Figure 79 with negative IMEP from Figure 73 indicates that the pressure losses over the tank valve are lower with the large valve than with the small valve. If focus is put on the TankVO, it can clearly be seen that the optimal TankVO for the large tank valve occurs considerably earlier compared to the optimal TankVO for the small tank valve. The reason for this behavior can once again be explained as inadequate amount of pressurized air supplied to the tank valve actuator and therefore the valve timing has to be advanced a number of CAD away from the real optimum, which contributes to a higher negative IMEP.

Figure 80 shows negative IMEP during optimal CM at three different engine speeds for the large tank valve setup. Comparing the result at 600 rpm displayed in Figure 80 with the result from the optimized test shown in Figure 74 indicates that there is only a difference the first 200 cycles during which the results obtained with the large tank valve setup show that IMEP is lower than the corresponding results obtained with the

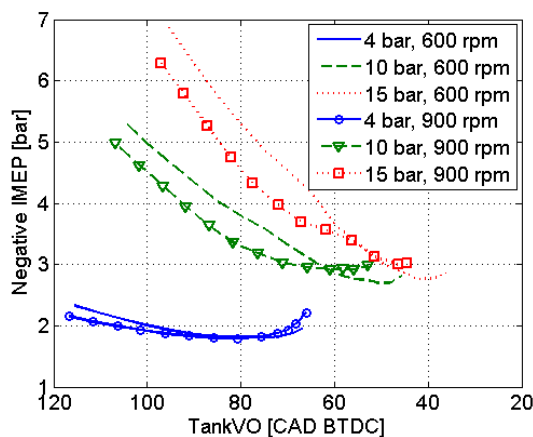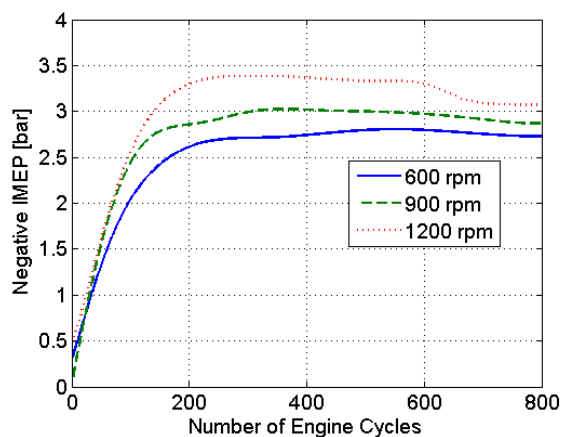**Figure 80 Negative IMEP during optimal CM as a function of engine cycle number at three different engine speeds for the large tank valve setup.**
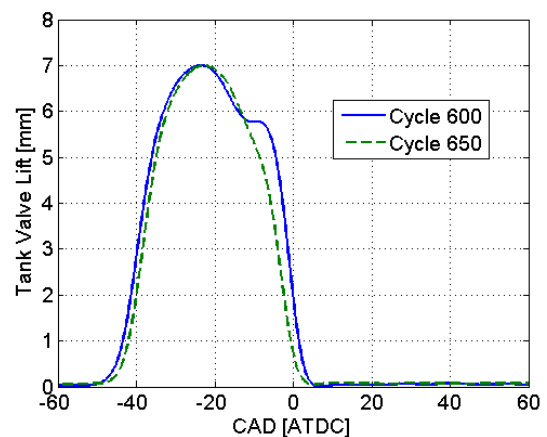
Figure 81 Tank valve lift at two different engine cycles and at an engine speed of 1200 rpm.

small tank valve setup. This verifies that increasing the tank valve diameter decreases the air flow resistance over the tank valve. The reason why negative IMEP is almost the same in both cases after 200 cycles is probably once again insufficient pressure in the compressed air supply line feeding the tank valve actuator.

From Figure 80 it can also be noticed that, at 1200 rpm negative IMEP suddenly starts to decrease after about 600 cycles. The reason for this behavior is that, due to inexplicable performance of the tank valve actuator, the valve lift duration is abruptly decreased after 600 cycles, see Figure 81. A shorter duration means that there will not be enough time to vent the cylinder from pressurized air and therefore the cylinder will still be filled with pressurized air at tank valve closing. This excess of compressed air pushes the piston as it moves towards BDC and thus contributes with positive IMEP, which in turn decreases negative IMEP for the whole cycle.

8.2.3   Initial testing of Air-Motor Mode

The AM can, as CM, mainly be executed in three ways – with optimal efficiency, power, or a trade-off between both. Achieving highest air-motor efficiency is done by a feedback control of both the tank valve and the intake valve. TankVO should occur at TDC and TankVC should be set in such a way that the pressurized air is expanded to atmospheric pressure at BDC. The intake valve should open at BDC and IVC should be set in such a way that when the piston reaches TDC, the inducted air is compressed to the same level as the tank pressure level.

In order to accelerate the vehicle more rapidly compared to the high-efficiency case, high power is needed. This can be achieved by prolonging the tank valve duration compared to the optimal timing and thereby induct more compressed air which increases the work done on the piston. Highest air-motor power is achieved with TankVC at BDC or shortly before. The inlet valve should be controlled in the same manner as with the high-efficiency method.

In a real application, a combination of the previously explained methods will be utilized. For instance, as long as the driver presses the gas pedal moderately, the AM will be operated at highest efficiency or close to it. As the driver continues to press the pedal towards its end position, the AM operation will drift away from highest efficiency towards maximum air-motor power.

This thesis focuses mainly on the first method, namely achieving as high AM efficiency as possible. All tests involving AM have been done at an engine speed of 600 rpm.

Table 11 shows the valve timing strategy used in this part of the experiment. The timings related to TankVC are chosen in order to achieve as high torque as possible. The different pressure levels that follow after @ relates to the starting tank pressure.

Table 11 Valve timing strategy during AM operation.

IVO	180 CAD ATDC
IVC	0 CAD ATDC
TankVO	5 CAD ATDC
TankVC@22 bar	40 CAD ATDC
TankVC@15 bar	60 CAD ATDC
TankVC@12.5 bar	70 CAD ATDC
TankVC@10 bar	80 CAD ATDC

Figure 82 and Figure 83 show the PV-diagram of one AM cycle during real engine testing at two different tank pressures. Comparing both figures with Figure 39 (ideal PV-diagram of one AM cycle), indicates a considerable difference. The lack of the isobaric event (the step between 1 and 2 in Figure 39) is due to a restricted air flow over the tank valve. The absence of the compression step between 4 and 1 found in Figure 39 can be explained by inappropriate IVC. In order to avoid a rush of compressed air into the cylinder, the air in the cylinder should be compressed to the same level as the tank pressure level prior to TankVO. Since IVC occurs at TDC, the pressure in the cylinder at TankVO will be atmospheric and the pressurized air from the tank will rush into the cylinder with high pressure losses as a result. Observe that in Figure 83 two enclosed loops can be noticed, a positive and a negative loop. The loop on the right side of the figure is the negative loop and it is contributing with negative IMEP. This is due to wrong tank or inlet valve timings. The amount of pressurized air charged into the cylinder is not enough in order to expand it to atmospheric pressure at BDC. Instead the pressure will decrease below atmospheric pressure and thus vacuum is created which is an energy consuming process. Since the inlet valve opens at BDC, the vacuum is canceled by the induction of fresh air into the cylinder and thereby the vacuum created cannot be used as an upward-acting force on the piston as it moves towards TDC.

There are two ways to prevent this occurrence. One is by not opening the inlet valve until the cylinder pressure reaches atmospheric pressure as the piston travels towards
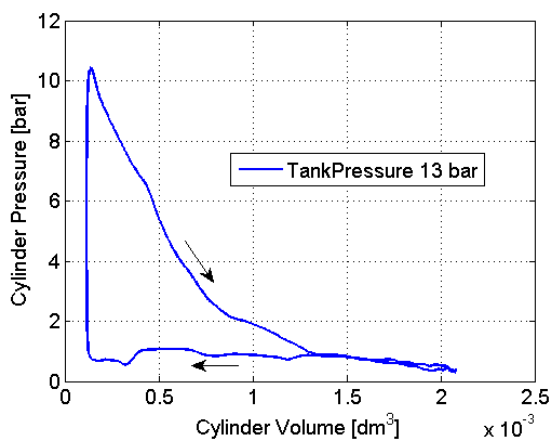
Figure 82 PV-diagram of one AM cycle at a tank pressure of 13 bar.
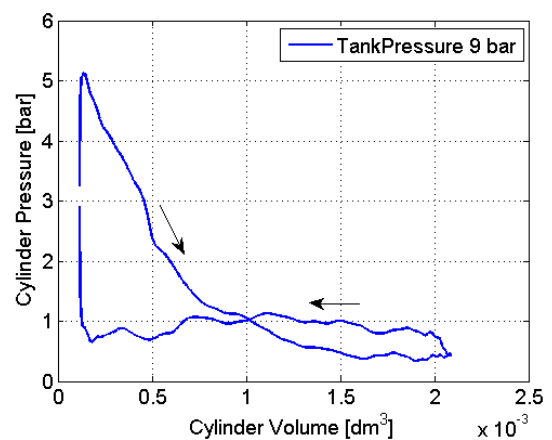
Figure 83 PV-diagram of one AM cycle at a tank pressure of 9 bar.

TDC. The second way is to have longer tank valve duration and thus induct more pressurized air. In this way the cylinder pressure will reach atmospheric pressure at BDC and the inlet valve can then open at BDC without the risk of creating any backflow of atmospheric air into the cylinder.

Figure 84 shows positive IMEP during 400 consecutive cycles of AM operation starting at four different tank pressures and Figure 85 shows the corresponding tank pressure. What can be noticed from both figures is that the positive IMEP becomes negative at some point during the test cycle even though the tank pressure is above atmospheric pressure. The larger than the positive loop and thus the work input has exceeded work output and therefore IMEP becomes negative.
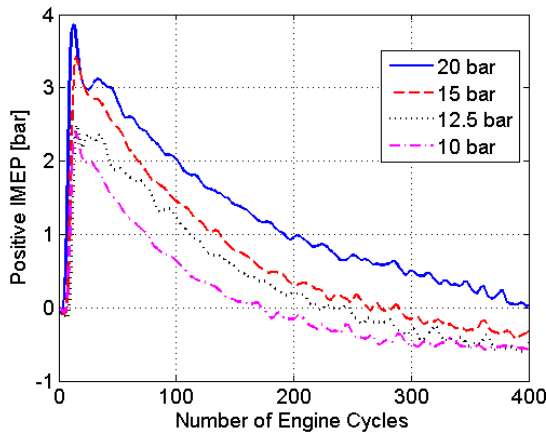
Figure 84 Positive IMEP during unoptimized AM with small tank valve setup as a function of engine cycle number. Legend indicates starting tank pressure.
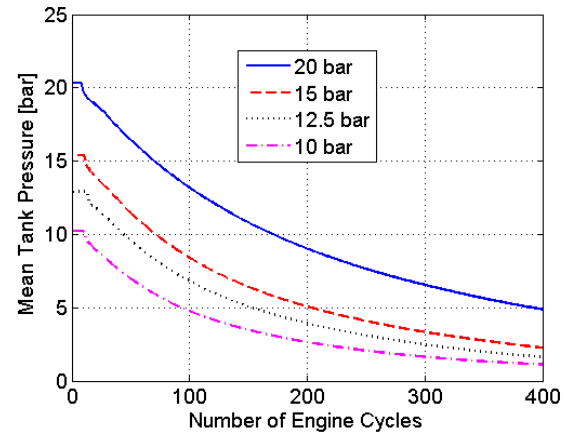
Figure 85 Mean tank pressure during unoptimized AM with small tank valve setup as a function of engine cycle number

8.2.4 Optimizing the air-motor mode

The optimization of AM has been done in terms of valve timing and valve geometry. The chosen valve timings used in previous section were not optimized in any way. The intent was to show that the concept works and thus the focus was mainly on function rather than optimal operation. However the results showed that proper valve timing is crucial for achieving good AM efficiency.

An attempt to use the polytropic compression law, in order to achieve a proper valve strategy during AM, has been done. TankVC is controlled in such way that at a certain tank pressure, a proper closing angle is calculated with the help of the polytropic compression law. Also IVC is calculated in a similar way. TankVO and IVO are set to a constant value of 0 CAD ATDC and 180 CAD BTDC, respectively. TankVC and corresponding positive IMEP obtained with this method can be seen in Figure 86. These results are quite poor compared to the results shown in Figure 84, where IMEP levels of almost 4 bars have been shown with constant valve timings. The reason is that, as stated before, the specific-heat ratio depends on the heat losses and setting this ratio to a constant value introduces some errors to the valve control algorithm. Also, the

polytropic relation does not take the pressure losses over the tank valve into account, and therefore the TankVC will be chosen closer to TDC than what would be optimal.
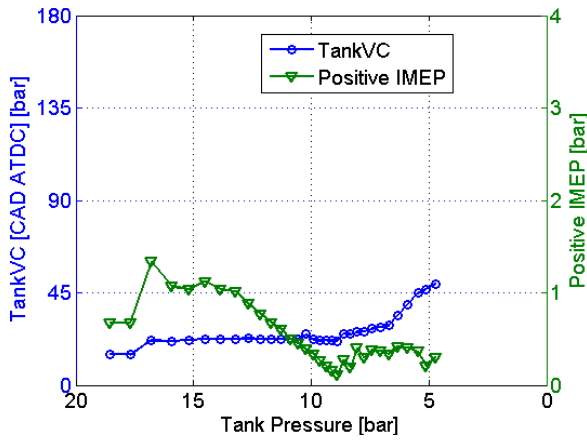
Figure 86 TankVO and corresponding positive IMEP during AM for the large tank valve setup as a function of tank pressure.
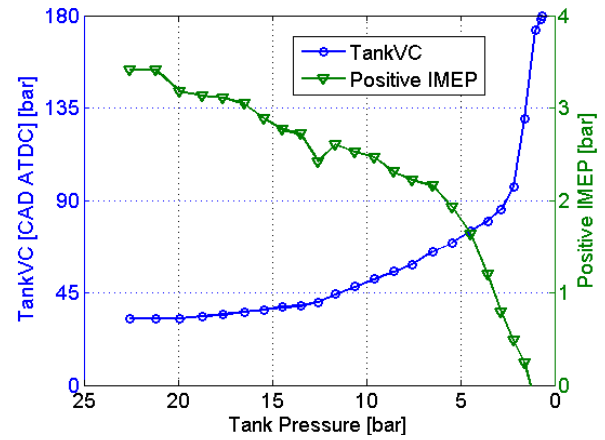
Figure 87 Optimized TankVO and corresponding positive IMEP during AM for the large valve setup as a function of tank pressure.

In order to optimize the AM, a method for finding the optimal valve timings is necessary. The steady-state method, used for optimizing the CM, cannot be used in order to optimize the AM, since there is no charging of the pressure tank during AM and thereby a steady-state tank pressure cannot be achieved.

A method for finding the optimal IVC has been developed. The idea is to vary IVC and thus the corresponding peak cylinder pressure will also be varied. In this way, a map containing IVC as a function of peak cylinder pressure can be created.

In order to find the optimal TankVC, results from the CM optimization, shown in Figure 79, have been used. During the compression stroke during optimal CM, the atmospheric air in the cylinder is compressed to the same pressure level as the tank pressure level before the tank valve opens. In AM, the procedure should be the opposite. The TankVO should occur around TDC. As the piston moves away from TDC, the compressed air will expand and when the in-cylinder pressure is the same as the tank pressure, the tank valve should close. This means that TankVO during CM corresponds to TankVC during AM. During CM the tank valve opens when pressure equilibrium is reached and during AM the tank valve closes at the same condition. Thereby the results obtained during CM optimization can, with some modification, be used to control the valve during AM. For instance, if it is determined that TankVO during CM should occur at 35 CAD BTDC, then TankVC during AM should occur at 35 CAD ATDC. In order to fit the results from CM to AM, some tuning of the valve timings had to be done.

Figure 87 shows the final results from AM testing where both IVC and TankVC have been optimized with the methods described above. Comparing the results from Figure 87 with the results from Figure 79 indicates that the curves bear a resemblance to one another. But there are some differences, mainly for the TankVC. For instance, at a tank pressure of 20 bar, the results in Figure 87 indicates a TankVC at approximately 33 CAD ATDC, while the results in Figure 79 indicates a TankVO at approximately 38 CAD BTDC.

The difference of 6 CAD is due to the fact that IVC during AM is chosen in such way that the peak in-cylinder pressure is lower than the tank pressure when the tank valve opens. Thereby, the deficit in the pressurized air supply line is compensated for.
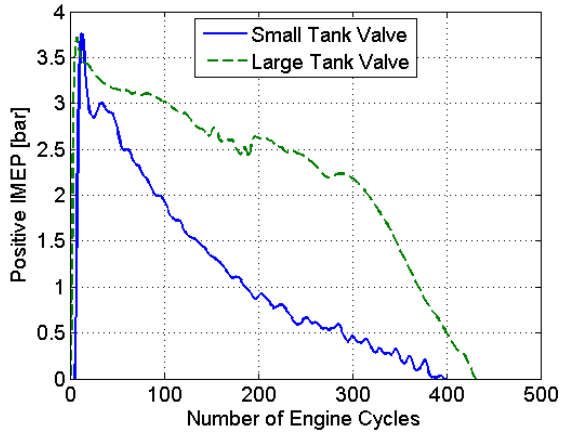
Figure 88 Positive IMEP for two different valve setups and valve strategies as a function of engine cycle number.
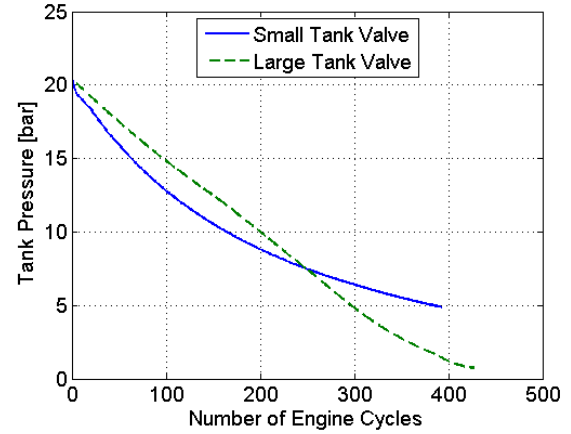
Figure 89 Mean tank pressure for two different valve setups and valve strategies.

Figure 88 shows positive IMEP obtained with two different tank valve setups and valve strategies during AM operation and the corresponding tank pressure can be seen in Figure 89. The small tank valve curve is the same as the one starting at 20 bar of tank pressure shown in Figure 84. The large tank valve curve has been obtained with the optimal valve timings shown in Figure 87. The starting tank pressure is about 20 bars in both cases. It can be realized that, an increase in valve head diameter together with optimal valve timings, has a large impact on the AM operation. This will in turn lead to a considerable increase in the AM total efficiency. The reason why IMEP for the large tank valve setup is much higher throughout the whole test compared to the small tank valve setup, is that the pressurized air is used in a much more efficient way. A larger tank valve diameter contributes to less pressure losses over the tank valve and an optimized valve control strategy contributes to a more efficient use of the pressurized air, and together they contribute to a higher positive IMEP.

Figure 90 and Figure 91 illustrates PV-diagrams for both tank valve setups at tank pressures of 16.5 and 6.5 bar, respectively. There are evident differences in peak cylinder pressure between the small tank valve setup and the large tank valve setup in both figures. The reason is that the flow over the small tank valve will become choked due to a very restricted flow area. With the larger tank valve, the flow area is increased more than three times compared to the small tank valve flow area and therefore the threshold for choked flow has been raised.
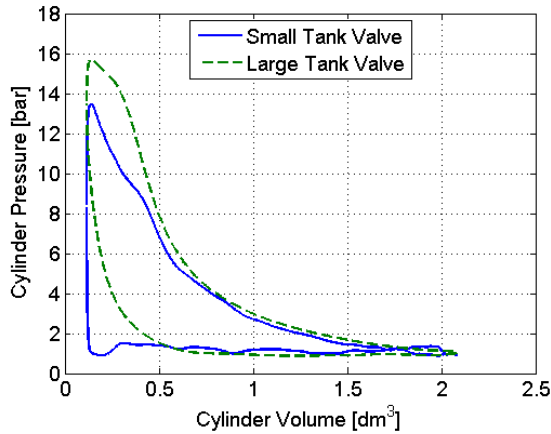
Figure 90 PV-diagram for two different tank valve setups and valve timing strategies at a tank pressure of 16.5 bar.
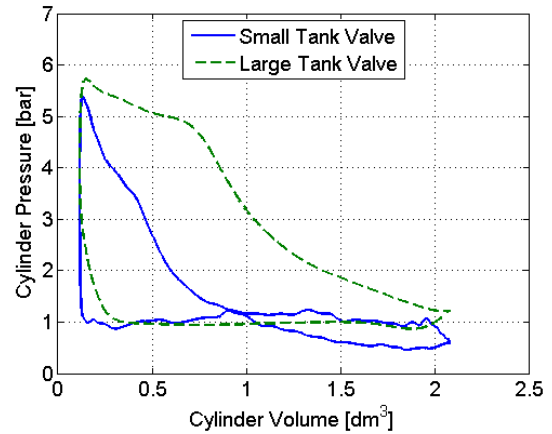
Figure 91 PV-diagram for two different tank valve setups and valve timing strategies at a tank pressure of 6.5 bar.

The PV-diagrams for the large tank valve setup bear a great resemblance to the ideal PV-diagram shown in Figure 39. The isobar step in the ideal PV-diagram has not been achieved, but it is much better than the corresponding step achieved with the small tank valve setup. There is now also a compression step present in the PV-diagram of the optimized AM comparable to the one found in the ideal PV-diagram.

8.2.5 Regenerative efficiency

In order to estimate the potential of the pneumatic hybrid, and introduce the possibility to compare different tests with each other, a regenerative efficiency has to be defined. The regenerative efficiency is the ratio between the energy recovered during AM and the energy consumed during CM. It can also be defined as the ratio between positive and negative IMEP:

$$\eta_{regen} = \frac{IMEP_+}{IMEP_-}$$

Table 12 shows the regenerative efficiency with different tank valve setups and valve strategies at three engine speeds. The small tank valve setup has a maximum regenerative efficiency of 33% at 900 rpm. The reason why the efficiency is higher at 900 rpm than at 600 rpm is that the unoptimized feedback controller by coincidence is better suited for the case at 900 rpm than at 600 rpm. The regenerative efficiency for the large tank valve setup indicates that with optimized tank valve timing, the maximum efficiency occurs at 600 rpm and decreases with increasing engine speed. A tremendous improvement has been achieved while switching from the small tank valve setup to the large tank valve setup. The improvement depends mainly on a larger tank valve head diameter and optimized tank valve timing during AM. A change in inlet valve strategy from constant IVC to open-loop controlled IVC, contributes to a further increase in regenerative efficiency.

Table 12 Calculated total regenerative efficiency for different tank valve setups and valve strategies at three different engine speeds.

	η_{regen}		
Engine speed	600	900	1200
Small tank valve setup	32	33	25
Large Tank valve setup, constant IVC during AM	44	40	37
Large tank valve setup	48	44	40

The pneumatic tank valve actuator consumes energy in the form of compressed air from the pressure tank. Since its energy consumption decreases the total energy stored in the pressure tank, it has to be seen as energy losses. These losses have automatically been taken into account in the calculation of regenerative efficiency. This is only valid for the large valve setup, since the pneumatic tank valve used in the small tank valve setup has been fed with compressed air generated from an external source. This means that the regenerative efficiency calculated for the large tank valve setup, is lower than it would be if the pneumatic valve actuator energy losses were excluded from the calculation.

It should be noticed that the regenerative efficiency, described in this paper is actually an indicated efficiency, apart from the included pneumatic valve actuator energy losses. This means that a real vehicle cannot utilize the energy to the same extent due, among other things, to engine and driveline friction losses, which will lead to a lower regenerative efficiency.

9 Summary

The work presented in this thesis consists of two parts: evaluation of a new type of VVA system and investigation of the pneumatic hybrid concept.

A VVA system is a very powerful tool in the field of engine research in order to study various combustion related phenomena and the effect of valve timings on engine performance. It is thus of great importance that such a system functions properly and stably.

Various tests have clearly shown the potential with electro-pneumatic VVA. The actuators have proven to be well developed and to offer a robust function. Results show the ability to operate in the desirable range associated with heavy duty engines. Valve lifts between 3 and 12 mm have been achieved at a speed interval between 300 and 2500 rpm. The system shows a great flexibility as valve lift and timing can be chosen almost without any constraints and independently of each other. Successful test runs with various valve strategies for HCCI combustion control have shown the great benefits with a fully variable VVA system.

The pneumatic hybrid is a promising concept with the possibility to reduce vehicle fuel consumption as well as exhaust emissions. The advantages with pneumatic hybrid compared to the electric hybrid are first and foremost simplicity combined with a great potential in cost reduction.

Initial testing of different pneumatic hybrid related modes of engine operation was conducted. Both compressor mode (CM) and air-motor mode (AM) were executed successfully and a regenerative efficiency of up to 33 % was achieved showing the potential with pneumatic hybridization.

In order to minimize pressure losses due to restricted flow into and out from the cylinder, the tank valve head diameter was changed from 16 mm to 28 mm. The large tank valve has been combined with an in-house developed pneumatic spring in order to secure proper valve timing. The evaluation has shown that there are some issues with the pneumatic valve spring concerning tank valve actuation. The problem has been identified and a possible solution has been suggested.

A method for optimizing both CM and AM in regard to efficiency has been developed and tested. The results indicate an increase in efficiency for both CM and AM. The impact of optimized valve timings was much more evident in AM compared to CM.

Optimized pneumatic hybrid operation together with the change of valve head geometry has shown an increase in regenerative efficiency from 33% to impressive 48%. However, this figure includes energy losses due to pressure tank fed valve actuation. Therefore, the increase in indicated efficiency is expected to be even higher.

10 Future work

The change of valve geometry has shown that this is an important factor in the optimization of pneumatic hybrid operation. However, a change in valve head diameter requires time consuming modifications. Therefore a GTPower model of the engine is under development. The aim is to develop a model as similar and accurate as possible to the real engine which will simplify the search for the optimal pneumatic hybrid. It is much easier to do a parametric study with a model than it would be with a real engine. A change in valve head for instance, can be done by simply changing the value in GTPower, while a change of valve diameter in a real engine requires exchange of valve seating and machining of the standard valve.

Results from the pneumatic hybrid model will also be combined with a standard driving cycle in order to investigate the potential of reduction in fuel consumption.

So far, only two pneumatic hybrid engine operation modes have been investigated. In the future also air-power-assist mode (APAM) will be explored. The different pneumatic hybrid modes of operation will also be used in combination with conventional combustion engine operation in order to study engine mode transient behavior and its effect on engine performance and exhaust emissions.

11 Summary of papers

11.1 Paper 1

FPGA Controlled Pneumatic Variable Valve Actuation
SAE Technical Paper 2006-01-0041
By Sasa Trajkovic, Alexandar Milosavljevic, Per Tunestål and Bengt Johansson
Presented by Sasa Trajkovic at the SAE World Congress, Detroit, MI, USA, April 2006

In this paper a pneumatic VVA system has been investigated and evaluated for use in a combustion engine. A control system for the VVA system has been developed in LabVIEW. The valves were first tested during motored operation, where its characteristics in form of valve lift and timing were explored. The extreme operating limits of the system were tested with good result. After proper function was assured by initial testing of the VVA system, three different valve strategies in order to control HCCI combustion were explored.

The results indicate that the VVA system is well developed with a stable function and offers a great flexibility in the choice of valve timing and lift. Investigation of the extreme limits together with results from the valve strategy tests have shown that the VVA system is suitable for heavy duty engines such as the Scania D12 Diesel engine used in this paper.

I did most the experiments, evaluated the data and wrote the paper. Some of the experiments were carried out together with A. Milosavljevic.

11.2 Paper 2

Introductory Study of Variable Valve Actuation for Pneumatic Hybridization
SAE Technical Paper 2007-01-0288
By Sasa Trajkovic, Per Tunestål and Bengt Johansson
Presented by Sasa Trajkovic at the SAE World Congress, Detroit, MI, USA, April 2007

In this paper the pneumatic hybrid concept has been investigated. A Scania D12 engine was converted for pneumatic hybrid operation and tested in a laboratory setup. Pneumatic valve actuators have been used to make the pneumatic hybrid possible. The intent with this paper was to test and evaluate two different modes of engine operation - compression mode (CM) where air is stored in an air tank during deceleration and air-motor mode (AM) where the previously stored air is used for acceleration of the vehicle. This paper also includes optimization of the compressor mode with respect to valve timing.

The results showed that the pneumatic hybrid has a potential in becoming a serious contender to the electric hybrid. The regenerative efficiency was below expected value, but still enough for a proof of concept. It was also realized that the chosen valve geometry was the main limiting parameter regarding regenerative efficiency.

I did the experiments, evaluated the data and wrote the paper.

11.3 Paper 3

Investigation of Different Valve Geometries and Valve Timing Strategies and their Effect on Regenerative Efficiency for a Pneumatic Hybrid with Variable Valve Actuation
SAE Technical Paper 2008-01-1715
By Sasa Trajkovic, Per Tunestål and Bengt Johansson
To be published at the SAE 2008 International Powertrains, Fuels and Lubricants Congress, Shanghai, China, June 2008

This paper can be seen as a continuation of Paper 2 where it was also realized that the chosen valve geometry was the main limiting parameter with regard to regenerative efficiency. In this paper the tank valve used in Paper 2 has been exchanged for a valve with a larger head diameter in combination with a pneumatic valve spring.

A comparison between the old and the new tank valve geometry and their effect on the pneumatic hybrid efficiency has been done. Also, optimization of the valve timings for both compressor mode and air-motor mode has been done in order to achieve further improvements of regenerative efficiency.

The results indicate that the increase in valve diameter reduces the pressure drop over the tank valve, contributing to a higher regenerative efficiency. Optimization of both tank valve timing and inlet valve timing for CM and AM contributes to a further increase in regenerative efficiency.

I did the experiments, evaluated the data and wrote the paper.

12 References

1. European Parliament, "*Beating global climate change*", (2005). Available at
    http://www.europarl.eu.int/omk/sipade3?PUBREF=-//EP//TEXT+TA+P6-TA-
    2005-
    0433+0+DOC+XML+V0//EN&L=EN&LEVEL=2&NAV=S&LSTDOC=Y&LSTDOC=N
    (May 19, 2008)

2. C. Thai, T-C Tsao, M. Levin, G. Barta and M. Schechter, "*Using Camless Valvetrain for Air Hybrid Optimization*", SAE Paper 2003-01-0038, 2003

3. M. Andersson, B. Johansson and A. Hultqvist, "*An Air Hybrid for High Power Absorption and Discharge*", SAE paper 2005-01-2137, 2005

4. Cargine Engineering AB," *Free Valve Technology*". Available at
    http://www.cargine.com/tech2.html, (April 3, 2008)

5. S. Trajkovic, A. Milosavljevic, P. Tunestål, B. Johansson, "*FPGA Controlled Pneumatic Variable Valve Actuation*", SAE Paper 2006-01-0041, 2006

6. M. Schechter, "*Regenerative Compression Braking – A low Cost Alternative to Electric Hybrids*", SAE Paper 2000-01-1025, 2000

7. M. Schechter, "*New Cycles for Automobile Engines*", SAE paper 1999-01-0623, 1999

8. P. Higelin, A. Charlet, Y. Chamaillard, "*Thermodynamic Simulation of a Hybrid Pneumatic-Combustion Engine Concept International Journal of Applied Thermodynamics*", Vol 5, No. 1, pp 1 – 11, ISSN 1301 9724, 2002

9. S. Trajkovic, P. Tunestål, and B. Johansson, "*Introductory Study of Variable Valve Actuation for Pneumatic Hybridization*", SAE Paper 2007-01-0288, 2007

10. S. Trajkovic, P. Tunestål and B. Johansson, "*Investigation of Different Valve Geometries and Valve Timing Strategies and their Effect on Regenerative Efficiency for a Pneumatic Hybrid with Variable Valve Actuation*", SAE Paper 2008-01-1715, 2008

11. John B. Heywood, "*Internal Combustion Engine Fundamentals*", McGraw-Hill, Inc, 1988

12. New Scientist, "*Clean-burn engine dodges ever tighter regulations*", issue 2534, 14 January 2006

13. M. Christensen, P. Einewall and B. Johansson, "*Homongeneous Charge Compression Ignition (HCCI) using Iso-octane, Ethanol and Natural Gas – A Comparison with Spark Ignition*", SAE Technical Paper 972874, 1997

14. G. Haraldsson, P. Tunestål, B. Johansson and J. Hyvönen, "*HCCI Combustion Phasing with Closed-Loop Combustion Control using Variable Compression Ratio in an Multi Cylinder Engine*", SAE Technical Paper 2003-01-1830, 2003

15. J. Olsson, P. Tunestål, G. Haraldsson and B. Johansson, "*A Turbocharged Dual Fuel HCCI Engine*", SAE Technical Paper 2001-01-1896, 2001

16. H. Persson, *Spark Assisted Compression Ignition (SACI) – Trapped Residuals and Optical Experiments*", Thesis for the degree of Licenciate in Engineering, ISRN LUTMDN/TMHP-06/7041-SE, Lund Institute of Technology, Lund, Sweden, 2006

17. P. Najt and D. Foster, "*Compression-Ignited Homogeneous Charge Combustion*", SAE Technical Paper 830264, 1983

18. Y. Wang, "*Introduction to Engine Valvetrains*", SAE international, Warrendale, PA, 2007

19. Wikipedia, "*Zylinderkopf*", Available at http://de.wikipedia.org/wiki/Zylinderkopf, (April 13, 2008)

20. Scania, "Valve gear actuation". Available at http://www.scania.co.uk/Trucks/technology/scania_modular_combustion_concept/gear_actuation.asp, (April 13, 2008)

21. G. Garcea, "*Timing variator for the timing system of a reciprocating internal combustion engine*", US Patent 4231330, November 1980

22. B. Johansson, *"Förbränningsmotorer del 2"*, 2004

23. H. Heisler, *"Advanced Engine Technology"*, SAE International, Warrendale, PA, 1995

24. M. Grohn, "*The New Camshaft Adjustment System by Mercedes-Benz -- Design and Application in 4-Valve Engines*", SAE Technical Paper 901727, 1990

25. Y. Moriya, A. Watanabe, H. Uda, H. Kawamura and M. Yoshioka, "*A Newly Developed Intelligent Variable Valve Timing System – Continuously Controlled Cam Phasing as Applied to a New 3 Liter Inline 6 Engine*", SAE Technical Paper 960579, 1996

26. K. Inoue, K. Nagahiro, Y. Ajiki and N. Kishi, "*A High Power, Wide Torque Range, Efficient Engine with a Newly Developed Variable-Valve-Lift and –Timing Mechanism*", SAE Technical Paper 890675, 1989

27. K. Hatano, K. Lida, H. Higashi, and S. Murata, "*Development of a New Multi-Mode Variable Valve Timing Engine*", SAE Technical Paper 930878, 1993

28. C. Brüstle and D. Schwarzenthal, "*The "Two-in-One" Engine – Porsche's Variable Valve System (VVS)*", SAE Technical Paper 980766, 1998

29. C. Brüstle and D. Schwarzenthal, "*VarioCam Plus – A Highlight of the Porsche 911 Turbo Engine*", SAE Technical Paper 2001-01-0245, 2001

30. S. Birch, "*Porsche developments*", Automotive Engineering International, July 2000

31. T. Shikida, Y. Nakamura, T. Nakakubo and H. Kawase, "*Development of the High Speed 2ZZ-GE Engine*", SAE Technical Paper 2000-01-0671

32. R. Flierl and M. Klüting, "*The Third Generation of Valvetrains – New Fully Variable Valvetrains for Throttle-Free Load Control*", SAE Technical Paper 2000-01-1227, 2000

33. J. Edgar, "*BMW's Valvetronic! The first petrol engine without a throttle butterfly?*", Autospeed, issue 144, August 2001. Available at http://www.autospeed.com/cms/A_1083/article.html, (May 19, 2008)

34. A. Titolo, "*The Variable Valve Timing System – Application on a V8 Engine*", SAE Technical Paper 910009, 1991

35. M. Theobald, B. Lequesne and R. Henry, "*Control of Engine Load via Electromagnetic Valve Actuators*", SAE Technical Paper 940816, 1994

36. B. Lequesne, "*Bistable electromechanical valve actuator*", US Patent 4779582, October 1988

37. D. Cope, A. Wright, C. Corcoran, K. Pasch and D. Fischer, "Fully Flexible Electromagnetic Valve Actuator: Design, Modeling and Measurement", SAE Technical Paper 2008-01-1350, 2008

38. L. Mianzo, B. Collins, I. Haskara and V. Kokotovic, "*Electromagnetic valve actuator with soft-seating*", US Patent 6817592, November 2004

39. M. Schechter and M. Levin, "*Camless Engine*", SAE Technical Paper 960581, 1996

40. J. Allen and D. Law, "*Production Elector-Hydraulic Variable Valve-Train for a New Generation of I.C. Engines*", SAE Technical Paper 2002-01-1109, 2002

41. J. Allen and Don law, "*Advanced Combustion Using a Lotus Active Valve Train. Internal Exhaust Gas Recirculation Promoted Auto Ignition*", IFP International Congress, 2001

42. N. Milovanovic, J. Turner, S Kenchington, G. Pitcher and D. Blundell, "*Active valvetrain for homogeneous charge compression ignition*", International Journal of Engine Research, Volume 6, Number 4, July 2005

43. J. Turner, S Kenchington and D. Stretch, "*Production AVT development: Lotus and Eaton's Electrohydarulic Closed-Loop Fully Variable Valve Train System*", 25th International Vienna Motor Symposium, 2004

44. J. Ma, H. Schock, U. Carlson, A. Höglund and M. Hedman, "*Analysis and Modeling of an Electronically Controlled Pneumatic Hydraulic Valve for an Automotive Engine*", SAE Technical Paper 2006-01-0042, 2006

45. J. Ma, T. Stuecken, H. Chock, G. Zhu and J. Winkelman, "*Model Reference Adaptive Control of a Pneumatic Valve Actuator for Infinitely Variable Valve Timing and Lift*", SAE Technical Paper 2007-01-1297, 2007

46. D.E. Johnson and D.S Johnson, "*Engine with pneumatic valve actuation*", US Patent 4702147, October 1987

47. W. Richeson and F. Erickson, "*Pneumatic actuator with permanent magnet control valve latching*", US Patent 4852528, August 1989

48. L. Gould, W. Richeson and F. Erickson, "*Performance Evaluation of a Camless Engine Using Valve Actuators with Programmable Timing*", SAE Technical Paper 910450, 1991

49. J. Watson and R. Wakeman, "*Simulation of a Pneumatic Valve Actuation System for Internal Combustion Engine*", SAE Technical Paper 2005-01-0771, 2005

50. J. Willand, R. Nieberding, G. Vent and C. Enderle, "*The Knocking Syndrome – Its Cures and Its Potential*", SAE Technical Paper 982483, 1998

51. G. Kontarakis, N. Collings and T. Ma, "*Demonstration of HCCI Using a Single Cylinder Four-stroke SI Engine with Modified Valve Timing*", SAE Technical Paper 2000-01-2870, 2000

52. O. Lang, W. Salber, J. Hahn, S. Pischinger, K. Hortmann and C. Brüker, "*Thermodynamical and Mechanical Approach Towards a Variable Valve Train for the Controlled Auto Ignition Combustion Process*", SAE Technical Paper 2005-01-0762, 2005

53. N. Kaahaaina, A. Simon, P. Caton and C. Edwards, "*Use of Dynamic Valving to Achieve Residual-Affected Combustion*", SAE Technical Paper 2001-01-0549, 2001

54. D. Law, D. Kemp, J. Allen, G. Kirkpatrick and T. Copland, "*Controlled Combustion in a IC-Engine with a Fully Variable Valve Train*", SAE Technical Paper 2001-01-0251, 2001

55. L. Cummins, "Internal Fire", Carnot Press, 2000

56. R. Miller, "*High-pressure supercharging system*", US Patent 2670595, March 1954

57. D. Luria, Y. Taitel and A. Stotter, "*The Otto-Atkinson Engine – A new Concept in Automotive Economy*", SAE Technical Paper 820352, 1982

58. Toyota, "*The heart and soul of hybrid synergy drive*". Available at http://www.toyota.com/html/hybridsynergyview/2004/october/heartandsoul.html, (May 3, 2008)

59. Fueleconomy.gov, "Advanced Technologies & Energy Efficiency". Available at www.fueleconomy.gov/feg/atv.shtml, (May 3, 2008)

60. Toyota, "*Hybrid Vehicle: The UN Definiton*"- Available at http://www.hybridsynergydrive.com/en/un_definition.html, (May 4, 2008)

61. The Sydney Morning Herald, "*Japan to launch first hybrid trains*". Available at http://www.smh.com.au/news/World/Japan-to-launch-first-hybrid-trains/2007/07/29/1185647720628.html, (May 4, 2008)

62. M. Samulski and C. Jackson, "*Effects of Steady-State and Transient Operation on Exhaust Emissions from Nonroad and Highway Diesel Engines*", SAE Technical Paper 982044, 1998

63. Toyota, "*Toyota Prius – 2008 Perfromance and Specifications*". Available at http://www.toyota.com/prius-hybrid/specs.html, (May 4, 2008)

64. Green Car Congress, "*Cumulative Reported US Sales of Hybrids Edge Past the One Million Mark in 2007*". Available at http://www.greencarcongress.com/2008/01/cumulative-repo.html, (May 5, 2008)

65. J. Ottoson, "Energy Management and Control of Electrical Drives in Hybrid Electrical Vehicles", Licenciate thesis, Department of Industrial Electrical Engineering and Automation, Lund University, Lund, 2006.

66. P. Bossche, "*The electric vehicle: raising the standards", PhD Thesis, Vrije Universiteit Brussel*, Belgium, 2003

67. M. Ehsani, Y. Gao, S. Gay and A. Emadi, "*Modern Electric, Hybrid Electric, and Fuel Cell Vehicles: Fundamentals, Theory, and Design*", CRC Press, 2004

68. J. K. Broderick, "*Combined internal combustion and compressed air engine*", US Patent 1013528, Jan 1912

69. W. Ochel, O. Beyermann and F. Gehrmann, "Multicylinder 4-stroke cycle diesel engine and compressor", US Patent 2676752, April 1954

70. R. Brown, "Compressed air engine", US Patent 3765180, October 1973

71. T. Ueno, "Convertible engine-air compressor apparatus for driving a vehicle", US Patent 3963379, June 1976

Appendix A – Drawing of the steel plate used for the mounting of the valve actuators
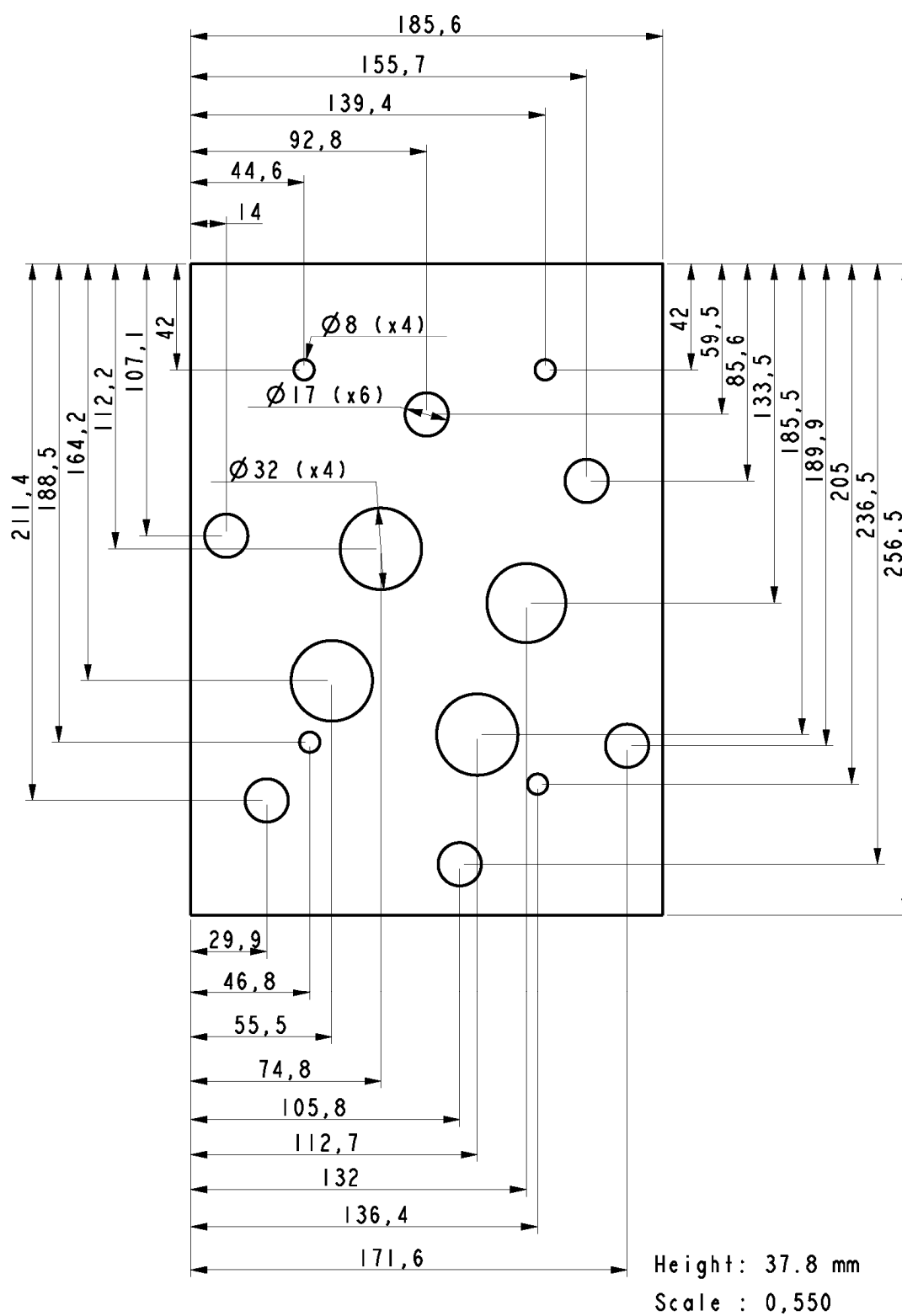
Height: 37.8 mm
Scale : 0,550

FPGA Controlled Pneumatic Variable Valve Actuation

Sasa Trajkovic, Alexandar Milosavljevic, Per Tunestål and Bengt Johansson

Division of Combustion Engines, Lund Institute of Technology

The Engineering Meetings Board has approved this paper for publication. It has successfully completed SAE's peer review process under the supervision of the session organizer. This process requires a minimum of three (3) reviews by industry experts.

For permission and licensing requests contact:

SAE Permissions
400 Commonwealth Drive
Warrendale, PA 15096-0001-USA
Email: permissions@sae.org
Tel: 724-772-4028
Fax: 724-776-3036

SAE®
Global Mobility Database®
All SAE papers, standards, and selected books are abstracted and indexed in the Global Mobility Database.

For multiple print copies contact:

SAE Customer Service
Tel: 877-606-7323 (inside USA and Canada)
Tel: 724-776-4970 (outside USA)
Fax: 724-776-0790
Email: CustomerService@sae.org

Positions and opinions advanced in this paper are those of the author(s) and not necessarily those of SAE. The author is solely responsible for the content of the paper. A process is available by which discussions will be printed with the paper if it is published in SAE Transactions.

Persons wishing to submit papers to be considered for presentation or publication by SAE should send the manuscript or a 300 word abstract to Secretary, Engineering Meetings Board, SAE.

Printed in USA

FPGA Controlled Pneumatic Variable Valve Actuation

Sasa Trajkovic, Alexandar Milosavljevic, Per Tunestål and Bengt Johansson
Division of Combustion Engines, Lund Institute of Technology

ABSTRACT

A control system for pneumatic variable valve actuation has been designed, implemented and tested in a single cylinder test engine with valve actuators provided by Cargine Engineering AB. The design goal for the valve control system was to achieve valve lifts between 2 and 12 mm over an engine speed interval of 300 to 2500 rpm. The control system was developed using LabView and implemented on the PCI 7831. The design goals were fulfilled with some limitations. Due to physical limitations in the actuators, stable operation with valve lifts below 2.6 mm were not possible. During the engine testing the valve lift was limited to 7 mm to guarantee piston clearance. Different valve strategies for residual gas HCCI combustion were generated on a single-cylinder test engine.

INTRODUCTION

Valve lift, timing and duration have generally fixed values for conventional valvetrains. These fixed values are usually optimized for the engine speed range most frequently used. They depend on what purpose the engine is made for and represent a compromise between stabile idle running and high engine speed performance. The ideal solution is to fully control when and how the valves should open and close. With such degrees of freedom one would be able to optimize the gas exchange for all operating conditions.

One way to achieve variable valve control, VVC, is through the use of pressurized air. A Swedish company, Cargine Engineering AB, has developed a pneumatic valve actuation system that offers fully variable valve control (see Appendix for physical dimensions). Pneumatic valve actuation could be easily implemented on heavy-duty vehicles since they have an existing system for pressurized air. On passenger cars it would require the addition of a compressor

This paper describes a control system, developed at Lund Institute of Technology, for the abovementioned VVC system. Test results are presented from a test rig consisting of the VVC system installed in a cylinder head with valves but also from actual engine operation with the VVC system. The objective is to offer a valve lift from 2 to 12 mm and a duration between 0 and 360 Crank Angle Degrees (CAD) over a range of engine speeds between 300 and 2500 rpm. A cylinder head from a Scania 12 liter engine with four valves was used for the test rig. The valves have to be controlled independently from each other with the possibility to deactivate them if desired.

After the evaluation of the program the whole system was implemented on a single-cylinder test engine for further testing. The engine testing consists of HCCI (Homogeneous Charge Compression Ignition) operation with three different valve strategies – Negative Valve overlap, Late/Early IVC and Rebreathe. The valve lift height will be limited to 7 mm to guarantee clearance from the moving piston.

PNEUMATIC VARIABLE VALVE ACTUATION

The system developed and delivered by Cargine Engineering AB consists of an actuator, two solenoids[1], an actuator piston and logical channels inside the housing. The actuator itself has to be seen as a "black box" due to company secrecy, but the concept will be described for better understanding.
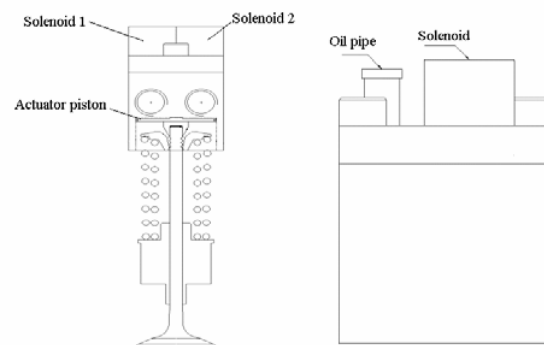

Figure 1 Sketch of the pneumatic valve actuator [2].

The right circle in Figure 1 is an intake port. Here the pressurized air should be connected. The left circle is the hole for outgoing air, which is released into

_____
[1] The solenoids are Bicron SP1913P2410

theatmosphere. When Solenoid 1 is activated pressurized air can enter the actuator, Solenoid 2 stops the filling. Each actuator requires one or two electrical signals, depending on if one or two solenoids are used. This means that it is possible to operate the actuator with only Solenoid 1 activated and then the lift is only dependent on the pressure supplied. By the use of both solenoids instead of one, it is possible to vary the lift at a given pressure. In this investigation a pressure of 2.5 bar has been used all the time, since this is sufficient for the entire valve lift interval from 2 to 12 mm.

The actuator is equipped with a hydraulic brake, whose function is to slow down the valve before seating. At the top of the valve, there is a valve stem cap. Its function is to make it possible to adjust the spacing between the actuator piston and the actuator itself. The adjustment is made with shims, which are simply very thin plates with various thicknesses. These are put between the top of the valve and the valve stem cap as shown in Figure 2.
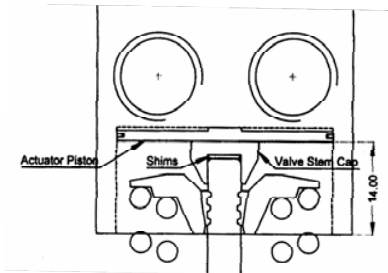

Figure 2 A close up of the pneumatic valve actuator [2].

If the clearance is too large, the hydraulic brake will not be able to slow down the valve enough, which leads to loud noise as the valve hits the seat. With insufficient clearance the pressurized air will not have full access to the actuator piston and the force will be insufficient to lift the valve.
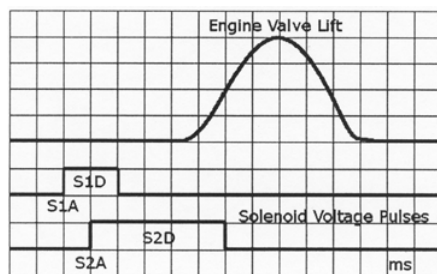

Figure 3 Schematic picture of solenoid voltage pulses and engine valve lift [2].

Figure 3 shows a schematically how the solenoid activation relates to the valve lift event..

Step 1 – Activation of Solenoid 1 (S1A) will open the inlet valve to the actuator[2] and thereby determine the starting point of the engine valve opening. The length of the activation time (S1D) determines the valve opening duration. Another function of Solenoid 1 is that when activated it turns on a hydraulic locking-mechanism that holds the valve at the desired lift where it dwells until the solenoid is deactivated.

Step 2 – Activation of Solenoid 2 (S2A) will close the inlet valve to the actuator. Hence the time difference between the two signals (S2A-S1A) will determine the engine valve lift height. S2D will affect neither the lift nor duration. However if S2D is chosen to end before S1D, this will result in another filling, which then leads to an incomplete closure of the valve. To avoid this, it is recommended to choose S2D to be as long as S1D.

Step 3 – The hydraulic brake will begin to slow down the valve about 3.0 mm from the end position during valve closing. In the interval 1.0 to 0.0 mm there is a ramp function, which means that the seating velocity is constant in that interval. The magnitude of this constant velocity is approximately 0.5 m/s according to the manufacturers. However this may change with different valve springs due to the precompression of the valve spring.

Figure 4 shows the actuators mounted on the test rig. Also the solenoids and the related hoses can be seen. Figure 5 shows the single cylinder test engine.
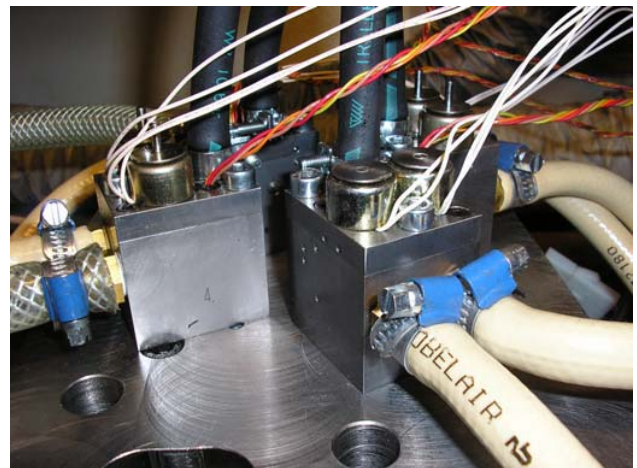

Figure 4 Valve test rig consisting of the actuators attached to a plate on the Scania D12 cylinder head.

---

[2] There is an inlet valve inside the actuator. This should not be mistaken for the engine inlet valve.

Figure 5 The Scania D12 single-cylinder test engine used in the study.

THE PROGRAM FOR VARIABLE VALVE CONTROL

INTRODUCTION

The valve control system has been developed in LabVIEW together with an FPGA device, both developed by National Instruments.

FPGA – Field Programmable Gate Array

A FPGA is a chip that consists of many unconfigured logic gates. It is possible to configure and reconfigure the FPGA for each application, unlike other chips with fixed functionality. This is a big advantage, since designing and manufacturing a new chip every time the application changes may be very costly.

The FPGA offers benefits such as precise timing, rapid decision making with loop rates up to 40 MHz and simultaneous execution of parallel tasks. FPGAs appear for example in devices such as consumer electronics, automobiles, aircraft and copy machines [3].

In this project a NI PCI-7831R (see Figure 6) device has been used. This device has 8 analog inputs, 8 analog outputs and 96 digital I/O [4].
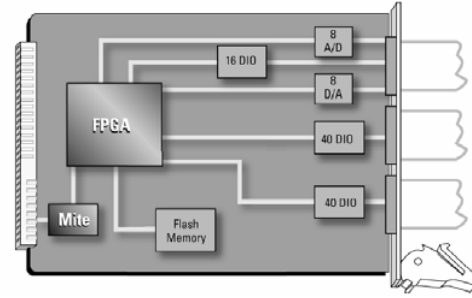

Figure 6 A schematic drawing of a NI PCI-7831R device [3].

THE PROGRAM

LabVIEW is an entirely graphical programming language. Instead of conventional programming, the user programs the algorithms with pre-programmed blocks. Any complete functional program made in LabVIEW is called a virtual instrument and is almost always referred to as a VI.

A LabVIEW VI consists of two "faces". These are the front panel and the block diagram. The front panel is the face that the user of the system works with when executing his program. Here the user can change input data, read output data and monitor graphs. The block diagram is almost the backside of the front panel and can be compared with for example the inside of an oscilloscope.

When combining FPGA with LabVIEW there is a certain development flow that should be followed, see Figure 7. Therefore the main program consists of two modules, one that will be compiled to the FPGA and one that will control the FPGA program and is called the Host VI. The FPGA should only be used for the parts that require fast operations.
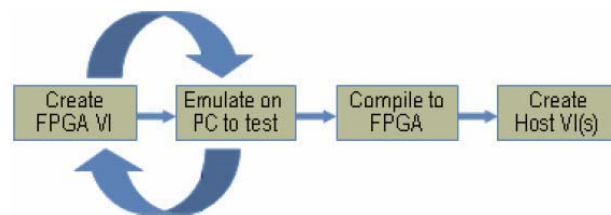

Figure 7 Application development flow [3].

The programs for each valve are quite similar with only minor differences and therefore the focus will be on describing the program for one inlet valve.

Host VI – Front panel

At the front panel the user has the possibility to choose engine speed, valve opening time, duration and valve lift, as seen in Figure 8. This can be done at any time, even while executing the program. There are some limitations in the program due to physical and programming constraints, and therefore there are indicators that for example indicate the smallest possible duration etc. Their task is to make the user aware of the limitations in the program and thus prevent the user from choosing unsuitable values.
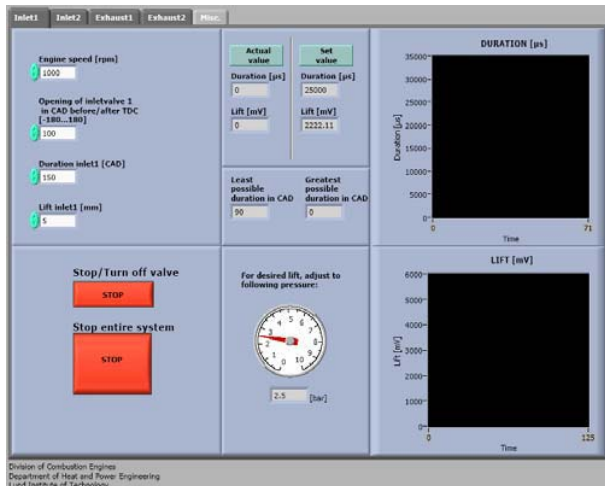

Figure 8 Front panel.

The upper part in the middle of the front panel contains four indicators that show the actual and the set values for duration and valve lift. Below them are two additional indicators. They indicate smallest and greatest possible duration. It is very important to stay in the interval suggested by the indicators, otherwise the system may not function as expected. The front panel is also equipped with a pressure gauge. It shows the pressure needed for the chosen valve lift. The right part of the front panel consists of two graph windows. They offer the user a possibility to monitor the cycle to cycle variation of the duration and valve lift as well as step responses when changes are made. At the top of the front panel there are 5 tabs, one for each valve and one miscellaneous tab where the user can change the integral constants and monitor the solenoid 1 activation duration, S1D, and the solenoid activation time difference, S2A-S1A. This tab should only be used by an advanced user that fully understands the system.

Host VI – Block diagram

As mentioned before the block diagram is the part of the VI where all the programming is done.

Figure 9 shows the block diagram of the host VI and will be described briefly below

Nbr 1 - Because the Host VI has to be connected to the FPGA VI, the following four functions are necessary. From the left there is a function that opens a specified FPGA VI, which means that it is activated for use in the Host VI. The following function invokes the FPGA VI and runs it. To be able to change input values to the FPGA VI, there is a need for another function called *Read/Write Control.* This control gives access to all controls and indicators on the FPGA VI. The left side is used for changing the controls while the right side is used for reading the indicators on the FPGA VI.

The FPGA works independently from the computer to avoid any possible disturbance. This means that even if the Windows operating system crashes, the FPGA will still run as long as it has power. Therefore there is a need for a final function that will stop the FPGA VI from running when wanted.
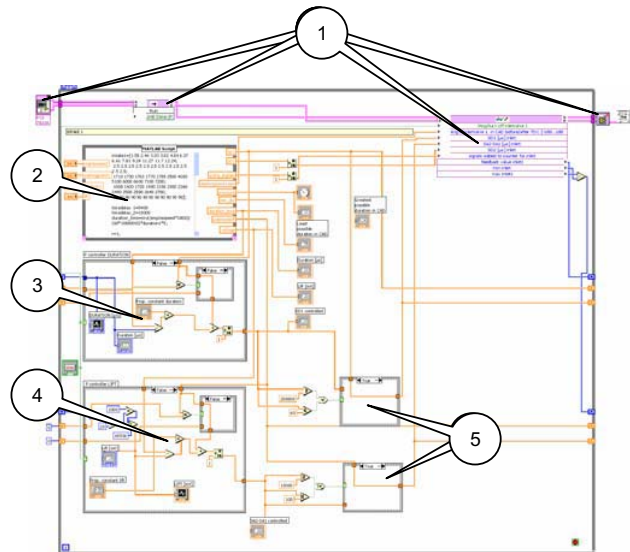

Figure 9 Block diagram for inlet valve 1¨

Nbr 2 - This section is called a *Matlab script* and as the name implies, it is used for connecting the Host VI to Matlab. Using Matlab in LabVIEW will simplify some calculations such as linear interpolation which has been used here.

The user sets the input values in the front panel, which are then processed in the Matlab script and calculated values are then passed on to other sections in the Host VI.

Nbr 3 - The Integral controller is a very important part of the system. It makes sure the actual valve lift duration is heading towards the set value. Without this, one can not be sure that the actual duration will be as desired. The following formula describes the integral controller.

$$U = \sum_{cycles} K(S - A)$$

where U = control signal

               K = integral constant

               S = set value

               A = actual value

The proportionality constant, K, is not a pre-defined parameter, which means that the user can use a value that best suits the application in question. An increasing K will give a faster controller to a certain point. Beyond this point it will make the system unstable. The controller in Section 3 regulates the duration. It adds U to S1D and thus introduces feedback. As long as there is a remaining error, U will keep growing in the direction opposing the error.

Nbr 4 - The lift also needs to be regulated. This is done by another integral controller that works in the same way as the previous one. The only difference is that U will instead be added to S2A-S1A.

Nbr 5 - The purpose of this section is to avoid absurd controller values. Such values can occur if for instance, the pressure is too low and insufficient for the desired lift or duration. Then U keeps growing out of bounds which is called integrator wind-up. Therefore there are intervals that only allow reasonable values.

FPGA VI – Block diagram

Nbr 6 - This part of the program begins with a so-called sequence. It looks like the frames of an old-fashioned film. The sequence function is used when the programmer wants to be sure that the algorithm runs in the right order.

The first frame in the sequence consists of a TDC detector. When TDC is detected, the program continues at the next frame.

Nbr 7 - This control makes it possible to turn off and on the valve during operation.
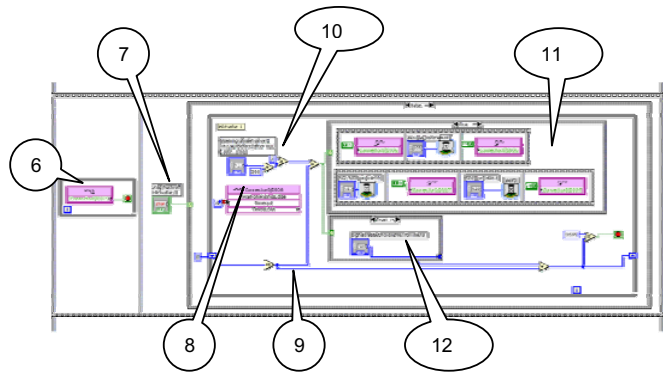

Figure 10 Controlling the solenoids.

Nbr 8 - An engine is assumed to be equipped with a crank pulse generator that provides 3600 pulses per cycle. To be able to open the valve at a desired crank angle the program needs a counter to count the pulses. LabVIEW has a function that makes the program wait until a rising edge of a digital signal is detected.

Nbr 9 - Every rising edge will be added to a counter. The sequence ends when the counter reaches 3595 pulses[3].

Nbr 10 - When the user sets the value for desired opening angle of the valve, the value is converted from CAD to a number of pulses. When the counter reaches the same value as the one that the user has set, the program will continue to Section 11.

Nbr 11 - Each solenoid is connected to a digital output. The first thing that will happen in Section 11 is that Solenoid 1 will be activated for a certain time. As mentioned before, this time will determine the duration of the valve actuation. While Solenoid 1 is activated, a wait function will delay the activation of Solenoid 2. This delay has also been mentioned before and it determines the valve lift.

Nbr 12 - While Section 11 is executing, the counter will stop counting. This means that when Section 11 ends and the counter continues counting the pulses, it will not take count of all the pulses that actually have been generated during this period of time. To avoid miscalculation of pulses, an extra algorithm has been made. It calculates the duration of Section 11, and with the help of the actual engine speed it converts this into pulses and in turn adds them to the counter.

EVALUATION OF THE PROGRAM

The purpose with this section is to show some typical curves obtained from an oscilloscope while executing

---

[3] The reason for using 3595 instead of 3600 pulses is to have a safety margin of 1 CAD which equals 5 pulses. This will avoid missing the TDC due to any lag of the program.

the program. The testing is performed on the test rig consisting of a Scania D12 cylinder head with the pneumatic valve actuators installed instead of the normal pushrods and rocker arms. Valve lift information is provided by lift sensors in the actuators. The sensors are optical and measure the amount of reflected light which decreases with valve lift. The voltage output from the sensor is highly nonlinear and has been linearized and calibrated to provide the correct lift in millmeters. The figures below show the behavior of one of the inlet valves during operation. The remaining valves show a similar pattern. Figure 11, Figure 12 and Figure 15 were obtained at an equivalent engine speed of 1000 rpm.
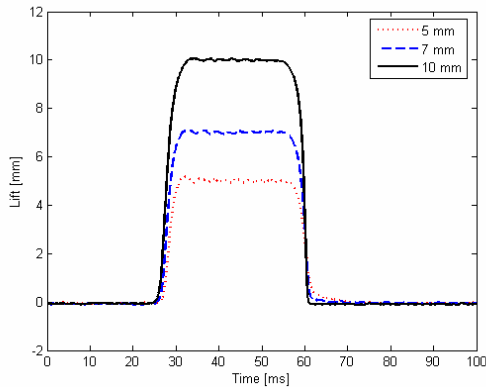

Figure 11 Three different valve lifts at a constant opening duration of 200 CAD.
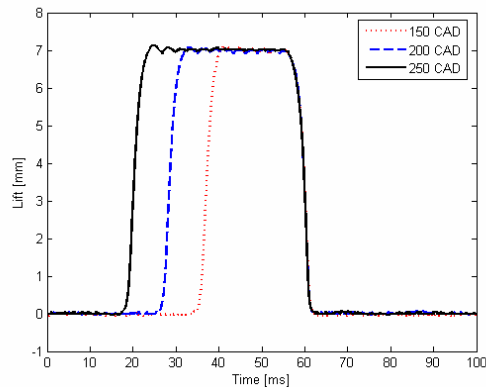

Figure 12 Three different opening durations at a constant valve lift of 7 mm.

Figure 11 shows that the duration remains constant when the valve lift is varied. At the valve closure, there is a slight difference between the valve lifts. This difference occurs because of the hydraulic brake. It seems like the braking is somewhat too effective at low valve lifts and the valve closure gets extended compared to at higher valve lift. The reason is that a higher valve lift has a higher returning velocity. Figure 12 shows how the lift remains unchanged for different opening durations.
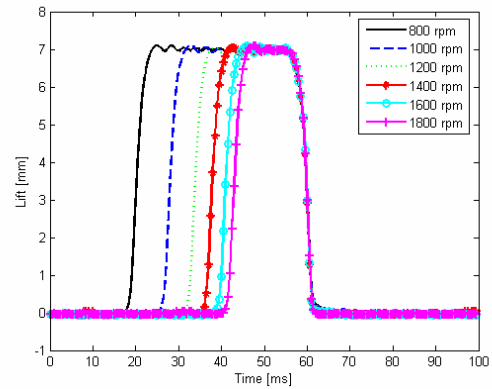

Figure 13 Six different engine speeds at a constant valve lift of 7 mm and a constant opening duration of 200 CAD.

Figure 13 shows how the valve lift is unaffected by the change of engine speed. The duration also remains unchanged, but this can't be seen in the figure. The reason for this is that duration in time varies with different engine speeds while duration in CAD remains the same.

Figure 14 shows how the valve lift remains stable at an engine speed of 2500 rpm, which was the upper limit, stated in the design goals.
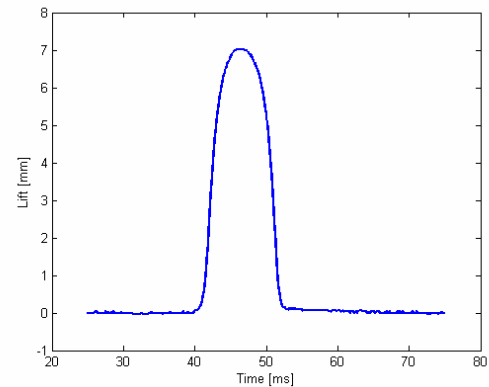

Figure 14 Valve lift of 7 mm at an opening duration of 200 CAD and an engine speed of 2500 rpm

The valve lift remains stable all the way down to 3 mm throughout the whole duration and engine speed interval. There exists a physical lower level limitation in valve lift, which is 2.6 mm. Below this value the system doesn't behave as expected and the lift tends to be very unstable. It is recommended to use 3 mm as a lower limit, thus providing a safety margin and avoiding any possible instability. Figure 15 shows a stable valve lift at the recommended minimum level.
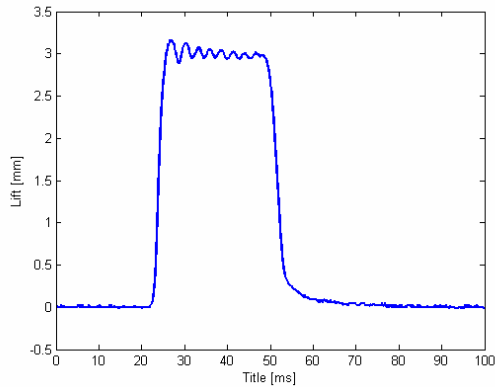
Figure 15 Valve lift of 3 mm at an engine speed of 1000 rpm and a valve opening duration of 200 CAD.

Figure 16, Figure 17, Figure 18 and Figure 19 show the step response when changing duration and valve lift. When changing the duration from a low to a high value, an immediate change is seen and then a last adjustment is made to reach the desired level. The opposite, i.e. changing from a high to a low value, also has an immediate effect on the duration. Now the value is set a little too low by the program, but the integral controller will adjust the error and eventually the desired level will be reached, as seen in Figure 16 and Figure 17. The same line of argument can be applied to Figure 18 and Figure 19, which show the step responses when changing valve lift.
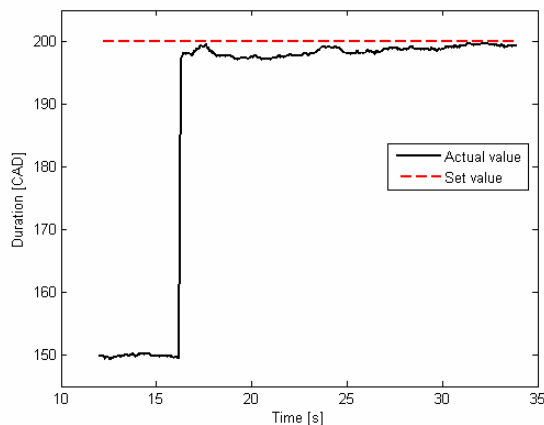

Figure 16 Step response when changing valve opening duration from 150 to 200 CAD.
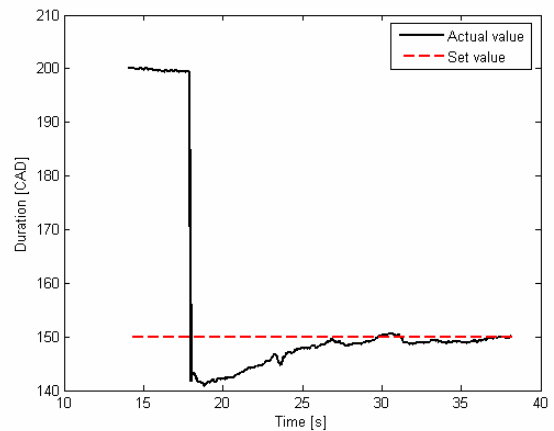

Figure 17 Step response when changing valve opening duration from 200 to 150 CAD.
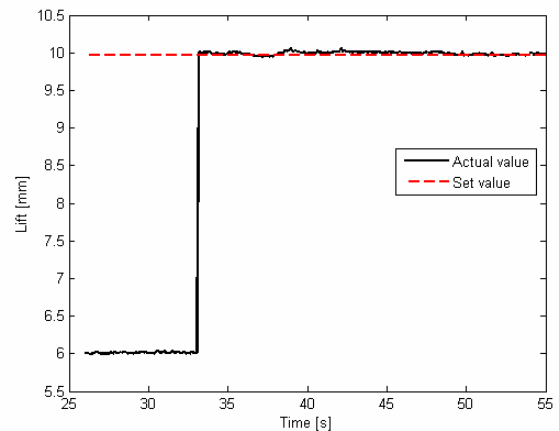

Figure 18 Step response when changing valve lift from 6 to 10 mm.
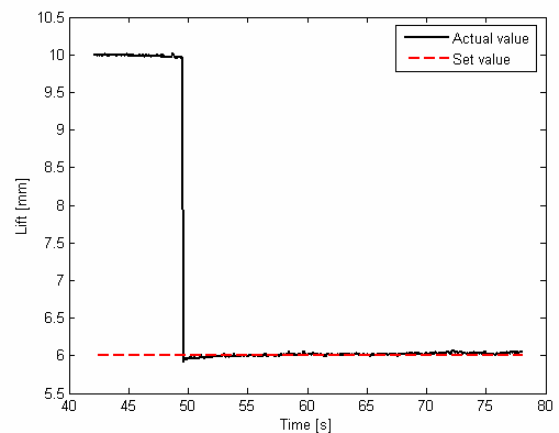

Figure 19 Step response when changing valve lift from 10 to 6 mm.

Figure 20 and Figure 21 show the cycle to cycle variation for duration and lift. It seems a little more dramatic than it actually is. The difference in percentage between the set value and the actual value is very small.
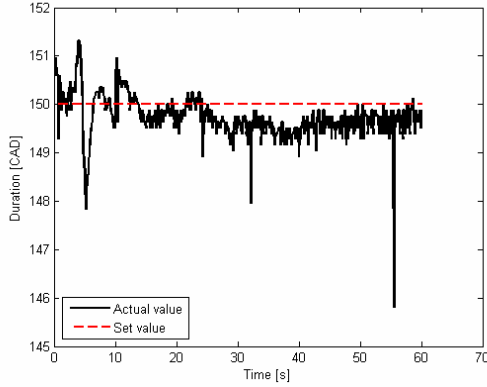

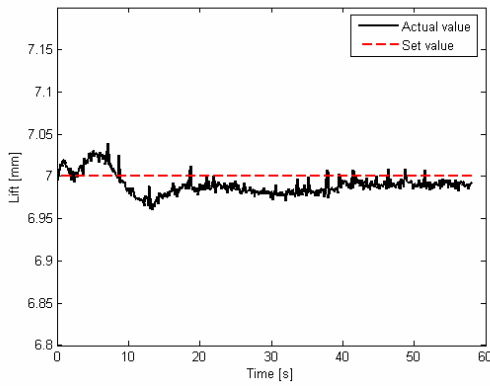**Figure 20 Cycle to cycle variations at a valve opening duration of 200 CAD.**

Figure 21 Cycle to cycle variation at a valve lift of 7 mm.

This study does not include any economic calculations, still it can be of great interest to investigate the consumption of pressurized air since this gives an indication how energy consuming the valve mechanism is. A simple rotameter was integrated into the system to measure the outgoing air flow from one actuator. The measurements were done at an ambient temperature of 20 degrees Celsius. It is assumed that the compressor uses 1 hp (736 W) to supply an air flow of 100 l_n/minute. This corresponds to a compressor efficiency of 40%. The power consumption of the compressor is subsequently used to compute a mean effective pressure, ValveMEP, which allows a comparison with the brake mean effective pressure produced by the engine.

$$ValveMEP = \frac{2P_{compressor}}{NV_d}$$

where N is the engine speed, V_d is the engine displacement volume and

$$P_{compressor} = \frac{Airflow}{100} * 736 \text{ W}$$

Figure 22 shows how the valve lift affects ValveMEP at a constant opening duration and engine speed. Figure 23 shows ValveMEP as a function of engine speed at constant opening duration and valve lift. Both measurements are compared with simulations done at the same conditions by Cargine Engineering AB.
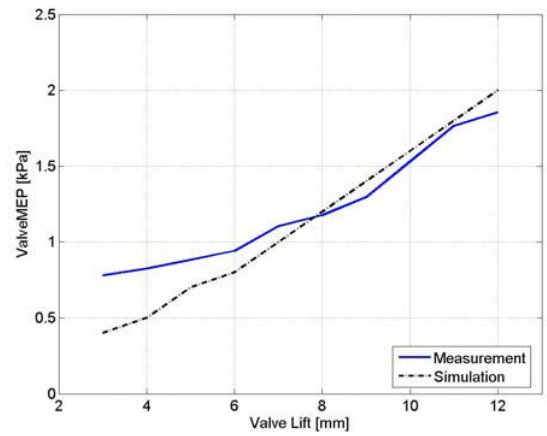
Figure 22 Valve mean effective pressure (single valve) as a function of valve lift at duration of 200 CAD and engine speed of 1000 rpm.

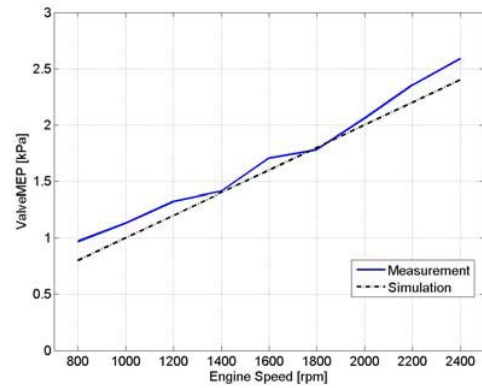**Figure 23 Valve mean effective pressure (single valve) as a function of engine speed at a duration of 200 CAD and a valve lift of 7 mm.**

ENGINE TESTING AND EVALUATION

The system has been implemented on a single-cylinder test engine to investigate if it is functioning as expected in a real application. The engine used is a Scania D12

engine where cylinders 1-5 have been deactivated and only cylinder 6 is operating. The operating parameters for the tests can be seen in Table 1

Table 1 Operating parameters

Actuator intake pressure	3 bar
Hydraulic brake pressure	4 bar
Valve spring constant	11.5 N/mm
Valve spring precompression	100 N
Maximum valve lift	7 mm
Compression ratio	18:01
Engine speed	1200 rpm
Fuel	Isooctane
Fuel energy per cycle	0.75 KJ
Displacement volume	1.96 l/cylinder

Each valve strategy began with valve timings according to Table 2.

Table 2 Initial valve timing

IVO	0 CAD ATDC
IVC	180 CAD ATDC
EVO	0 CAD ABDC
EVC	180 CAD ABDC

A new and promising combustion concept is HCCI (Homogeneous Charge Compression Ignition), which promises high efficiency, and low NO_x. Retained or rebreathed residual / exhaust gas can be used to increase the charge temperature and achieve HCCI combustion. Below, the variable valve system is used to enable these strategies. Only low loads have been tested in this study. The maximum load during the tests was 2.2 bar net indicated mean effective pressure (IMEPn) which corresponds to about 35% of the maximum achievable load with HCCI and naturally aspirated conditions. It is however only about 10% of the maximum load achievable with turbocharged Diesel operation.

NEGATIVE VALVE OVERLAP

With negative valve overlap, NVO, the amount of trapped residual gases can be changed and can be seen as "internal EGR". The basic idea with NVO is that the exhaust valve should close early and the intake valve should open late which leads to a higher fraction of residual gas. Figure 24 shows how the exhaust valve closing and the inlet valve opening vary with NVO. It can also be seen that with increasing NVO the pressure during the gas exchange increases. Observe that the right valve lift is the exhaust valve and the left valve lift is the intake valve.
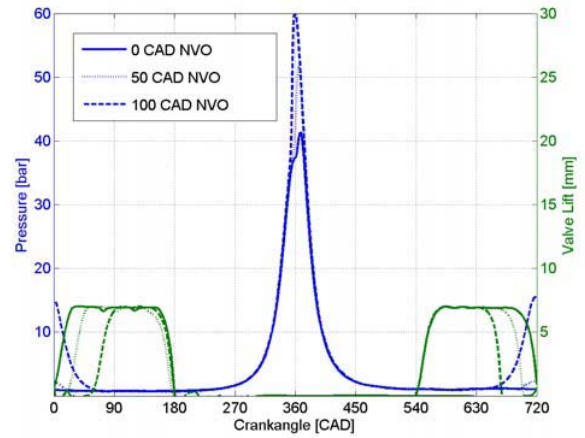

Figure 24 An illustration of how the NVO works.

As mentioned the amount of residual gas increases with increasing NVO. With more residual gas the in-cylinder temperature increases and therefore the combustion will start progressively earlier.

Figure 25 shows how CA50 varies with NVO. CA50 is the crank angle where 50% of the energy from combustion has been released. This parameter is very useful combustion timing indicator.
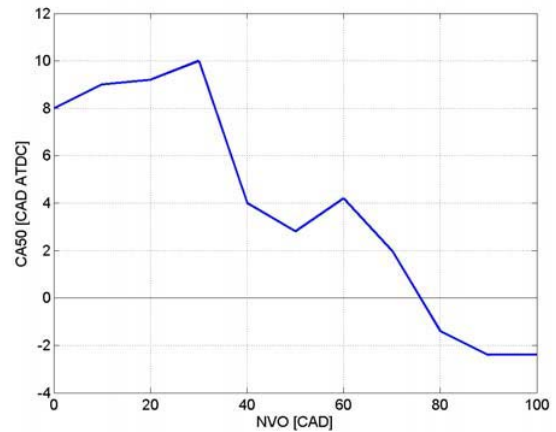
Figure 25 CA50 as a function of NVO

It can also be seen that there is an insufficient charge temperature for NVO less than 30 CAD and therefore the combustion is delayed. The explanation for this behavior is probably that the combustion is very poor. When NVO is increased beyond 30 CAD, the combustion improves and combustion timing advances with increasing NVO.

In Figure 26 it is clearly visible that the combustion efficiency is very bad between 0 and 40 CAD NVO. Both IMEPg (gross indicated mean effective pressure) and IMEPn (net indicated mean effective pressure) show low values in this interval.

Figure 26 IMEP and PMEP as a function of NVO

As the combustion improves, IMEPg and IMEPn increase and after 40 CAD of NVO they are almost constant at a value of about 2.4 bar and 2.1 bar respectively. The Pumping Mean Effective Pressure (PMEP) seems to be constant throughout the whole interval.
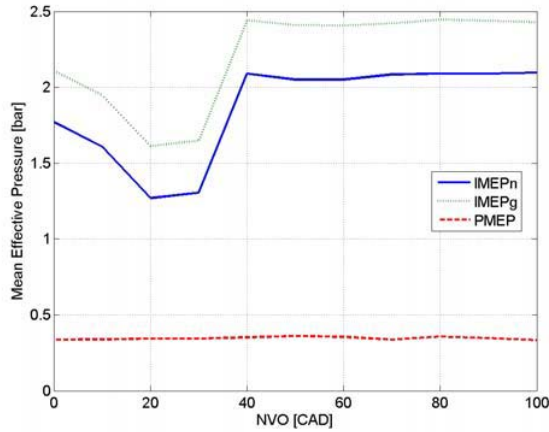
NVO displaces some of the air in the combustion chamber and thus the air/fuel ratio should decrease. Figure 27 shows exactly this behavior.
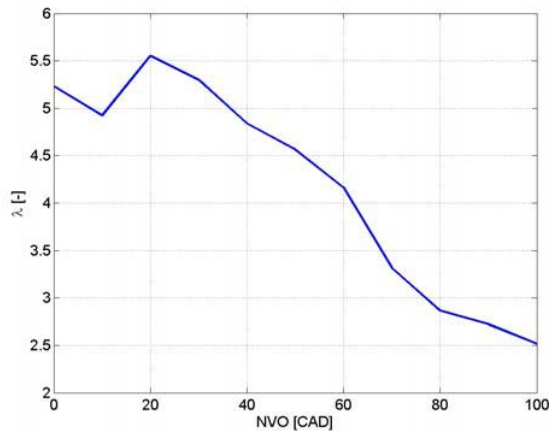
Figure 28 Total Hydrocarbon emission (THC) as a function of NVO

Better combustion due to higher temperature and lower air/fuel ratio leads to lower hydrocarbon emissions. Combustion of some of hydrocarbons in the retained burned gas also contributes.

NOx and NO are below measurable levels (<1 ppm) and therefore they are not considered in this paper. This also applies to the rest of the valve strategies.

REBREATHE STRATEGY

The idea with the rebreathe strategy is to open the exhaust valve a second time a short while after it has closed the first time which can be seen in Figure 29. It is very similar compared to NVO. The amount of rebreathed exhaust gas increases with increasing duration of the rebreathe opening and the difference is that with the rebreathe strategy the burned gas is not compressed during the gas exchange.

Figure 27 Lambda as a function of NVO

The poor combustion in the interval from 0 to 40 CAD NVO can once again be seen in Figure 28. The hydrocarbon levels in this interval are fairly high compared to when the combustion is more effective.
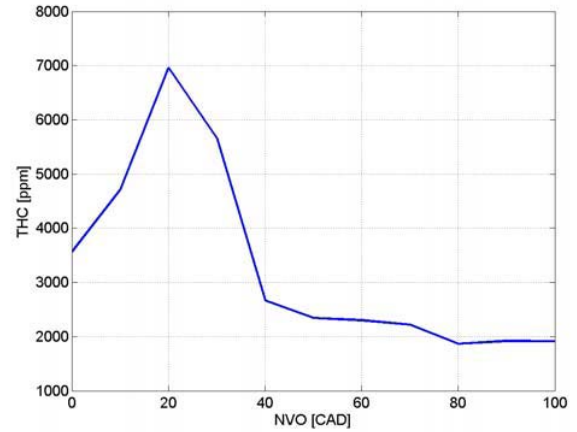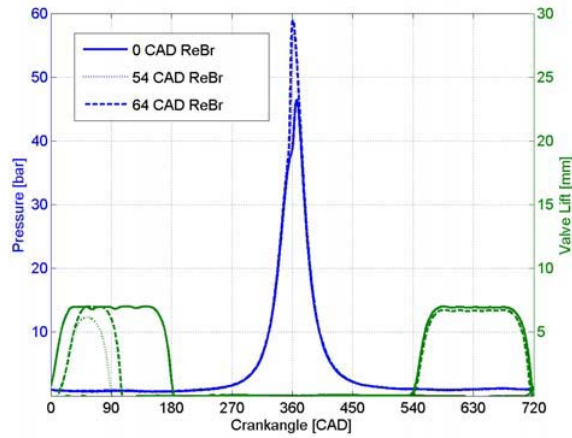
Figure 29 An illustration of how the rebreathe strategy works. The dashed and dotted valve profiles in the 0-90 CAD interval represent the rebreathe opening of the exhaust valves
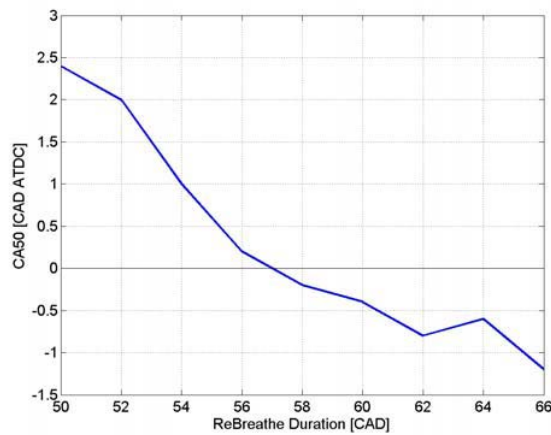
Figure 30 CA50 as a function of rebreathe duration

The behaviour of combustion timing in Figure 30 with respect to rebreathe duration is as expected. Both the decrease in air/fuel ratio and the increase in charge temperature contribute.
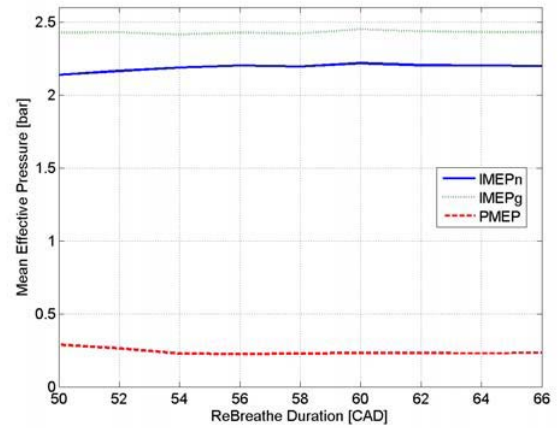
Figure 31 IMEP and PMEP as functions of the rebreathe duration

The IMEPg in Figure 31 shows that the combustion is good since it is essentially constant throughout the whole interval. It should also be noted that the pumping work is lower with rebreathe than with negative valve overlap since there is no recompression of burned gas.
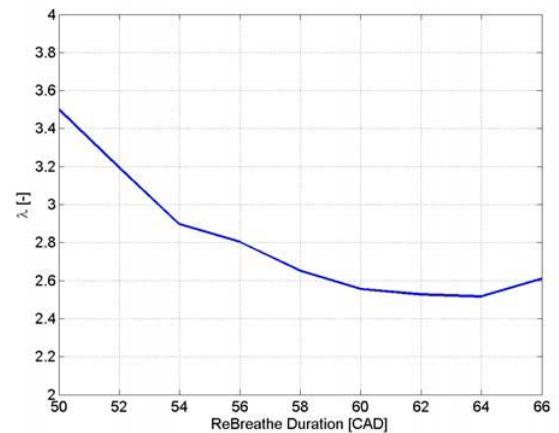
Figure 32 Lambda as a function of rebreathe duration

Rebreathing of exhaust displaces some of the air in the combustion chamber and thus the air/fuel ratio decreases which is clearly visible in Figure 32.
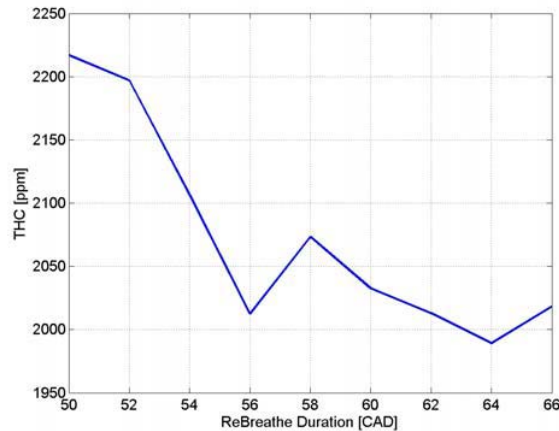
Figure 33 THC as a function of rebreathe duration

Figure 33 shows that the combustion is, as with NVO, better due to higher temperature and lower lambda which leads to lower hydrocarbon emissions. Also here, combustion of some of the rebreathed hydrocarbons contributes.

MILLER STRATEGY

With the Miller strategy the effective compression ratio can be varied by either closing the inlet valve early or late. The decrease of the compression ratio, and thus the compression work, leads to a decrease in charge temperature after compression. Figure 34 shows how the Miller strategy affects the in-cylinder pressure.
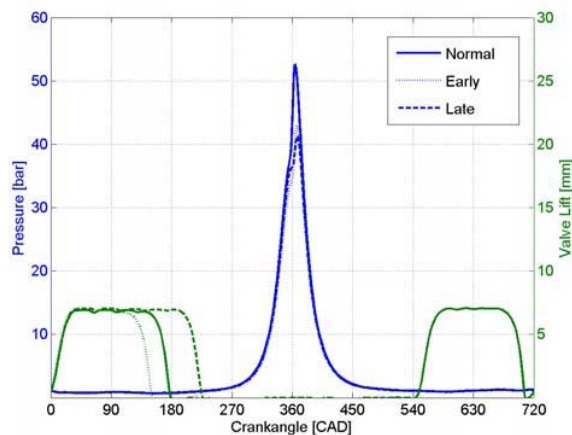

Figure 34 An illustration of how the Miller strategy works
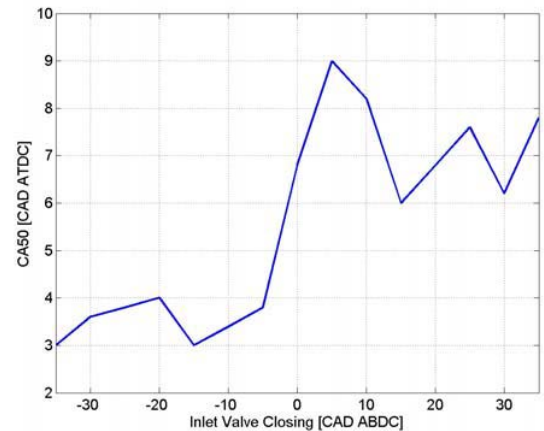
Figure 35 CA50 as a function of IVC angle

Late IVC gives higher volumetric efficiency due to tuning effects. This in combination with somewhat cooler charge causes poor combustion, which can be seen in Figure 35. With early IVC, combustion is satisfactory and there are two effects competing to decide the combustion timing. Decreased air/fuel ratio causes earlier combustion whereas decreased effective compression ratio causes later combustion. The result is that combustion timing stays relatively constant independent of IVC.
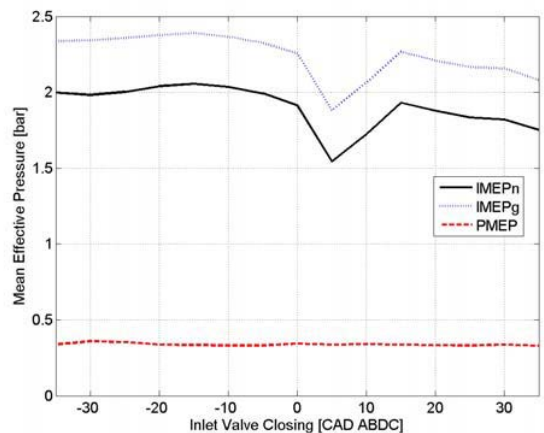
Figure 36 IMEP and PMEP as a function of IVC

On the right side of BDC in Figure 36 it is clearly visible that with inlet valve closing at 5 CAD ABDC the combustion is really poor and after that point is seems like the combustion improves a little but for IVC later than 15 CAD ABDC combustion deteriorates again.

With inlet valve closing at 5 CAD ABDC in Figure 37 the lambda value is much higher than in the rest of the interval. This can be explained by a higher volymetric efficiency in this point or that the poor combustion causes an increase in the lambda measurement.
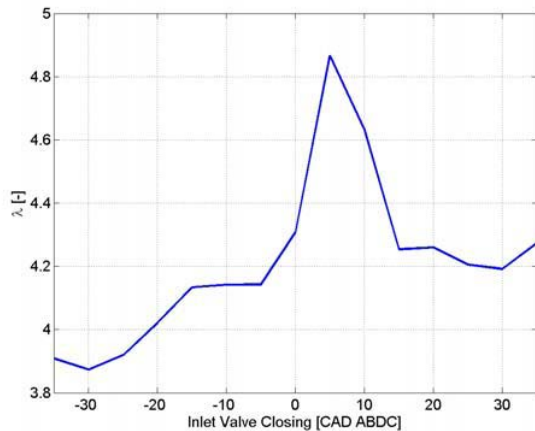
Figure 37 Lambda as a function of IVC

On both sides away from this point lambda decreases because less air is sucked into the cylinder.

Figure 38 shows high hydrocarbon levels with late intake valve closing and low levels with early closing which indicates better combustion with early valve closing than with late. There are two contributing reasons for this. One reason is that the charge temperature is lower with late closing since more intake air enters the combustion chamber and cools the charge. The other reason is that there is a certain tuning effect with late closing which increases the volumetric efficiency and thus the air/fuel ratio. This is one of the reasons why there is always a positive valve overlap on production engines.
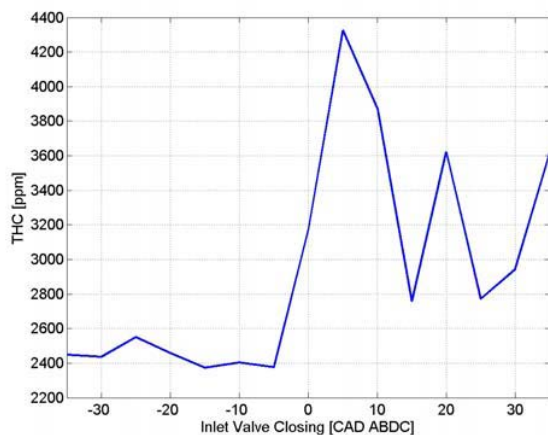
Figure 38 THC as a function of IVC

FUTURE WORK

The next logical step is to test the system for a range of engine speeds and loads combined with various valve strategies. The variable valve system can then also be used for closed-loop HCCI engine control.

CONCLUSIONS

The results achieved during this project clearly show the potential with pneumatic variable valve control. The actuators have proven to be well developed, with very little oil leakage and good reliability during long test runs. There are only remarks regarding time-consuming work such as air drainage and finding the right shims level.

The design goal to control the valves between 2 and 12 mm throughout an engine speed interval between 300 and 2500 rpm has been essentially fulfilled. The only exception is that valve lifts below 2.6 mm are unstable due to physical limitations of the actuators. In the engine tests the valve lift was limited to 7 mm in order to guarantee piston clearance.

Test runs with various valve strategies for HCCI combustion control on a single-cylinder test engine have shown that the system works as well in an engine as in the test rig. The engine tests were performed at a fairly low load level in order to prevent equipment damage in this early test stage. Negative valve overlap, rebreathe of exhaust and Miller cycle were all possible to achieve with the variable valve control system. It was seen that the NVO and rebreathe strategies had a large impact on the HCCI combustion timing.whereas the Miller strategy had less impact due to the competing effects of charge temperature and dilution.

REFERENCES

[1]   Gregory M. Shaver, J. Christian Gerdes, Parag Jain, P.A. Caton and C.F. Edwards, "Modeling for Control of HCCI Engines". Proceedings of the 2003 American Control Conference, Denver, CO, pp. 749-754.

[2]   Personal contact with Urban Carlson and Anders Höglund at Cargine Engineering AB

[3]   http://digital.ni.com/devzone%5Cconceptd.nsf/w ebmain/91F92C8E4585F16986256CFE005FE6B7 /$File/WP2329.pdf, 2004-11-25

[4]   http://www.ni.com/pdf/products/us/04_3632_301 _101.pdf, 2004-11-25

[5]   J. Willand, R.G. Nieberding, G. Vent, C. Enderle, "The knocking syndrome – its cure and its potential", SAE Technical Paper Series, SAE paper 982483, 1998

[6] A. Fuerhapter, W.F. Piock, G.K. Fraidl, "CSI - Controlled Auto Ignition – the best solution for the fuel consumption – versus emissions trade-off?", SAE Technical Paper Series, SAE paper 2003-01-0754, 2003

[7] P. Strandh, J. Bengtsson, R. Johansson, P. Tunestål, B. Johansson, "Variable Valve Actuation for Timing Control of a Homogeneous Charge Compression Ignition Engine", SAE Technical Paper Series, SAE paper 2005-01-0147, 2005

CONTACT

Sasa Trajkovic, MSc M. E.

E-mail: sit111@hotmail.com

DEFINITIONS, ACRONYMS, ABBREVIATIONS

A   Actual Value

ABDC   After Bottom Dead Center

ATDC   After Top Dead Center

BMEP   Brake Mean Efficiency Pressure

CA50   Crank Angle of 50% mass fraction burned

CAD   Crank Angle Degree

FPGA   Field Programmable Gate Array

HCCI   Homogeneous Charge Compression Ignition

HP   Horse Power

IMEP   Indicated Mean Effective Pressure

IMEPg Gross IMEP (compression and expansion only)

IMEPn Net IMEP (full cycle)

K   Integral Constant

NVO   Negative Valve Overlap

PMEP   Pumping Mean Effective Pressure

RPM   Revolutions Per Minute

S   Set Value

S1A   Solenoid 1 Activation

S2A   Solenoid 2 Activation

S1D   Solenoid 1 Duration

S2D   Solenoid 2 Duration

TDC   Top Dead Center

THC   Total Hydrocarbons

U   Control Signal

VI   Virtual Instrument

VVC   Variable Valve Control

APPENDIX

Version date: 2004-05-13
Scale: 3:1
Copyright: Cargine Engineering AB

Oil pipe

Solenoid

Recommended
screw shape
and dimensions (3x).

D10.00

7.00

D6.00h9

46.50

D4.50

44.00

Side view

M6

Ø39.76
Ø6,00H9(3x)
Ø31,90
44.00
39.00
19.00
5.00
5.00
19.00
33.00
38.00

Bottom view

G1/4

G1/4

60.00

46.00

23.50

13.00

9.00

19.00

29.00

38.00

Actuator piston

Engine valve stem
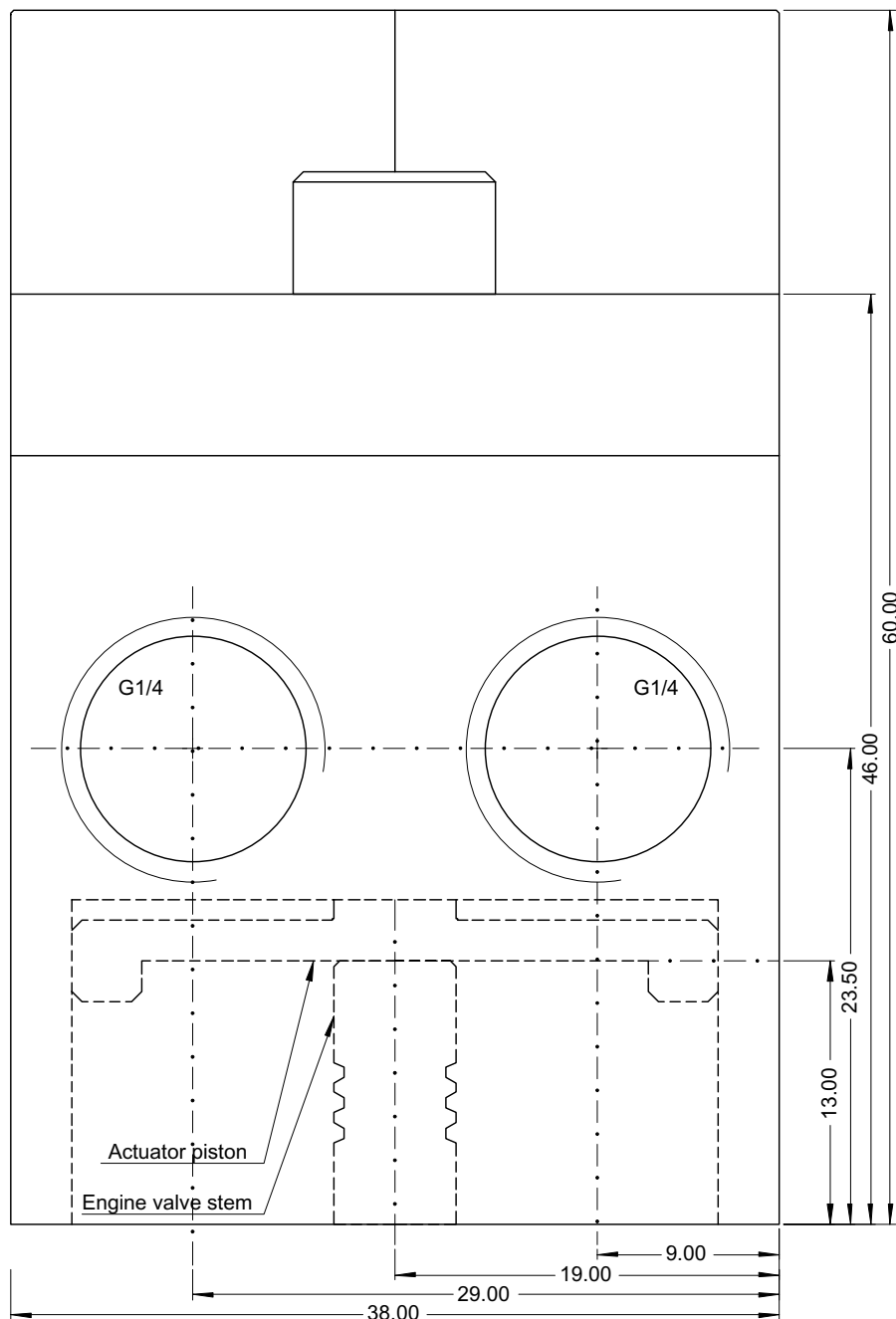
Front view

Introductory Study of Variable Valve Actuation for Pneumatic Hybridization

Sasa Trajkovic, Per Tunestål and Bengt Johansson
Division of Combustion Engines, Lund University, Faculty of Engineering

Urban Carlson and Anders Höglund
Cargine Engineering AB

ABSTRACT

Urban traffic involves frequent acceleration and deceleration. During deceleration, the energy previously used to accelerate the vehicle is mainly wasted on heat generated by the friction brakes. If this energy that is wasted in traditional IC engines could be saved, the fuel economy would improve. One solution to this is a pneumatic hybrid using variable valve timing to compress air during deceleration and expand air during acceleration. The compressed air can also be utilized to supercharge the engine in order to get higher load in the first few cycles when accelerating.

A Scania D12 single-cylinder diesel engine has been converted for pneumatic hybrid operation and tested in a laboratory setup. Pneumatic valve actuators have been used to make the pneumatic hybrid possible. The actuators have been mounted on top of the cylinder head of the engine. A pressure tank has been connected to one of the inlet ports and one of the inlet valves has been modified to work as a tank valve. The goal has been to test and evaluate 2 different modes – compression mode (CM) where air is stored in an air tank during deceleration and air-motor mode (AM) where the previously stored pressurized air is used for accelerating the vehicle. This paper also includes an optimization of the CM.

INTRODUCTION

As fuel prices increase, together with more stringent pollution standards, the demand for better fuel economy increases. Today there are several solutions to meet this demand and one of them is electric hybrids. In urban traffic the vehicle has to accelerate and decelerate frequently. In conventional vehicles the energy used for acceleration of the vehicle is wasted in the form of heat generated by the friction brakes during deceleration. This leads to a higher fuel consumption during city driving compared with freeway driving. The idea with electric hybridization is to reduce the fuel consumption by taking advantage of the, otherwise lost, brake energy. Hybrid operation can also allow the combustion engine to operate at its best operating point in terms of load and speed. An electric hybrid consists of two power sources, an ICE (Internal Combustion Engine) and an electric motor that can be used separately or combined. During deceleration the electric motor transforms the kinetic energy of the vehicle to electric power which it then stores in the batteries. The energy stored in the batteries will then be used when the vehicle accelerates. The disadvantage with electric hybrids is that they require an extra propulsion system and large heavy battery. All this costs the manufacturers a lot of money, which naturally leads to a higher price for the consumers to pay. One way to keep the costs down is the introduction of pneumatic hybrid. It doesn't need an expensive extra propulsion source and it works in a way similar to the electric hybrid. During deceleration of the vehicle, the engine is used as a compressor and stores the compressed air into a pressure tank. After a standstill the engine is used as an air-motor that uses the pressurized air from the tank in order to accelerate the vehicle. During a full stop the engine can be shut off. All these features of the pneumatic hybrid contribute to lower fuel consumption. Simulations made by Tai et al. [4] show a so called "roundtrip" efficiency of 36% and fuel economy improvement as high as 64% in city driving. This indicates that the pneumatic hybrid can be a promising alternative to the traditional vehicles of today and a serious contender to the better known electric hybrid. Andersson et al. [3] describes simulations of a dual pressure tank system for heavy vehicles with a regenerative efficiency as high as 55% and promising fuel savings.

PNEUMATIC HYBRID

The main idea with pneumatic hybrid is to use the ICE in order to compress atmospheric air and store it in a pressure tank during vehicle deceleration. The stored compressed air can then be used either to accelerate

the vehicle or to supercharge the engine in order to achieve higher loads when needed. It is also possible to completely shut off the engine at for instance a stoplight, which in turn contributes to lower fuel consumption. [1, 4]

In this study a single cylinder engine was used. In reality, in for instance a heavy duty truck, one cylinder will not be enough to take full advantage of the pneumatic hybrid. A pneumatic hybrid vehicle will most probably utilize multiple cylinders. The number of cylinders that will be converted for pneumatic hybrid operation for a certain vehicle is hard to estimate at this point. It depends on, among other things, the vehicle weight and the maximum braking torque needed. Drive cycle simulations will be conducted in a near future in order to find the optimal number of converted cylinders.

PNEUMATIC VARIABLE VALVE ACTUATION

In order to be able to switch between all these modes of engine operation, a variable valve system is needed. In this study a pneumatic variable valve actuating system has been used. The valve system is designed and manufactured by a Swedish company named Cargine Engineering AB. The system uses compressed air in order to drive the valves and the motion of the valves are controlled by a combination of electronics and hydraulics. The system is a fully variable valve system, which means that the valve lift, valve timing and valve lift duration can be completely controlled, independently of each other. The pneumatic valve system in question and the control program has been more thoroughly described by Trajkovic et al. [2].

TANK VALVE

In order to run the engine as a pneumatic hybrid, a pressure air tank has to be connected to the cylinder head. Tai et al. [4] describes an intake air switching system in which one inlet valve per cylinder is feed by either fresh intake air or compressed air. Andersson et al. [3] describes a dual valve system where one of the intake ports has two valves, one of whom is connected to the air tank. A third solution would be to add an extra port, to the cylinder head, that will be connected to the air tank. Since these three solutions demand significant modifications to a standard engine a simpler solution, where one of the existing inlet valves has been converted to a tank valve, has been chosen for this study. Since the engine used in this study has separated air inlet ports, there will be no interference between the intake system and the compressed air system. The drawback with this solution is that there will be a significant reduction in peak power, and reduced ability to generate and control swirl for good combustion.

MODES OF ENGINE OPERATION

In this paper two different engine modes have been investigated – compressor mode (CM) and air-motor mode (AM) and they will be described more thoroughly below.

COMPRESSOR MODE

In CM the engine is used as a 2-stroke compressor in order to decelerate the vehicle. The inlet valve opens a number of CAD after TDC and brings fresh air to the cylinder and closes around BDC. The moving piston compresses the air after BDC and the tank valve opens somewhere between BDC and TDC, depending on how much braking torque is needed and closes around TDC. The compressed air generated during CM is stored in a pressure tank that is connected to the cylinder head. A simple illustration of CM can be seen in Figure 1.
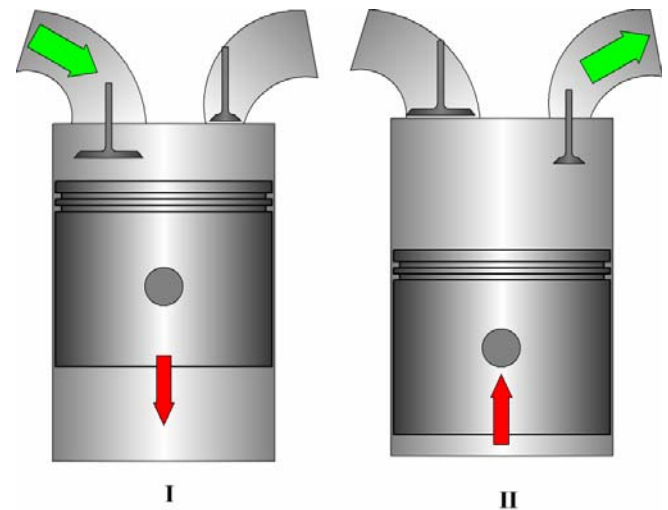
Figure 1 Illustration of CM. I) Intake of fresh air, II) Compression of air and pressure tank charging.

AIR-MOTOR MODE

In AM the engine is used as a 2-stroke air-motor that uses the compressed air from the pressure tank in order to accelerate the vehicle. The tank valve opens at TDC or shortly after and the compressed air fills the cylinder to give the torque needed in order to accelerate the vehicle. Somewhere between TDC and BDC the tank valve will close, depending on how much torque the driver demands. Increasing tank valve duration will increase the torque generated by the compressed air. The inlet valve opens around BDC in order to avoid compression of the air in the cylinder. The AM is illustrated in Figure 2.

Figure 2 Illustration of AM. I) Intake of compressed air, II) Air venting

EXPERIMENTAL SETUP

The engine used in this study is a single-cylinder Scania D12 diesel engine together with the pneumatic variable valve actuating system described earlier in this paper. The geometric properties of the engine can be seen in Table 1. Figure 3 shows a close-up of the pneumatic valve actuators mounted on top of the Scania cylinder head.

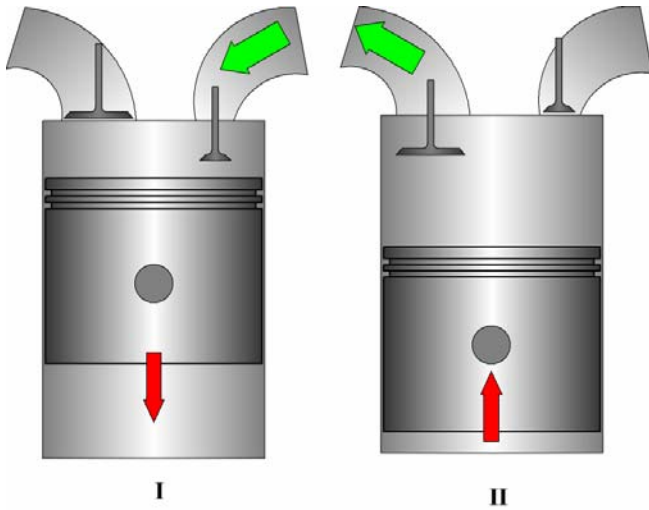The engine has two separated inlet ports and therefore they are suitable to use with the pneumatic hybrid since there will be no interference between the intake air and the compressed air. One of the inlet valves was therefore converted to a tank valve.

The exhaust valves were deactivated throughout the whole study because no fuel was injected and thus there was no need for exhaust gas venting.

The pressure tank used in this study is an AGA 50 litre pressure tank suitable for pressures up to 200 bars and it is shown in Figure 4. Note that this testing involved a one-tank hybrid system, unlike the two-tank system described in [3]. The tank size in the current system is selected based on availability rather than optimality, but in the future the tank volume will be an important parameter for the optimization of the system.

Table 1 Engine geometric properties.

Displaced Volume	1966 cm3
Bore	127.5 mm
Stroke	154 mm
Connecting Rod Length	255 mm
Number of Valves	4
Compression Ratio	18:1
Piston type	Flat
Inlet valve diameter	45 mm
Tank valve diameter	16 mm
Piston clearance	7.3 mm

Table 2 shows some valve parameters. The maximum valve lift height in this study is limited to 7 mm in order to avoid valve to piston contact. The valve system can, when unlimited, offer a valve lift height of about 12 mm.

Table 2 Valve parameters

Inlet valve supply pressure	4 bar
Tank valve supply pressure	6 bar
Hydraulic brake pressure	4 bar
Inlet valve spring preloading	100 N
Tank valve spring preloading	340 N
Maximum valve lift	7 mm

MODIFICATIONS TO TANK VALVE

In order to open the tank valve at high in-cylinder pressures some modifications of the tank valve had to be introduced. The valve diameter had to be decreased from 45 mm to 16 mm. The tank valve spring preloading had to be changed from 100 to 340 N in order to keep the tank valve completely closed for tank pressures up to 25 bars.

MODIFICATIONS TO CYLINDER HEAD

In order to use the modified tank valve the original valve seating had to be exchanged for a smaller seating.

The inlet port related to the tank valve has been connected to the pressure tank with metal tubing resistant to high temperatures and pressures.

Figure 3 The pneumatic valve actuators mounted on the Scania cylinder head

Figure 4 The pressure tank connected to the cylinder head by metal tubing.

ENGINE EXPERIMENTAL RESULTS

Both CM and AM have been tested in this study. Also results from optimization of CM will be shown. The results will be discussed thoroughly. Notice that all presented pressure values are absolute.

COMPRESSOR MODE

The CM tests can be done in two ways. The first one is to achieve as high compression efficiency as possible. This is done by the introduction of a feedback control of the tank valve. The tank valve then opens when the in-cylinder pressure is equal to the tank pressure.

The second one is to achieve as much braking torque as possible. The maximum braking torque is achieved when the tank valve opens at or shortly after BDC. This strategy will lead to a blowdown of pressurized air from the pressure tank into the cylinder and thus the cylinder will be charged with air at current tank pressure instead

of atmospheric air. This paper focuses more on the first method, i.e. achieving higher compression efficiency.

Table 3 shows the valve strategy used in this part of the experiment. The tank valve opening is feedback controlled and depends on the in-cylinder pressure and the tank pressure. The feedback control is based on the isentropic compression law:

$$p_2 = p_1 \left(\frac{V_1}{V_2} \right)^{\gamma} \qquad (1)$$

p_1 corresponds to the pressure at BDC and p_2 is the pressure at any other point in the cycle. V_1 is the maximal volume in the cylinder and V_2 is the cylinder volume when the cylinder pressure is p_2. By setting p_2 equal to the tank pressure, the volume at the given pressure can be calculated and from that it is possible to calculate the correct tank valve timings.

Table 3 Valve strategy in CM

	Cylinder pressure ≈ tank pressure
Tank valve opening	
Tank valve closing	10 CAD ATDC
Inlet valve opening	35 CAD ATDC
Inlet valve closing	180 CAD ATDC

Figure 5 and Figure 6 show the in-cylinder pressure and the tank pressure during one engine revolution in 2-stroke. Normally the maximum in-cylinder pressure occurs at TDC or shortly before, but in Figure 5 the peak of the in-cylinder pressure trace has moved more than 20 CAD away from TDC. The reason for this phenomenon is that the pressurized air in the cylinder escapes into the tank once the tank valve opens.
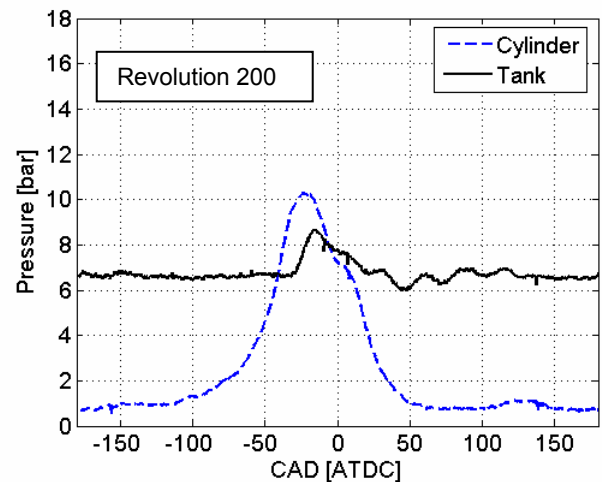

Figure 5 In-cylinder pressure and tank pressure in CM at revolution 200 and an engine speed of 600 rpm
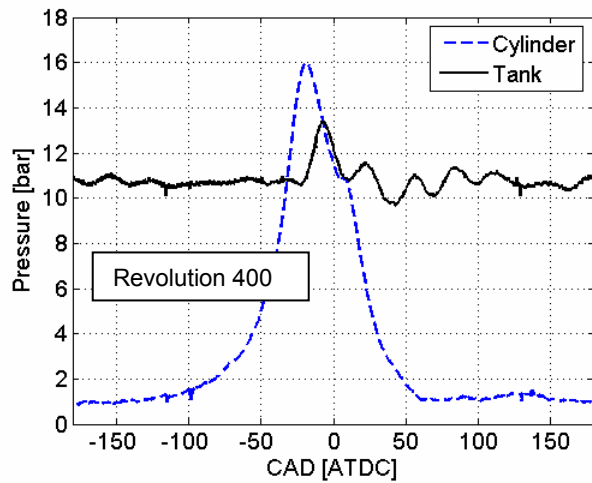
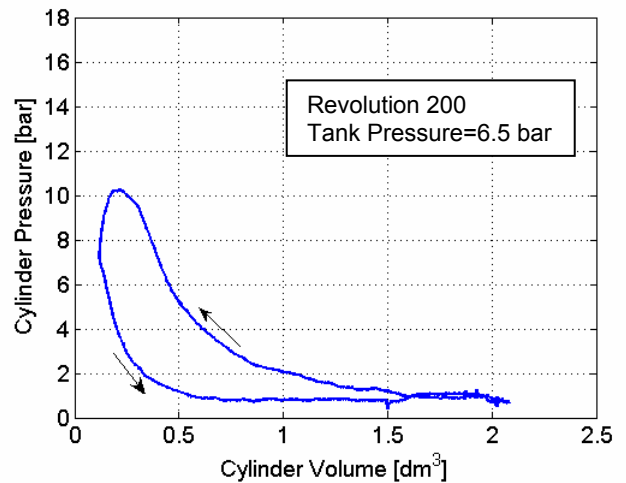**Figure 6 In-cylinder pressure and tank pressure in CM at revolution 400 and an engine speed of 600 rpm**
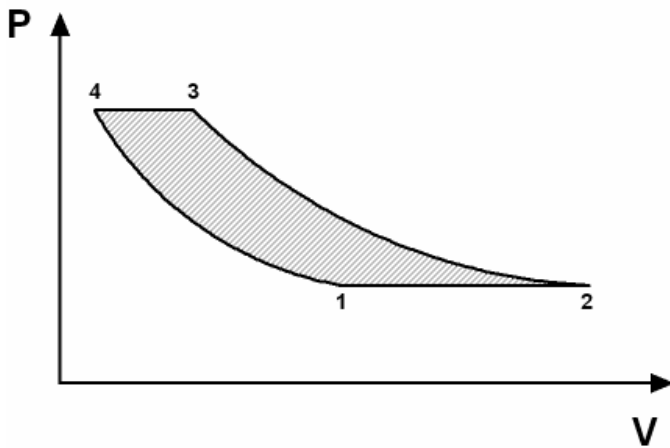

Figure 7 Illustration of an ideal PV-diagram of one CM revolution.

Figure 7 illustrates an ideal PV-diagram of one revolution in CM. At point 1 the inlet valve opens and fresh air enters the cylinder. The inlet valve closes at point 2 and the piston starts to compress the air until equilibrium between the tank and the cylinder pressure exists. At point 3 the tank valve opens and most of the compressed air is transferred to the pressure tank until the tank valve closes at point 4. The step between point 3 and 4 is isobar, which means that the cylinder pressure will remain constant while the tank valve is open. Between point 4 and 1, the remaining compressed air is expanded.

Figure 8 and Figure 9 shows the PV-diagram from real engine testing at two different tank pressures. Comparing Figure 7 with Figure 8 and Figure 9 clearly indicates that there is an absence of the isobar event in the real engine testing. The reason for this is that choking occurs over the tank valve which limits the air

flow and thereby the pressure will increase. This overshoot in pressure can probably be lowered dramatically if the small tank valve diameter is increased.

Figure 8 PV-diagram from engine testing at engine revolution number 200 and an engine speed of 600 rpm.
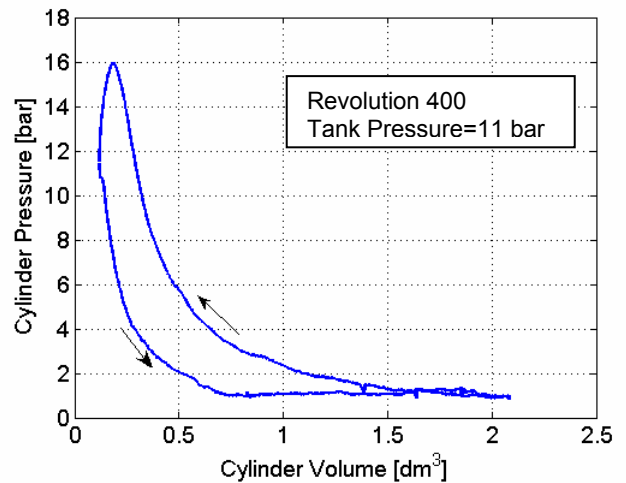

Figure 9 PV-diagram from engine testing at engine revolution number 400 and an engine speed of 600 rpm.

Figure 10 shows how the tank pressure increases with time during CM for three different engine speeds. Figure 11 shows the same data with the timescale changed from seconds to number of engine revolutions.
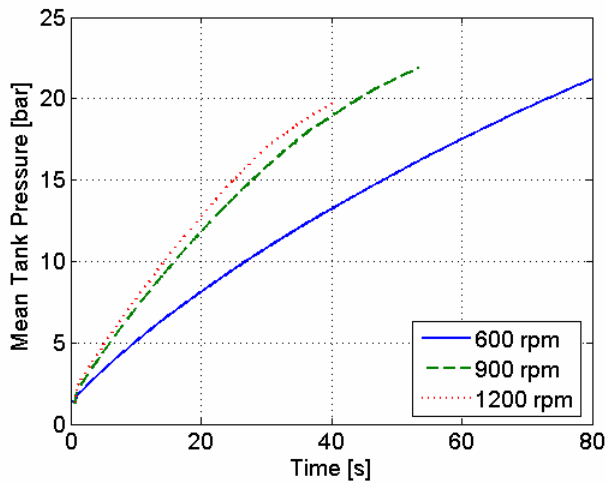
Figure 10 Mean tank pressure as a function of time for three different engine speeds.
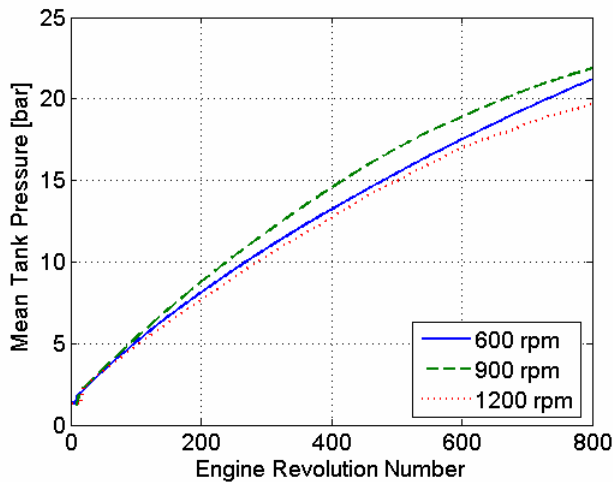

Figure 11 Mean tank pressure as a function of engine revolutions for three different engine speeds.

It is noticeable from Figure 11 that there is a difference between the tank pressures for different engine speeds. The reason for this is probably that the control program by coincidence is better optimized for the case at 900 rpm than at the other two cases.

Figure 12 Negative BMEP as a function of engine revolutions for three different engine speeds.

Figure 12 shows negative BMEP during CM for three different engine speeds. The reason why BMEP is decreasing after about 500 revolutions at 900 and 1200 rpm is that the tank valve closing is not feedback controlled but set to a constant value. This leads to a premature tank valve closing when the tank pressure is high. The cylinder is then still filled with pressurized air that pushes the cylinder and thereby contributes with positive BMEP which decreases BMEP for the whole revolution. This phenomenon is engine speed dependant and it is not visible at 600 rpm. If the tank valve closing would be controlled in the same way as the opening, then the BMEP curve would probably be flat throughout the whole test run.
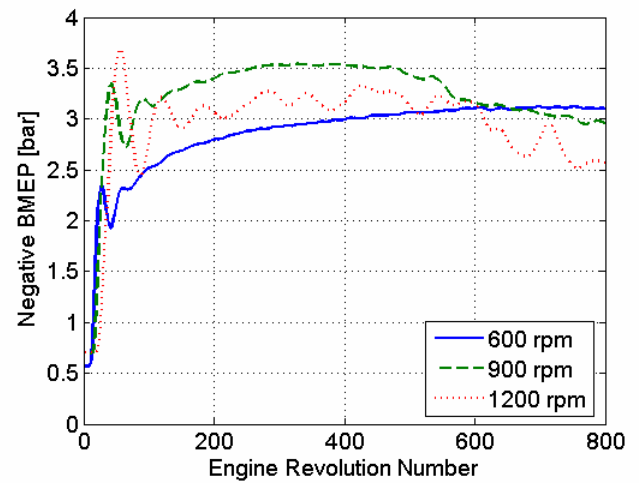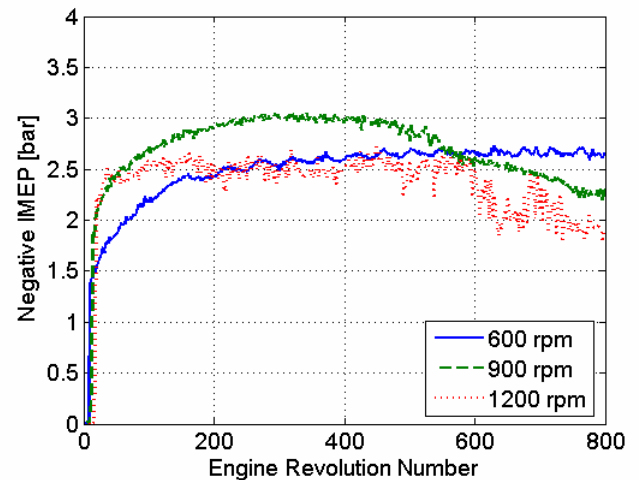

Figure 13 Negative IMEP as a function of engine revolutions for three different engine speeds.

Figure 13 shows IMEP during CM for the three different engine speeds. The same line of argument as for Figure 12 can be used in explaining Figure 13.

BMEP and IMEP in Figure 12 and Figure 13 have been calculated by two different methods. BMEP has been calculated as a function of torque and IMEP as a function of in-cylinder pressure. Figure 12 and Figure 13 can then be used to evaluate both methods. Since the graphs of IMEP and BMEP look almost the same, the methods can be seen as reliable.

Figure 14 shows clearly how the pressure losses over the tank valve increases with increasing engine speed. The pressure losses at 600 rpm are surprisingly low considering that the tank valve has a very small diameter.
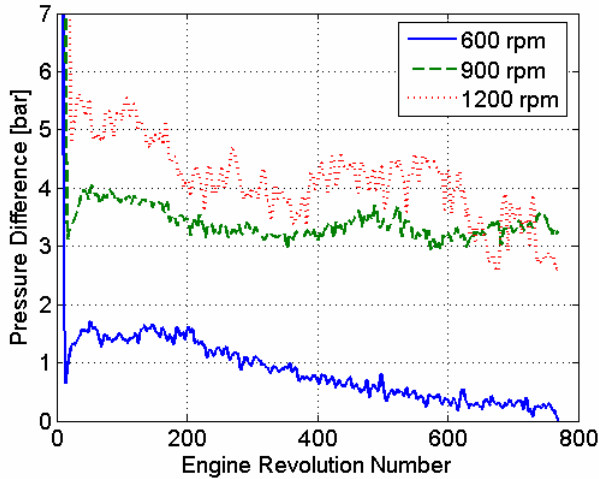

Figure 14 Pressure difference between maximum in-cylinder and tank pressure at various engine speeds.

OPTIMIZING THE COMPRESSOR MODE

Equation (1) described earlier in this paper is an isentropic relation between the pressure and the volume for various values of γ. γ is the specific-heat ratio and depends on the heat losses but in this study γ has been set to a constant value of 1.4. This will introduce some errors to the tank valve control algorithm and in order to avoid this, a method for optimizing CM mode has been tested.

The main idea with this method is to find the most optimal valve timing at a given tank pressure and, in order to do that, the tank pressure needs to be constant throughout the whole testing interval. Since the amount of air charged into the tank should equal the amount of air released from the tank in order to keep the tank pressure constant, a pressure relief valve is connected to the tank. It is then possible to achieve the desired steady state tank pressure by adjusting the pressure relief valve opening angle. The greater the opening angle the lower the steady state tank pressure.

This paper describes only the optimization of the tank valve opening.

Notice that BMEP and IMEP in the figures in this section are given in 4-stroke scale (doubled).

Figure 15 Negative IMEP as a function of valve opening timing during optimization of CM at various tank pressures and an engine speed of 600 rpm.

Figure 15 and Figure 16 show how negative IMEP and BMEP are affected by the tank valve opening timing during optimization of CM. From the figures it can be seen that there is an optimal tank valve opening timing for every tank pressure when taking highest efficiency into consideration. Highest efficiency corresponds to the minimum in each curve. This means that it takes less power to compress air at this point than at any other point on the curve at a given tank pressure. If higher braking power is needed, the efficiency has to be sacrificed.
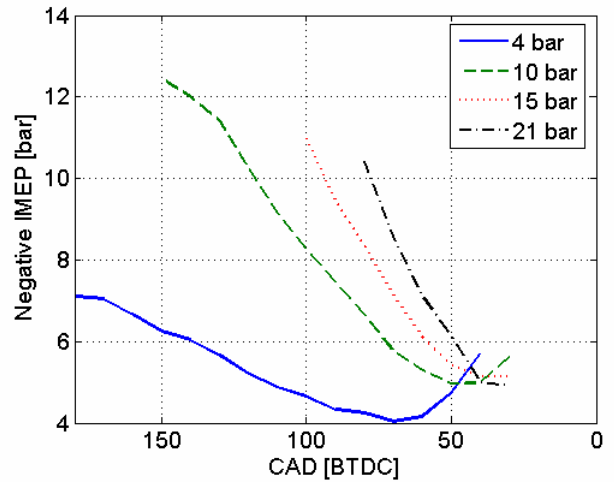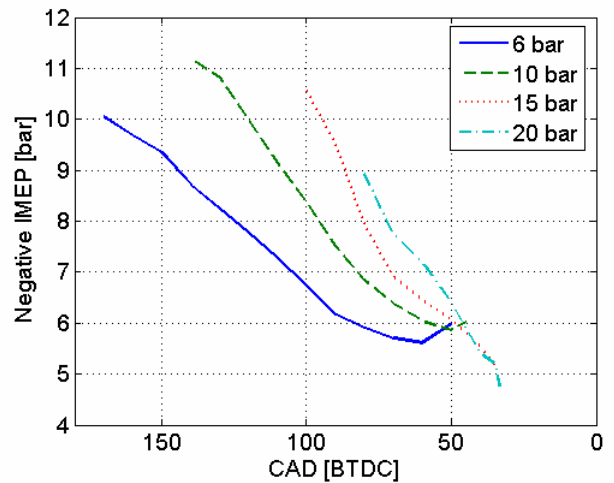

Figure 16 Negative IMEP as a function of valve opening timing during optimization of CM at various tank pressures and an engine speed of 900 rpm.

Figure 17 and Figure 18 show how the pressure difference between the maximum in-cylinder pressure and maximum tank pressure are affected by the tank valve opening during optimization of CM. The higher the differences are the higher the pressure losses are. The smallest differences occur at the same points as the minimum in the 4 previous figures. This verifies that the highest efficiency is achieved in these points.
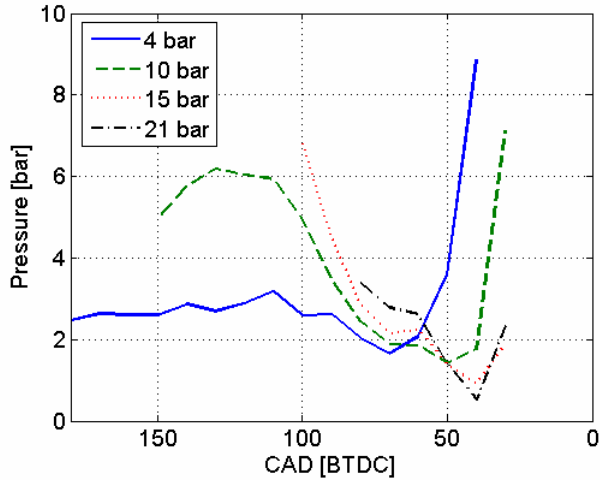
Figure 17 Pressure difference between maximum in-cylinder pressure and maximum tank pressure as a function of valve opening during optimization of CM at various tank pressures and an engine speed of 600 rpm.
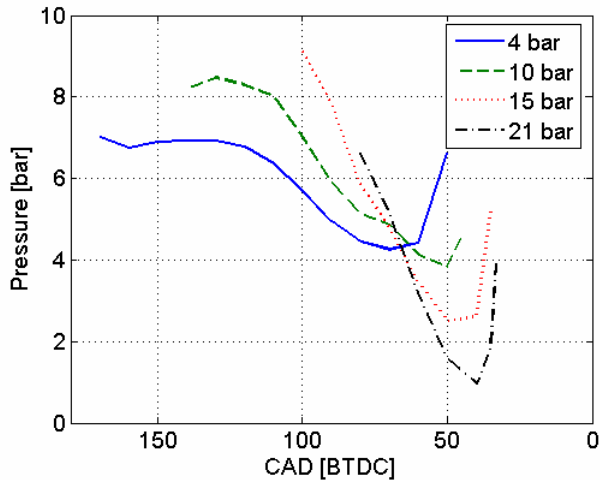
Figure 18 Pressure difference between maximum in-cylinder pressure and maximum tank pressure as a function of valve opening during optimization of CM at various tank pressures and an engine speed of 900 rpm.

AIR-MOTOR MODE

The AM can, as CM, be executed in two ways, either in regard to efficiency or brake power. The latter one has been used in this study. An optimization of AM similar to the one performed for CM will be presented in a future publication.

The tank valve opening is set to 5 CAD BTDC while the closing is varied with various tank pressures in order to get the highest torque. The inlet valve opens at BDC and closes at TDC. Table 4 shows the tank valve closings used in this experiment.

Table 4 Tank valve closing at various tank pressures in AM.

TankVC@22 bar	40 CAD ATDC
TankVC@15 bar	60 CAD ATDC
TankVC@12.5 bar	70 CAD ATDC
TankVC@10 bar	80 CAD ATDC

Figure 19 indicates that in order to achieve as high torque as possible, a valve control strategy involving valve timings similar to the valve timings in Table 4 has to be used.

Figure 19 Positive IMEP in AM at an engine speed of 600 rpm.

Figure 20 Mean tank pressure during AM at an engine speed of 600 rpm.

Figure 21 PV-diagram illustrates why IMEP is below 0 bars at some point during AM.

REGENERATIVE EFFICIENCY

It can be seen in Figure 20 that when the pressure is as high as 22 bars, it lasts for over 40 seconds at the current engine speed and valve timings. This time duration can be extended if the tank valve duration is decreased and thereby the AM efficiency would be increased.

Notice that when the tank pressure reaches a value below 4.5 bars, IMEP becomes negative. This is due to wrong tank or inlet valve timings. The amount of pressurized air charged into the c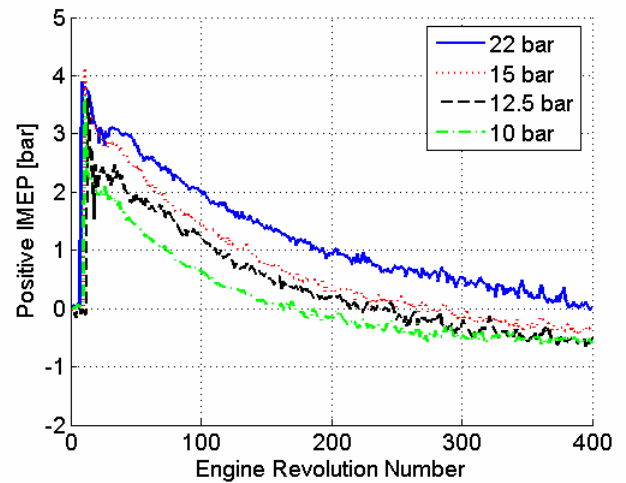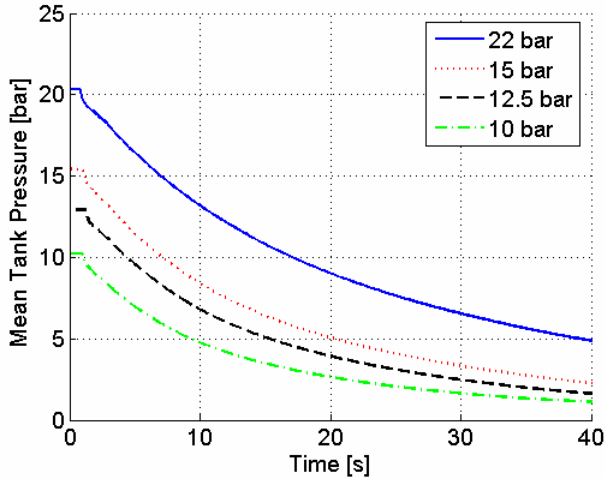ylinder is not enough in order to expand it to atmospheric pressure at BDC. Instead the pressure will decrease bellow atmospheric pressure and since the inlet valve opens at BDC there will be a blowdown of atmospheric air into the cylinder which leads to negative IMEP. This event is illustrated in Figure 21. In order to avoid this, the inlet valve should not open until the cylinder pressure reaches atmospheric pressure. Another way to avoid negative IMEP in this case is to have longer tank valve duration. In this way the cylinder pressure will reach atmospheric pressure at BDC and the inlet valve can then open at BDC without any backflow of atmospheric air into the cylinder.

In order to estimate the potential of the pneumatic hybrid, the regenerative efficiency has to be calculated. The regenerative efficiency is defined as the ratio between the energy produced during AM and the energy stored during CM. It can also be defined as the ratio between the positive and negative IMEP:

$$\eta_{regen} = \frac{IMEP_+}{IMEP_-} \tag{2}$$

It can also be interesting to see the efficiencies for every revolution during CM and AM. They are defined as:

$$\eta_{CM} = \frac{P_{tank,CM}}{P_{engine-}} \tag{3}$$

and

$$\eta_{AM} = \frac{P_{engine+}}{P_{tank,AM}} \tag{4}$$

where $P_{engine-}$ is the engine motoring power during CM and $P_{engine+}$ is the engine brake power during AM.

P_{tank} in (3) and (4) is defined as the change of energy in the tank per time unit:

$$P_{tank,CM} = -P_{tank,AM} = \frac{\Delta E_{stored}}{\Delta t} \tag{5}$$

Figure 22 and Figure 23 show the efficiency in CM and AM, respectively. The reason why all the efficiency curves are going towards zero in Figure 23 is that IMEP

is going towards 0 bars. These really low, near zero, efficiencies are not desirable and it is then better to use the remaining pressurized air to supercharge the engine as described by Schechter et al. [1, 4].

Figure 24 and Figure 25 show the total efficiency in CM and AM, respectively.
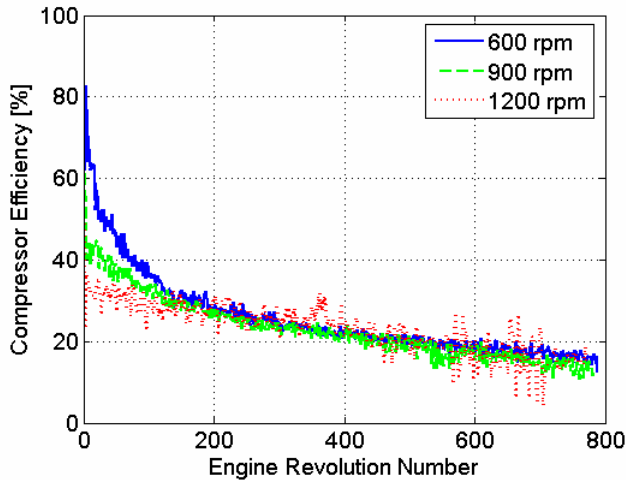
Figure 22 Compressor efficiency calculated for every engine revolution during CM at three different engine speeds.
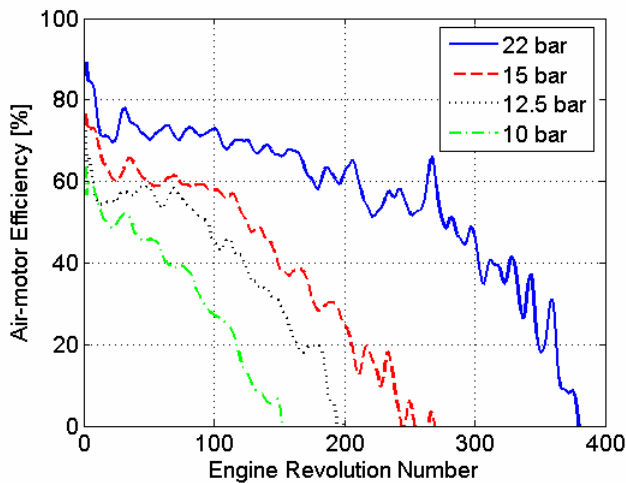
Figure 23 Air-motor efficiency calculated for every engine revolution during CM at various tank pressures and at an engine speed of 600 rpm
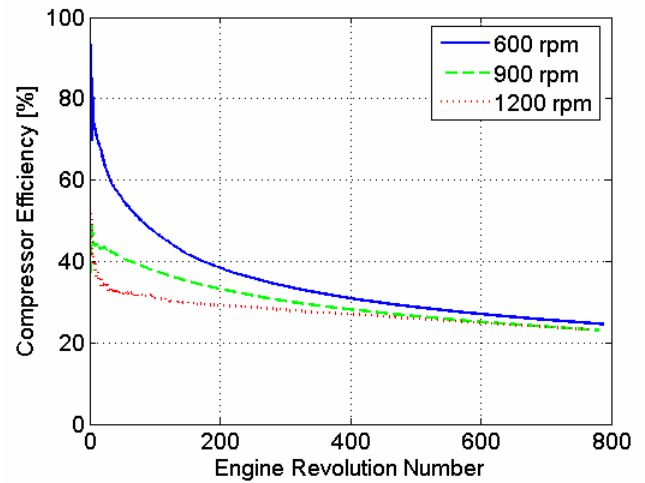
Figure 24 Total compressor efficiency as a function of engine revolutions during CM at three different engine speeds.
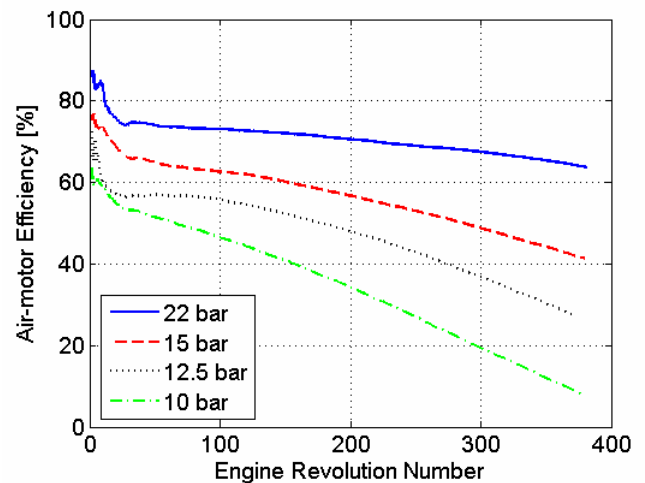
Figure 25 Total air-motor efficiency as a function of engine revolutions during CM at various tank pressures and an engine speed of 600 rpm.

Next step is to calculate the regenerative efficiency. First thing to do is to calculate how much work has been used in order to compress air from 5 bars to 22 bars in the three different CM runs. These numbers have been chosen because the starting tank pressure in AM is about 22 bars and 5 bars corresponds to the remaining air pressure when IMEP is around zero in AM. The total work used during CM is then divided with the total work recovered during AM. The calculated regenerative efficiency can be seen in Table 5 and the results shows that the run at 900 rpm was the most optimized as stated in one of the previous sections.

Table 5 Total calculated regenerative efficiency for three different engine speeds.

	η_{regen} [%]
CM@600rpm	32
CM@900rpm	33
CM@1200rpm	25

FUTURE WORK

- A third engine mode will be tested, namely the supercharge mode also called air-power-assisted mode by Schechter et al. [1, 4]. The idea with this mode is to use the compressed air in order to supercharge the engine and thereby achieve higher loads.
- The tank valve diameter will be increased as an attempt to lower the pressure losses.
- The pressure tank and the connecting tubing will be insulated in order to prevent cooling of the hot compressed air with increased efficiency as a result.
- This paper describes only the optimization of the tank valve opening in CM. Therefore optimization of valve closing and inlet valve timings will be done. All the obtained optimal measurements will then be introduced into a look up table in the control program.
- AM will be optimized in a similar way as CM.
- The engine testing described in this study will be simulated in GT-Power, in order to verify the real-life results. The simulations can be a useful tool in future optimization of the pneumatic hybrid.

CONCLUSION

The results achieved during the study show the potential with the pneumatic hybrid. Compared with simulations made by Tai et al. [4] the maximum regenerative efficiency obtained in this study (33 %) is a little lower, but still promising considering that it is an almost unoptimized system. The regenerative efficiency of 55% described by Anderson et al. [3] seems to be out of reach with the use of only one pressure tank.

The main factors that affect the efficiency negatively are probably the pressure losses over the valve and the heat losses due to poor insulation. The pressure losses can easily be lowered by switching to another tank valve with larger diameter. The heat losses can be lowered significantly by the introduction of some sort of insulation to the tank and the connecting tubing.

The results show that there is a pretty simple way to optimize the valve timings in order to increase the efficiency in CM. They also indicate on how to change the valve timing in order to achieve higher braking torque when needed.

REFERENCES

1. M. Schechter, "Regenerative Compression Braking – a Low Cost Alternative to Electric Hybrids", SAE Paper 2000-01-1025, 2000.
2. S. Trajkovic, A. Milosavljevic, P. Tunestål, B. Johansson, "FPGA Controlled Pneumatic Variable Valve Actuation" SAE Paper 2006-01-0041, 2006.
3. M. Andersson, B. Johansson, A. Hultqvist, "An Air Hybrid for High Power Absorption and Discharge", SAE Paper 2005-01-2137, 2005.
4. C. Tai, T-C Tsao, M. Levin, G. Barta and M. Schechter, "Using Camless Valvetrain for Air Hybrid Optimization", SAE Paper 2003-01-0038, 2003.

CONTACT

Sasa Trajkovic, PhD student, Msc M. E.

E-mail: Sasa.Trajkovic@vok.lth.se

NOMENCLATURE

AM: Air-motor Mode

ATDC: After Top Dead Centre

BDC: Bottom Dead Centre

BMEP: Brake Mean Effective Pressure

BTDC: Before Top Dead Centre

CAD: Crank Angle Degree

CM: Compressor Mode

E_{stored}: Energy stored in the tank

η_{AM} :   Air-motor Mode efficiency [%]

η_{CM} :   Compressor Mode efficiency [%]

η_{regen} : Regenerative efficiency [%]

γ :   Specific heat ratio [-]

ICE: Internal combustion Engine

IMEP: Indicated Mean Effective Pressure

p: In-cylinder pressure [bar]

P_{engine}: Engine power [W]

P_{tank}:   Change of energy in the tank [J/s]

t: Time [s]

TDC: Top Dead Centre

RPM: Revolutions Per Minute

V: Cylinder volume [m^3]

Investigation of Different Valve Geometries and Valve Timing Strategies and their Effect on Regenerative Efficiency for a Pneumatic Hybrid with Variable Valve Actuation

Sasa Trajkovic, Per Tunestål and Bengt Johansson
Division of Combustion Engines, Lund University, Faculty of Engineering

ABSTRACT

In the study presented in this paper a single-cylinder Scania D12 diesel engine has been converted to work as a pneumatic hybrid. During pneumatic hybrid operation the engine can be used as a 2-stroke compressor for generation of compressed air during vehicle deceleration and during vehicle acceleration the engine can be operated as an air-motor driven by the previously stored pressurized air.

The compressed air is stored in a pressure tank connected to one of the inlet ports. One of the engine inlet valves has been modified to work as a tank valve in order to control the pressurized air flow to and from the pressure tank.

In order to switch between different modes of engine operation there is a need for a VVT system and the engine used in this study is equipped with pneumatic valve actuators that uses compressed air in order to drive the valves and the motion of the valves are controlled by a combination of electronics and hydraulics.

This paper describes the introduction of new tank valve geometry to the system with the intent to increase the pneumatic hybrid regenerative efficiency. The new tank valve has a larger valve head diameter than the previously used setup described in [1], in order to decrease the pressure drop over the tank valve. In order to ensure tank valve operation during high in-cylinder pressures the valve is combined with an in-house developed pneumatic valve spring which makes the tank valve pressure compensated.

A comparison between the old and the new tank valve geometry and their effect on the pneumatic hybrid efficiency has been done. Also, optimization of the valve timings for both CM (Compressor Mode) and AM (Air-motor Mode) has been done in order to achieve further improvements on regenerative efficiency.

INTRODUCTION

As the pollution standards are becoming more stringent going towards zero emissions together with increasing fuel prices, engine developers are looking for alternative engine management to meet the increasing demand for better fuel economy. Of great importance is to improve the fuel economy at part-load, especially during city driving since it involves frequent acceleration and deceleration. In conventional vehicles all the kinetic energy built up during acceleration is lost during declaration in the form of heat generated by the friction brakes. This leads to a higher fuel consumption during city driving compared with freeway driving where acceleration and deceleration is less frequent.

Today there are several solutions to meet the demand for better fuel economy and one of them is electric hybrids. The idea with electric hybridization is to reduce the fuel consumption by taking advantage of the, otherwise lost, brake energy. Hybrid operation in combination with engine downsizing can also allow the combustion engine to operate at its best operating points in terms of load and speed.

An electric hybrid consists of two power sources, an ICE (Internal Combustion Engine) and an electric motor that can be used separately or combined. During deceleration the electric motor transforms the kinetic energy of the vehicle to electric power which it then stores in the batteries. The energy stored in the batteries will then be used when the vehicle accelerates. The main disadvantage with electric hybrids is that they require an extra propulsion system and large heavy battery. All this costs the manufacturers a lot of money, which is compensated by a higher end-product price.

One way of keeping the extra cost as low as possible compared to a conventional vehicle, is the introduction of pneumatic hybrid. It doesn't require an expensive extra propulsion source and it works in a way similar to the electric hybrid. During deceleration of the vehicle, the

engine is used as a compressor that converts the kinetic energy contained in the vehicle into energy in the form of compressed air which is stored in a pressure tank. After a standstill the engine is used as an air-motor that utilizes the pressurized air from the tank in order to accelerate the vehicle. During a full stop the engine can be shut off.

Tai et al. [2] describes simulations with a so called "round-trip" efficiency of 36% and an improvement of 64% on fuel economy in city driving. Simulations made by Andersson et al. [3] show a regenerative efficiency as high as 55% for a dual pressure tank system for heavy vehicles. Real engine studies made by Trajkovic et al. [1] shows that the pneumatic hybrid has a promising potential in the reality and a regenerative efficiency of 33% has been achieved.

All these features of the pneumatic hybrid contribute to lower fuel consumption and in combination with the simplicity of the system, the pneumatic hybrid can be a promising alternative to the traditional vehicles of today and a serious contender to the better known electric hybrid.

PNEUMATIC HYBRID

Pneumatic hybrid operation introduces new operating modes in addition to conventional ICE operation. The main idea with pneumatic hybrid is to use the ICE in order to compress atmospheric air and store it in a pressure tank when retarding the vehicle. The stored compressed air can then be used either to accelerate the vehicle or to supercharge the engine in order to achieve higher loads when needed. The pneumatic hybrid also makes it possible to completely shut off the engine at idling like for instance at a stoplight, which in turn contributes to lower fuel consumption. [2,4,5,6]

In this study a single-cylinder engine was used. In reality, in for instance a heavy duty truck, one cylinder will not be enough to take full advantage of the pneumatic hybrid. A pneumatic hybrid will most probably utilize multiple cylinders. The number of cylinders that will be converted for pneumatic hybrid operation for a certain vehicle is hard to estimate at this point. It depends on, among other things, the vehicle weight and the maximum braking torque needed. Drive cycle simulations using data from engine experiments obtained in this study will be conducted in a near future in order to find optimal parameters like required number of converted cylinders and optimal tank volume, just to mention a few.

PNEUMATIC VARIABLE VALVE ACTUATION

In order to be able to switch between all pneumatic hybrid operations and conventional ICE operations, a variable valve actuating system is needed. In this study a pneumatic variable valve actuating system has been used. The valve system is designed and manufactured by a Swedish company named Cargine Engineering AB.

The system uses compressed air in order to drive the valves and the motion of the valves are controlled by a combination of electronics and hydraulics. The system is a fully variable valve actuating system, which means that the valve lift, valve timing and valve lift duration can be completely controlled, independently of each other. The pneumatic valve system in question and the control program has been more thoroughly described by Trajkovic et al. [7].

TANK VALVE

In order to run the engine as a pneumatic hybrid, a pressure tank has to be connected to the cylinder head. Tai et al. [2] describes an intake air switching system in which one inlet valve per cylinder is feed by either fresh intake air or compressed air from the pressure tank. Andersson et al. [3] describes a dual valve system where one of the intake ports has two valves, one of whom is connected to the air tank. A third solution would be to add an extra port to the cylinder head, which would be connected to the air tank. Since these three solutions demand significant modifications to a standard engine a simpler solution, where one of the existing inlet valves has been converted to a tank valve, has been chosen for this study. Since the engine used in this study has separated air inlet ports, there will be no interference between the intake system and the compressed air system. The drawback with this solution is that there will be a significant reduction in peak power, and reduced ability to generate and control swirl for good combustion.

MODES OF ENGINE OPERATION

The main pneumatic hybrid vehicle operations are compressor mode (CM) and air-motor mode (AM). Both modes have been tested in the study described in this paper and an attempt to optimize them has been carried out. The optimization of both CM and AM will be presented later on in this paper.

COMPRESSOR MODE

In CM the engine is used as a 2-stroke compressor in order to decelerate the vehicle. The kinetic energy of the moving vehicle is converted to potential energy in the form of compressed air.

During CM the inlet valve opens a number of CAD after TDC and brings fresh air to the cylinder, and closes around BDC. The moving piston starts to compress the air contained in the cylinder after BDC and the tank valve opens somewhere between BDC and TDC, depending on how much braking torque is needed, and closes shortly after TDC. The compressed air generated during CM is stored in a pressure tank that is connected to the cylinder head.

AIR-MOTOR MODE

In AM the engine is used as a 2-stroke air-motor that uses the compressed air from the pressure tank in order

to accelerate the vehicle. The potential energy in the form of compressed air is converted to mechanical energy on the crankshaft which in the end is converted to kinetic energy.

During AM the tank valve opens at TDC or shortly after and the compressed air fills the cylinder to give the torque needed in order to accelerate the vehicle. Somewhere between TDC and BDC the tank valve closes, depending on how much torque the driver demands. Increasing the tank valve duration will increase the torque generated by the compressed air. The inlet valve opens around BDC in order to avoid compression.

PRESSURE COMPENSATED TANK VALVE

In experiments done by Trajkovic et al. [1], one of the intake valves was chosen to work as tank valve. The intake valve had to be modified in order to make it possible to achieve desired TankVO (Tank Valve Opening) at high in-cylinder pressures. The tank valve diameter had to be reduced from the original size of 45 mm, down to 16 mm. Also the tank valve spring preloading had to be changed from 100 N to 340 N in order to keep the tank valve completely closed at tank pressures up to 25 bars. Both modifications lead to some complications. The reduced valve diameter increases the pressure losses over the tank valve and thus the regenerative efficiency will be reduced. The increased spring pre-loading will affect the pneumatic valve actuator energy consumption, but this is only of importance in a real vehicle where the actuators have to be feed with pressurized air from a compressor.

In an attempt to avoid the pressure losses over the tank valve, an in-house designed pneumatic valve spring has been developed and has replaced the conventional tank valve spring. Figure 1 shows a simple cross section illustration of the pneumatic valve spring arrangement mounted on the cylinder head. The pneumatic spring is constructed in such way, that it uses the tank pressure to keep the valve closed. A cylinder (indicated by number 1) is placed on the top of the cylinder head (indicated by number 4), with the tank valve (indicated by number 3) in the center of the cylinder. The cylinder is sealed in the bottom against the cylinder head and on the top the cylinder is sealed with the valve spring retainer (indicated by number 2). The space between the bottom sealing and the tank valve spring retainer is the pneumatic valve spring and it is connected to the tank valve port (indicated by number 6) and thus to the compressed air through 4 passages machined on the tank valve (indicated by number 5). The pressurized air enters the air passages on the valve and is guided up to the pneumatic valve spring, as indicated by the blue arrows. The passages are made in such way, that the pneumatic spring will be connected to the tank valve port at any time and any valve lift. Since the compressed air in the pneumatic spring works on the underside of the tank valve spring retainer and the compressed air in the tank valve port acts on the upside of the tank valve

head, as indicated by the yellow arrows, the net force should be zero, and thus the valve should be pressure compensated. This means that the tank will be kept closed without using any valve spring and the valve diameter can now be increased in order to reduce the pressure drop over the valve. In the study presented in this paper, the tank valve diameter has been increased to 28 mm, which is almost the double of what has been used before. Figure 2 shows a picture of the two tank valves used in this study. Geometrical properties of the pneumatic spring arrangement can be seen in Table 1.
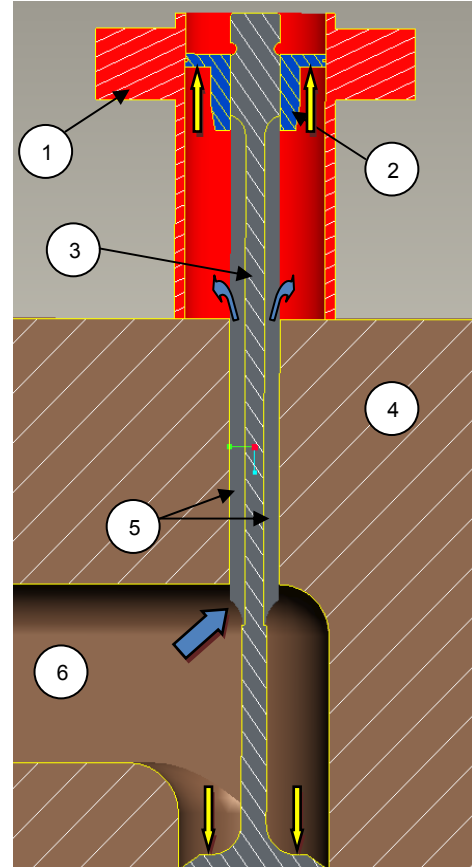

Figure 1 A simple cross section illustration of the pneumatic valve spring arrangement mounted on the cylinder head

When the valve is open the force generated by the pressurized air acting on the upside of the tank valve head is canceled. This means that there now only exist a considerable force on the undersurface of the valve spring retainer trying to close the tank valve. In order to overcome this problem, the tank valve actuator is feed with compressed air from the tank. This means that the pressure at a certain time is the same in the pneumatic valve spring as in the valve actuator. Since the actuator piston has a larger diameter than the tank valve spring retainer, the actuator will always have enough power to open the valve and maintain it open for as long as desired.

Figure 2 Picture illustrating the difference between the "small tank valve" and the "large tank valve"

Figure 3 The engine used in this study

Table 1 Geometric properties of the spring

Pneumatic spring cylinder inner diameter	28 mm
Tank valve spring retainer diameter	28 mm
Tank valve poppet diameter	28 mm
Actuator piston diameter	32 mm
Compressed air guiding passage cross-section area	6 mm^2

MODIFICATIONS TO THE PNEUMATIC SPRING

After some initial testing, some issues have been observed with the pneumatic valve spring. The issue of greatest importance is that the tank valve self-opens at certain running conditions during testing. The reason behind this behavior of the valve is high pressure oscillations in the tank valve port which haven't been taken into consideration. When a high pressure pulse arrives to the tank valve, the force acting on the tank valve head will be increased. The tank valve will no longer be pressure compensated and the net force acting on the valve will not be zero, and as a result of this the valve will self-open. In order to eliminate this problem a valve spring with 220 N preloading has been added to the tank valve, which means that there will always be a net force acting to keep the tank valve closed.

EXPERIMENTAL SETUP

The engine used in this study can be seen in Figure 3. It is a 6-cylinder Scania D12 diesel engine converted to a single-cylinder engine. The engine is equipped with the pneumatic variable valve actuating system described earlier in this paper. The geometric properties of the engine can be seen in Table 2. Figure 4 shows a close-up of the pneumatic valve actuators mounted on top of the Scania cylinder head.
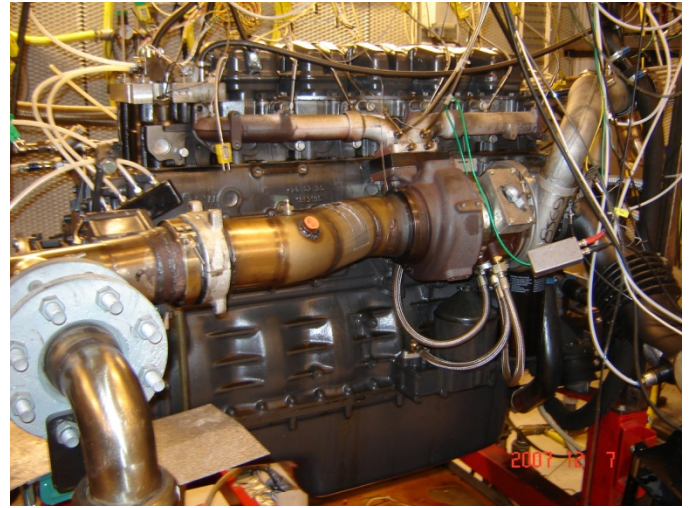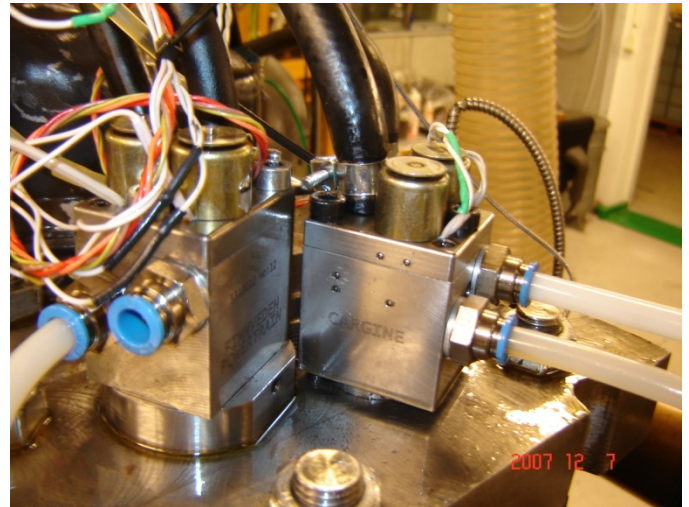

Figure 4 The pneumatic valve actuators mounted on the Scania cylinder head

The engine has two separated inlet ports and therefore they are suitable to use with the pneumatic hybrid since there will be no interference between the intake air and the compressed air. One of the inlet valves was therefore converted to a tank valve.

The exhaust valves were deactivated throughout the whole study because no fuel was injected and thus there was no need for exhaust gas venting.

Table 2 Engine geometric properties

Displaced Volume	1966 cm3
Bore	127.5 mm
Stroke	154 mm
Connecting Rod Length	255 mm
Number of Valves	4
Compression Ratio	18:1
Piston type	Flat
Inlet valve diameter	45 mm
Tank valve diameter	16 and 28 mm
Piston clearance	7.3 mm

The pressure tank used in this study is an AGA 50 litre pressure tank suitable for pressures up to 200 bars and it is shown in Figure 5. The pressure tank is connected to the cylinder head by metal tubing. In order to eliminate the metal tubing as a potential bottleneck on account of air flow choking, the diameter of the tubing was doubled at the same time as the small tank valve was replaced by the large tank valve. The tank size in the current system is selected based on availability rather than optimality, but in the future the tank volume will be an important parameter for the optimization of the system.

Figure 5 The pressure tank connected to the cylinder head by metal tubing

Table 3 shows some valve parameters. The maximum valve lift height in this study is limited to 7 mm in order to avoid valve to piston contact. The valve system can, when unlimited, offer a valve lift height of about 12 mm.

Table 3 Valve parameters

Inlet valve supply pressure	4 bar
Tank valve supply pressure	6 bar
Hydraulic brake pressure	4 bar
Inlet valve spring preloading	100 N
Tank valve spring preloading	220 N
Maximum valve lift	7 mm

Since the pneumatic valve spring arrangement require the actuator to be fed by compressed air from the tank, an extra pressurized air supply line had to be added. A problem with the actuator being fed with tank pressure is that there is a pressure threshold below which the pneumatic valve actuator will not work as expected. This means that the actuator has to be fed with compressed air from an external source. This adds thereby the need of having a pressure source switch. The switching system used in this study is built up by two check-valves which are arranged in such way that the source feeding the valve actuator will always be the source with the highest pressure. For instance if the external source of compressed air is set to 6 bars it will be the main feeding source until the pressure in the pressure tank exceeds 6 bars. A picture of the pressure source switching system is shown in Figure 6.

Figure 6 Pressurized air switching system built up by two check-valves

ENGINE EXPERIMENTAL RESULTS

Both CM and AM have been tested in the study described in this paper. Main focus have been on the optimization of CM and AM and comparison between the old and new setup. The results will be discussed thoroughly. Note that all presented pressure values are absolute and IMEP is given in 2-stroke scale.

COMPRESSOR MODE

The CM operation can mainly be done in three ways. The first way is to achieve as high compression efficiency as possible. This is done by the introduction of a feedback control of the tank valve. The tank valve then opens when the in-cylinder pressure is equal to the tank pressure.

The second way is to achieve as much braking torque as possible. The maximum braking torque is achieved when the tank valve opens at or shortly after BDC. This strategy will lead to a blowdown of pressurized air from the pressure tank into the cylinder and thus the cylinder will be charged with air at current tank pressure instead of atmospheric air.

Finally, the third way is actually a combination of the previous two and is the one that will be used in a real application. For instance, if the driver releases the gas pedal, the engine will be operating as a CM at highest efficiency. If the driver then presses the brake pedal, the CM operation will drift away from highest efficiency towards highest braking torque.

This study focuses mainly on the first method, i.e. achieving as high CM efficiency as possible.

The experiments described below are done for both the old setup with a tank valve head diameter of 16 mm and for the new setup with a pressure compensated tank valve with a tank valve head diameter of 28 mm.

From now and further on the tank valve with a valve head diameter of 16 mm will be referred to as "small tank valve" and the pressure compensated valve with a valve head diameter of 28 mm will be referred to as "large tank valve".

Optimizing the compressor mode, small tank valve

Trajkovic et al. [1] focused mainly on a valve strategy based on the polytropic compression law:

$$p_2 = p_1 \left(\frac{V_1}{V_2}\right)^{\kappa} \tag{1}$$

where p_1 corresponds to the pressure at BDC and p_2 is the pressure at any point in the cycle. V_1 is the maximal volume in the cylinder and V_2 is the cylinder volume at cylinder pressure p_2. By setting p_2 equal to the tank pressure, the volume at the given pressure can be calculated and from that it is possible to calculate proper tank valve timings. A drawback with this strategy is that the polytropic exponent, κ, depends on the heat losses and setting this ratio to constant value introducers some errors to the tank valve control algorithm. In order to avoid this error, a method for optimizing the CM has been suggested by Trajkovic et al. [1]. The main idea with this method is to find the most optimal valve timing at a given tank pressure and, in order to do that, the tank pressure needs to be constant throughout the whole

testing interval. With the aid of a pressure relief valve it is possible to change the pressure level in the system. The pressure in the tank will become constant when the amount of air charged into the tank is equal to the amount of air released from the tank and by adjusting the pressure relief valve opening angle it is possible to set a desired steady-state tank pressure.

Figure 7 shows a TankVO optimization sweep for the small tank valve at various steady-state tank pressures. TankVC, IVO and IVC were set to a constant value at this optimization. It can clearly be seen how negative IMEP is affected by TankVO timing during optimization of CM. The figure shows that there is an optimal TankVO timing for every tank pressure when taking highest efficiency into consideration, highest efficiency corresponds to the minimum in each curve. This means that it takes less power to compress the inducted air at this point than at any other point on the curve at a given tank pressure. If higher braking torque is needed, the efficiency has to be sacrificed.

The reason why negative IMEP increase at early TankVO is that when the tank valve opens earlier than optimal, there will be a blowdown of compressed air into the cylinder due to the fact that the pressure level in the cylinder is lower than in the pressure tank. At a certain premature TankVO, negative IMEP will dramatically increase with increasing tank pressure, due to a larger pressure level difference between the cylinder and the pressure tank.
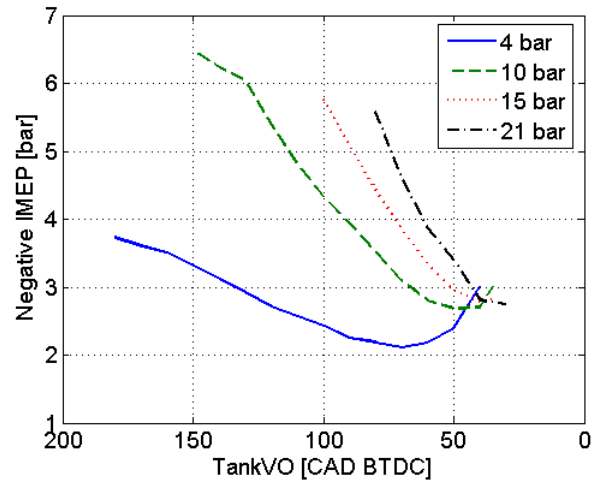

Figure 7 Negative IMEP obtained during steady-state CM as a function of TankVO for the small tank valve setup during optimization of CM at various tank pressures and an engine speed of 600 rpm

Figure 8 shows how optimal TankVO and corresponding negative IMEP varies with increasing tank pressure. The reason why the negative IMEP decrease after a tank pressure of approximately 14 bar, is that the optimization has been done with focus on TankVO while TankVC has been set to a constant value of 10 CAD ATDC. Constant

TankVC will affect the negative IMEP at higher tank pressures because ideally TankVC should be retarded towards TDC with increasing tank pressure. IVO should be set in such way that the pressurized air trapped in the cylinder after TankVC will be expanded to atmospheric pressure. At higher tank pressures, a late TankVC means that the in-cylinder pressure is higher than desired, and this excess pressure pushes the piston as it moves towards BDC and thereby contributes with positive IMEP which decreases the negative IMEP for the whole cycle.
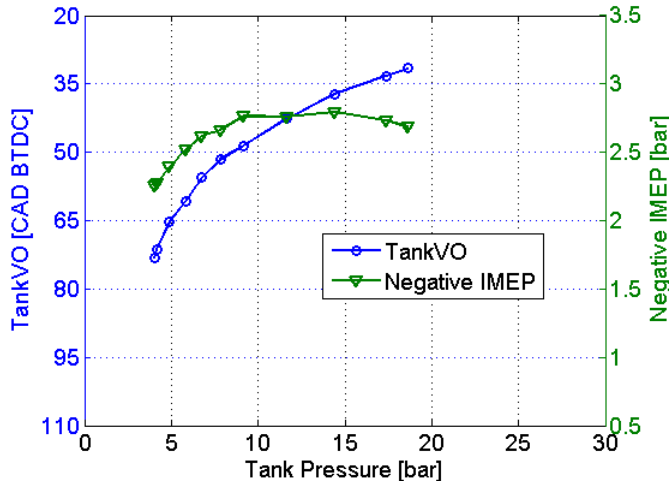

Figure 8 TankVO and negative IMEP as a function of tank pressure for the small tank valve setup at an engine speed of 600 rpm
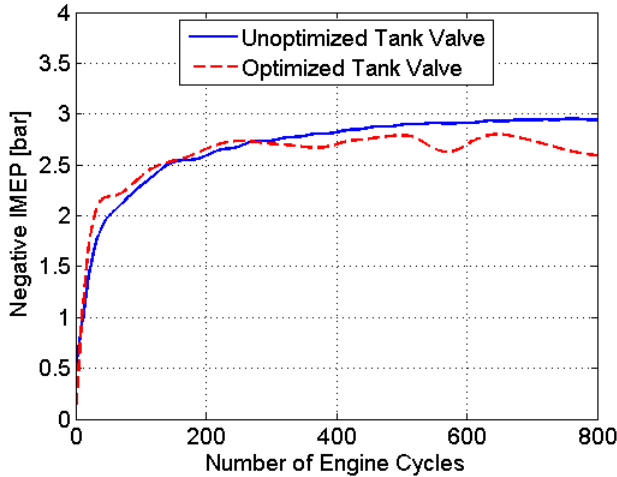

Figure 9 Comparison of negative IMEP for unoptimized and optimized TankVO as a function of engine cycle number during CM operation for the small tank valve setup. End tank pressure is about 21 bars in both cases

CM operation testing has been done both with an unoptimized tank valve, i.e. the feedback control of the tank valve was based on equation (1), and with the optimal TankVO timings seen in Figure 8. The result can

be seen in Figure 9 where negative IMEP for both the unoptimized tank valve and the optimized tank valve is shown. Initially, negative IMEP for the unoptimized tank valve is similar to negative IMEP for the optimized tank valve, but after about 300 engine cycles negative IMEP for the optimized tank valve remains reasonably constant while negative IMEP for the unoptimized tank valve continues to increase throughout the rest of the test.

The reason why negative IMEP is decreasing during optimized tank valve operation between 600 and 800 engine cycles is that the optimization is based on the valve timings shown in Figure 8, and thus the same IMEP behavior is expected.

Optimizing the compressor mode, large tank valve

In order to reduce the pressure drop over the tank valve the small valve has been replaced with a valve that has a larger valve head diameter in combination with the previously described pneumatic spring arrangement.
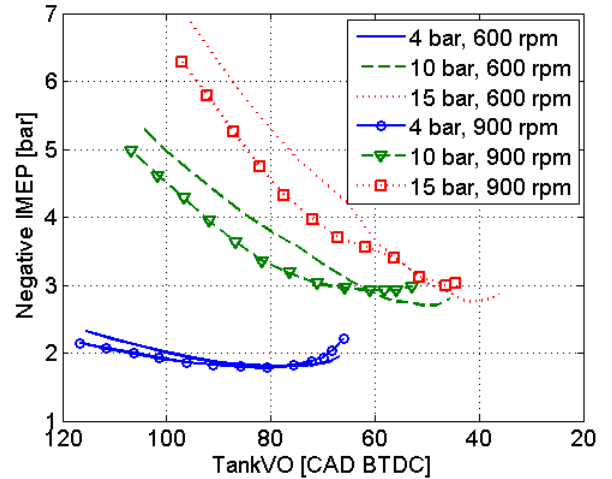

Figure 10 Negative IMEP obtained during steady-state CM as a function of TankVO for the large tank valve setup at various tank pressures for engine speeds of 600 and 900 rpm

Figure 10 shows a TankVO optimization sweep for the large tank valve at various steady-state tank pressures, similar to the TankVO sweep in Figure 7. With the larger valve, the negative IMEP at a tank pressure of 4 bar and at optimal TankVO for both 600 and 900 rpm is lower compared to the negative IMEP in Figure 7 at the same tank pressure. This is because the pressure drop is decreased due to the larger tank valve head diameter. At 10 and 15 bars, there is hardly any difference between negative IMEP for the large tank valve compared to the small tank valve. The only difference is that the optimal TankVO for the large tank valve is advanced a number of CAD compared to TankVO for the small valve. One of the reasons for this behavior is most likely that there is a blowdown of pressurized air into the cylinder through the

tank valve. It seems as the tank valve is not completely pressure compensated as expected and thus there exist a net force acting to open the tank valve. Another reason is that there is some pressure losses in the pressurized air supply line between the tank and the pneumatic valve actuator, which means that the pressurized air fed to the valve actuator at a certain time is not the same as the mean tank pressure at the corresponding time and therefore the ability to open the tank valve at optimal timing is lost and has to be advanced. An advance in TankVO compared to optimal timing means that there will be a blowdown of pressurized air into the cylinder and thus negative IMEP will increase. The reason why negative IMEP for the large tank valve is considerably lower than for the small tank valve at 4 bars tank pressure is that at this tank pressure level, the actuator is fed with 6 bars of compressed air from an external source. This means that, at this point there is a surplus of 2 bars feeding the valve actuator and thus the optimal TankVO timing can be achieved.

Another observation that can be made from Figure 10 is that at a certain tank pressure, there is a difference in negative IMEP between the case at 600 rpm and the case at 900 rpm. The reason is that at a higher engine speed, there will be less time for the blowdown process previously described and thereby its effect on the negative IMEP will be less.

Figure 11, Figure 12 and Figure 13 show how optimal TankVO and corresponding negative IMEP varies with increasing tank pressure at various engine speeds for the large tank valve setup. Comparing negative IMEP from Figure 11 with negative IMEP from Figure 8 indicates that the pressure losses over the valve are lower with the large valve than with the small valve. If focus is put on the TankVO, it can clearly be seen that the optimal TankVO for the large tank valve is occurs considerably earlier compared to the optimal TankVO for the small tank valve. The reason for this behavior can once again be explained as inadequate amount of pressurized air supplied to the tank valve actuator and therefore the valve timing has to be advanced a number of CAD away from the real optimum, which contributes to a higher negative IMEP.

It can also be seen that TankVO advances with engine speed at the same tank pressure with the reason being the same as stated previously. As the engine speed increase, the pressure tank charging rate increase faster than the supply rate of compressed air to the actuator due to restrictions in the pressurized air supply line between the pressure tank and the valve actuator. The result is that at a certain time, mean tank pressure will be higher than actuator supply pressure. As engine speed increase, the pressure difference between the tank pressure and the actuator supply pressure will also increase. Therefore TankVO has to be advanced with increasing engine speed.
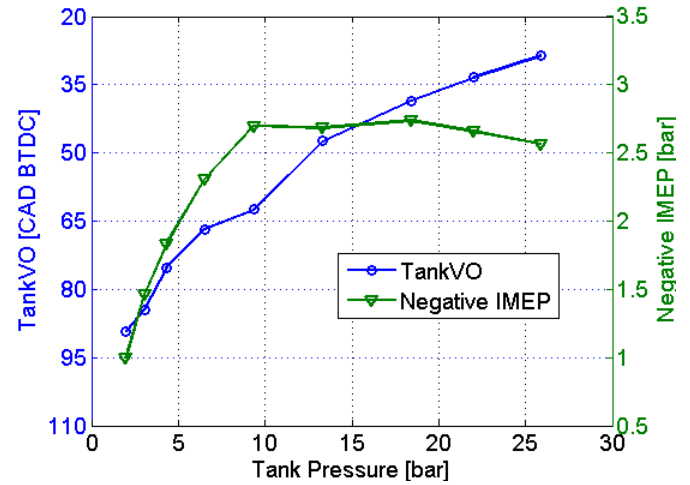

Figure 11 Optimized TankVO timing and corresponding negative IMEP during CM optimization as a function of tank pressure for the large tank valve setup at an engine speed of 600 rpm
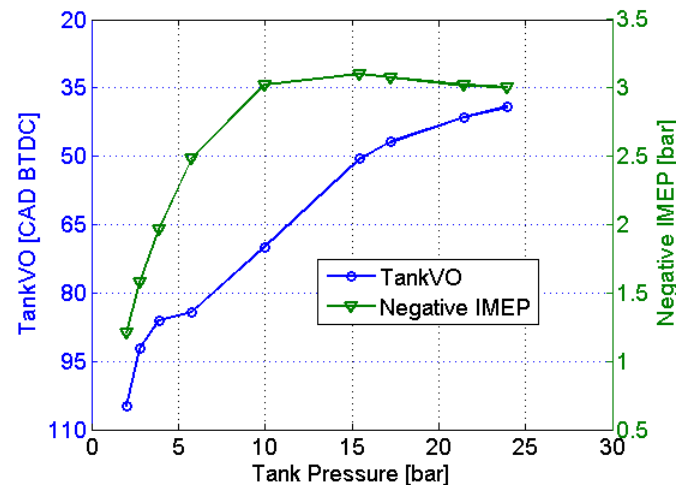

Figure 12 Optimized TankVO timing and corresponding negative IMEP during CM optimization as a function of tank pressure for the large tank valve setup at an engine speed of 900 rpm

Notice that at a tank pressure of 4 bars, negative IMEP at all three engine speeds presented in Figure 11, Figure 12 and Figure 13, are lower than negative IMEP shown in Figure 8. This is once again due to the surplus of 2 bars in the pressurized air supply line feeding the tank valve actuator since the compressed air source is external with an air pressure set to 6 bars. This indicates that in order to achieve optimal TankVO timing, there should always be a surplus of minimum 2 bars in the supply line to compensate for all the pressure losses through it.
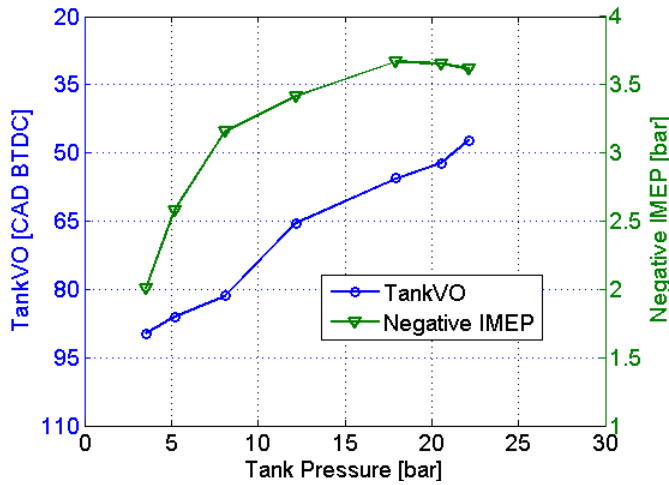
Figure 13 Optimized TankVO timing and corresponding negative IMEP during CM optimization as a function of tank pressure for the large tank valve setup at an engine speed of 1200 rpm

Comparing Figure 11, Figure 12 and Figure 13 with one another indicates that at equal tank pressure, negative IMEP increases with engine speed. This is due to the fact that with increasing engine speed there is less time to vent the cylinder from compressed air and thus there will be an overshoot in cylinder pressure which increases with increasing engine speed. This is illustrated in Figure 14.
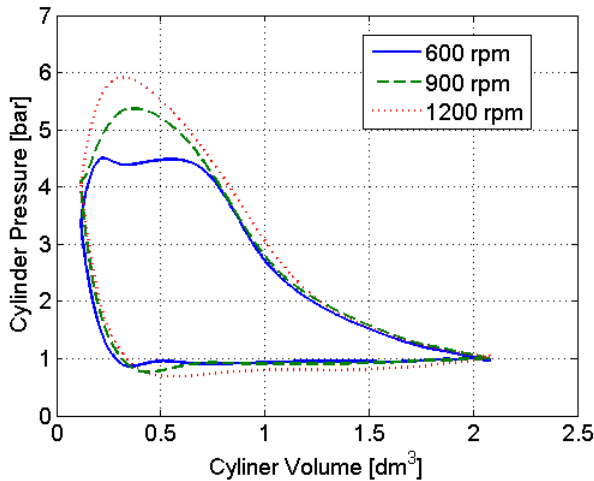

Figure 14 PV-diagram during CM for three different engine speeds at 4 bars of tank pressure

Figure 15 shows negative IMEP during optimal CM at three different engine speeds for the large tank valve setup. Comparing the result displayed in Figure 15 with the result from the optimized test shown in Figure 9 indicates that there is only a difference the first 200 cycles. The results obtained with the large tank valve shows that IMEP is lower than the corresponding results

obtained with the small tank valve which verifies that increasing the tank valve diameter decreases the pressure drop over the tank valve. The reason why negative IMEP is almost the same in both cases after 200 cycles is probably once again insufficient pressure in the compressed air supply line feeding the tank valve actuator.
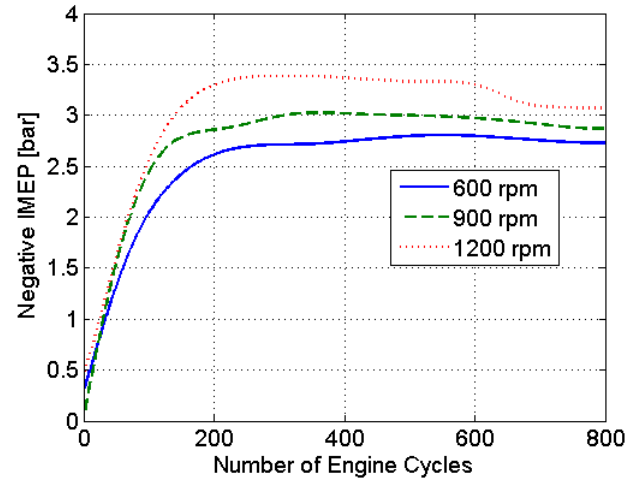

Figure 15 Negative IMEP during optimal CM as a function of engine cycle number at three different engine speeds for the tank valve setup

The corresponding mean tank pressure as a function of engine cycle number at three different engine speeds can be seen in Figure 16. There is a slight difference between the curves. The end pressure at 900 rpm is higher than at both 600 and 1200 rpm. This can probably be explained with tank pressure leakage into the cylinder through the tank valve. This would mean that there exists a net force acting to open the tank valve and in that case the tank valve is not pressure compensated. Since leakage of compressed air through an orifice is constant in time at a constant pressure, the amount of air inducted into the cylinder per cycle due to leakage will decrease with increasing engine speed, and thus the end tank pressure should reach a higher level. At 1200 rpm, this explanation is not enough since the end tank pressure is at the same level as at 600 rpm. Careful observation of the tank pressure curve at 1200 rpm in Figure 16, indicates that it follow the tank pressure curve at 900 rpm quite well up to approximately 600 engine cycles and then it starts to deviate and ends at the same pressure level as at 600 rpm. The reason is probably that, during this specific test run, the tank valve actuator didn't behave as expected. This can be verified from Figure 15, where negative IMEP at 1200 rpm starts to decrease at about 600 cycles. The reason for this behavior is that, due to inexplicable performance of the tank valve actuator, the duration of maximum valve lift abruptly decreases after 600 cycles, as displayed in Figure 17. A shorter duration means that there will not be enough time to vent the cylinder on pressurized air and therefore the cylinder will still be filled with pressurized air at tank valve closing. This excess of

compressed air pushes the piston as it moves towards BDC and thus contributes with positive IMEP, which in turn decreases negative IMEP for the whole cycle.
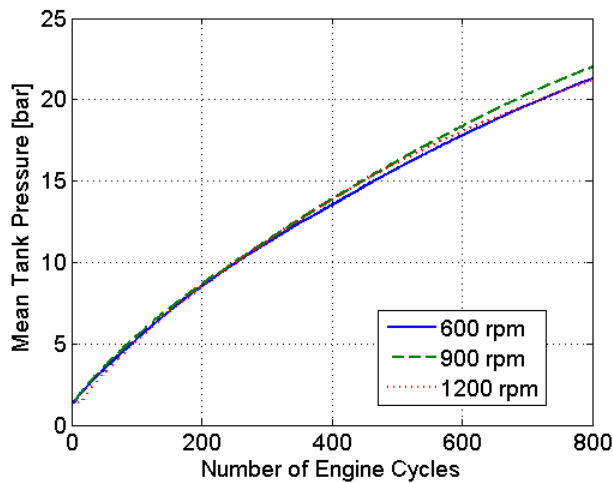

Figure 16 Mean tank pressure as a function of engine cycle number at three different engine speeds
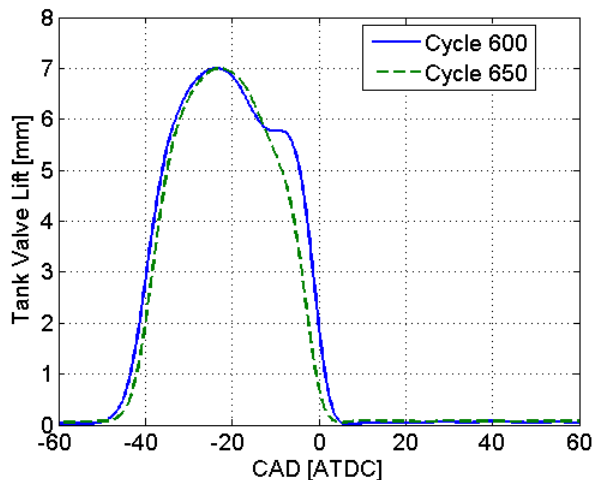

Figure 17 Tank valve lift at two different engine cycles at an engine speed of 1200 rpm

Figure 18 and Figure 19 displays the port temperature immediately after the tank valve and the temperature in the pressure tank, respectively, at three different engine speeds. The results indicate that there is a considerable amount of heat losses through the system. The explanation is that the metal tubing, which connects the cylinder head with the tank, and the pressure tank are not heat insulated in any way. Therefore, a considerable amount of the total thermal energy generated during CM will be transferred to the surroundings and thus the total efficiency of the pneumatic hybrid will be decreased.
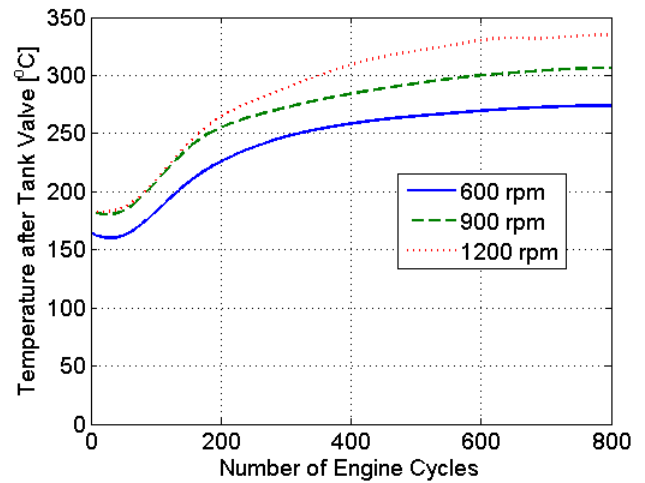

Figure 18 Temperature after tank valve (port temperature) as a function of engine cycle number at three different engine speeds
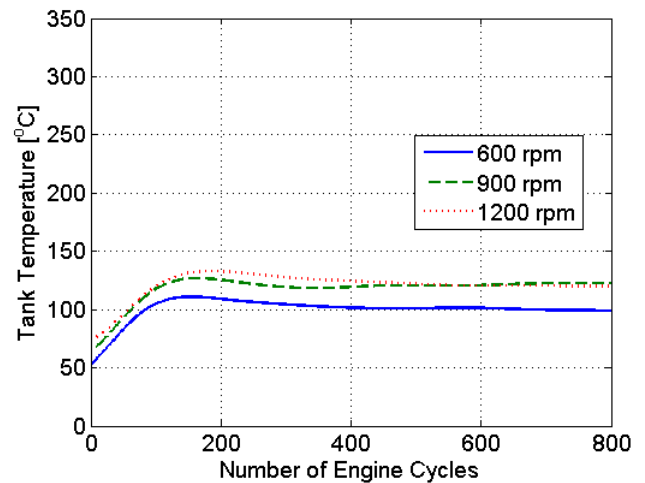

Figure 19 Pressure tank temperature as a function of engine cycle number at three different engine speeds

Figure 20 and Figure 21 illustrates the pressure drop over the small tank valve and the large valve, respectively, obtained at three different engine speeds during CM. The hump-like behavior between 100 and 200 engine cycles at both 900 and 120 rpm in Figure 21 occurs due to the pressurized air source switching system described earlier. As the tank pressure is reaching a pressure level close to the switching pressure level, the tank valve lift height is decreasing, as can be seen in Figure 22. The tank valve lift has decreased by almost 1 mm at engine cycle 150 compared to cycle 100. At cycle 200 the tank valve lift height has nearly returned to a maximum. The reason for this behavior is thought to be bad interaction between the check-valves due to pressure oscillations in the pressurized air supply line. During normal running conditions one of the check-valves will be completely open, but during the transition period, both check-valves will open and close frequently

due to the pressure oscillations, which lead to a deficit in pressure and thus the valve lift will decrease.
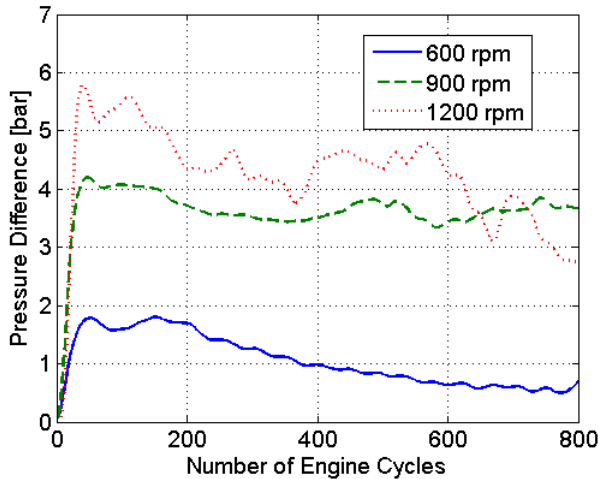

Figure 20 Pressure difference between maximum in-cylinder pressure and maximum pressure after the tank valve (port pressure) as a function of engine cycle number at various speeds. Tank valve with small diameter was used during this test.
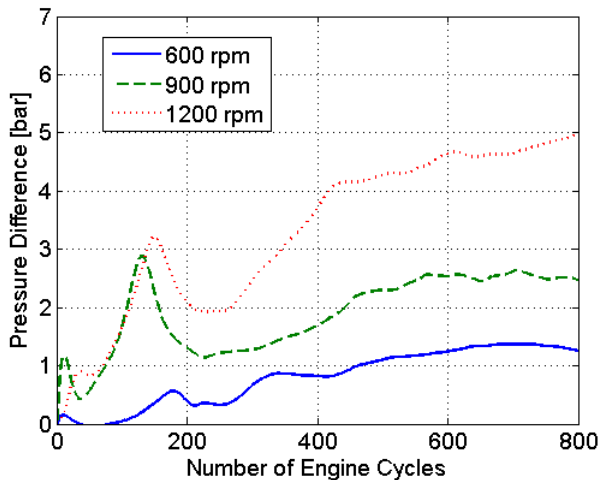

Figure 21 Pressure difference between maximum in-cylinder and maximum pressure after the tank valve (port pressure) as a function of engine cycle number at various engine speeds. Tank valve with large diameter was used during this test.

Another observation made from Figure 20 and Figure 21 is that the curves displayed in Figure 21 are indicating an increasing trend, while the curves in Figure 20 are decreasing or somewhat constant throughout the whole test. The reason is, as stated before, insufficient pressure in the pressurized air supply line feeding the tank valve actuator which forces TankVO to deviate from the optimal timing, and thereby the pressure difference between the pressure after the valve and the cylinder pressure will increase.
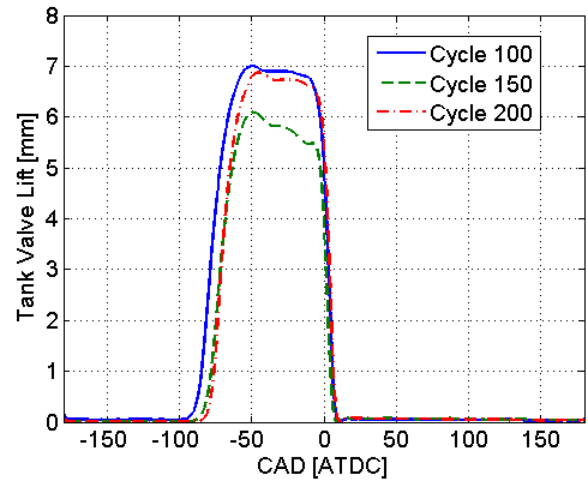

Figure 22 Tank valve lift at three different engine cycles and at an engine speed of 1200 rpm

Figure 23 and Figure 24 show cylinder pressure at a mean tank pressure of 8 bars for the small tank valve setup and the large tank valve setup, respectively. It can clearly be seen that the pressure losses over the small tank valve are considerably higher than they are with the larger tank valve. This is mainly because choking occurs over the small tank valve which limits the air flow and thereby the pressure will increase. Figure 23 and Figure 24 indicates that this overshoot in pressure can be lowered dramatically if the small tank valve diameter is increased.
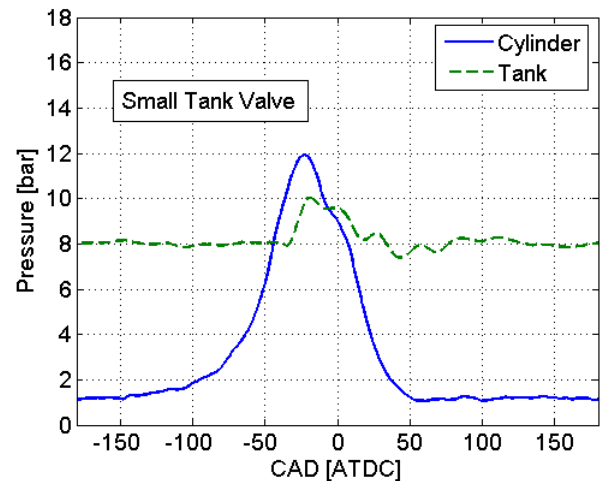

Figure 23 In-cylinder pressure and tank pressure during CM with a small valve diameter at revolution 200 and an engine speed of 600 rpm
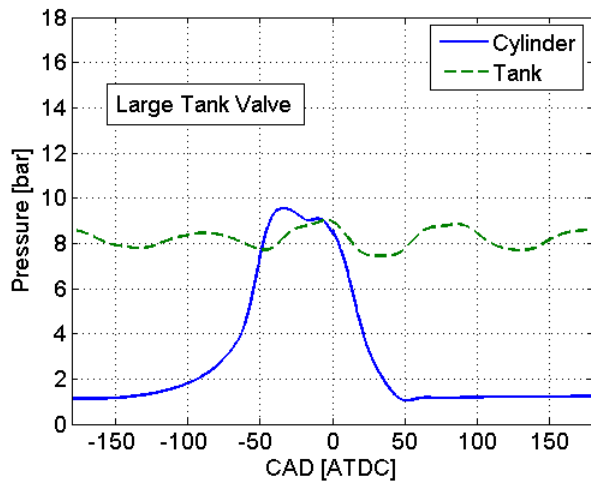
Figure 24 In-cylinder pressure and tank pressure during CM with a large valve diameter at revolution 200 and an engine speed of 600 rpm

The cylinder pressure curves from Figure 23 and Figure 24 can be seen in the form of PV-diagrams in Figure 25. The PV-diagram for the large tank valve setup, bear a great resemblance to an ideal CM PV-diagram, with an almost constant cylinder pressure between cylinder volume 0.5 and 0.2 dm^3. It can be noticed that for the case with the large tank valve, at approximately 0.7 dm^3, the cylinder pressure deviates from the small tank valve pressure trace. The cause is that TankVO is advanced a number of CAD in comparison to optimal tank valve timing due to reasons already stated in this paper, namely insufficient pressure in the compressed air supply line feeding the tank valve actuator.
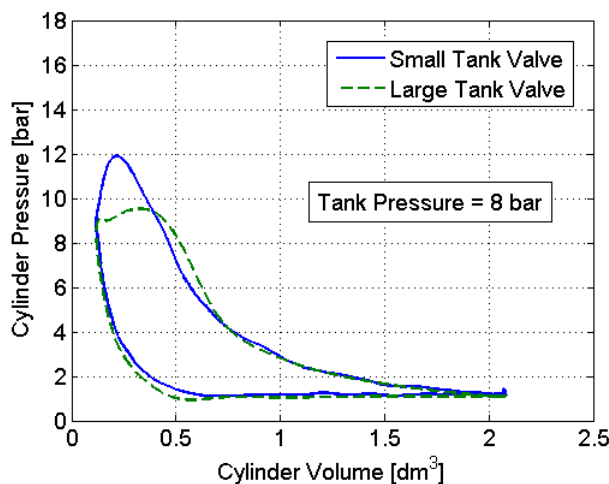

Figure 25 PV-diagrams for two different tank valve diameters at a tank pressure of 8 bars

Figure 26 illustrates how the pressure in the port, immediately after the tank valve varies during one engine cycle for both the small tank valve setup and the large valve setup. The major difference between the curves is the large pressure oscillation during the entire cycle for the test carried out with the large tank valve.

The reason for this occurrence is that the metal tubing for the large tank valve setup has a larger diameter than for the small valve setup. The increase in diameter eliminates the possibility of having any choking in the tubing, but instead the pressure oscillations through it increase. If the tank valve opens when the pressure oscillation at the valve is at a local maximum, the cylinder will be filled with some additional air, which in turn leads to a higher negative IMEP.
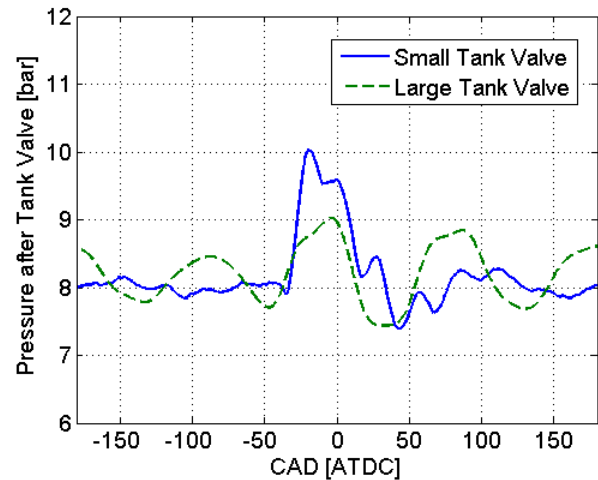

Figure 26 Pressure after the tank valve for two different tank valve diameters

AIR-MOTOR MODE

The AM can, as CM, mainly be executed in three ways – in regards to efficiency, power, or a combination of both. Achieving highest air-motor efficiency is done by a feedback control of both the tank valve and the intake valve. The tank valve should open at TDC and TankVC should be set in such way that the pressurized air is expanded to atmospheric pressure at BDC. The intake valve should open at BDC and IVC should be set in such way that when the piston reaches TDC, the inducted air is compressed to the same level as the tank pressure level.

In order to accelerate the vehicle more rapidly compared to the high-efficiency case, high power is needed. This can be achieved by prolonging the tank valve duration compared to the optimal timing and thereby induct more compressed air which increases the work done on the piston. Highest air-motor power is achieved with TankVC at BDC or shortly before. The inlet valve should be controlled in the same manner as with the high-efficiency method.

In a real application, a combination of the previously explained methods will be utilized. For instance, as long as the driver presses the gas pedal moderately, the AM will be operated at highest efficiency or close to it. As the driver continues to press the pedal towards its end

position, the AM operation will drift away from highest efficiency towards maximum air-motor power.

This study focuses mainly on the first method, namely achieving as high AM efficiency as possible.

Optimizing the air-motor mode

An attempt to use the polytropic compression law, in order to achieve a proper valve strategy during AM, has been done. TankVC is controlled in such way that at a certain tank pressure, a proper closing angle is calculated with the help of the polytropic relation. Also the IVC is calculated in a similar way. TankVO and IVO are set to a constant value of 0 CAD ATDC and 180 CAD BTDC, respectively. TankVC and corresponding positive IMEP obtained with this method can be seen in Figure 27. These results are quite poor compared to the results shown by Trajkovic et al [1], where IMEP levels of 4 bars have been shown with constant valve timings. The reason is that, as stated before, the specific-heat ratio depends on the heat losses and setting this ratio to a constant value introduces some errors to the valve control algorithm. Also, the polytropic relation doesn't take the pressure losses over the tank valve into account, and therefore the TankVC will be chosen closer to TDC than what would be optimal.
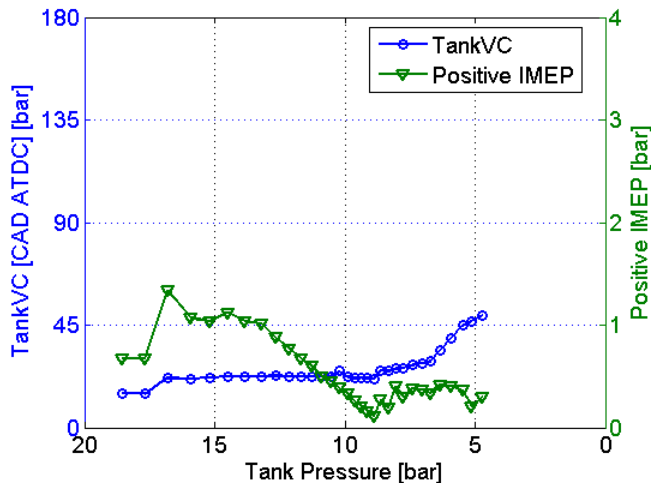

Figure 27 TankVO and corresponding positive IMEP during AM as a function of tank pressure for the large tank valve setup at an engine speed of 600 rpm. TankVO timings are based on the polytropic relation.

In order to optimize the AM, there is a need for a method that can help finding the optimal valve timings. The steady-state method, used for optimizing the CM, cannot be used in order to optimize the AM, since there is no charging of the pressure tank during AM and thereby a steady-state tank pressure cannot be achieved.

A method for finding the optimal IVC has been developed. The idea is to vary IVC and thus the corresponding peak cylinder pressure will also be varied.

In that way a map, containing IVC as a function of peak cylinder pressure can be created.

In order to find the optimal TankVC, results from the CM optimization, shown in Figure 11, have been used. During the compression stroke in CM, the atmospheric air in the cylinder is compressed to the same pressure level as the tank pressure level before the tank valve opens. In AM, the procedure should be the opposite. The pressure level in the cylinder is the same as the tank pressure level when the tank valve is supposed to close. The pressurized air is then expanded to the atmospheric pressure level. Thereby the results obtained during CM optimization can, with some modification, be used to control the valve during AM. In order to fit the results from CM to AM, some tuning of the valve timings had to be done.

Figure 28 shows the final results from AM testing where both IVC and TankVC have been optimized with the methods described above. Comparing the results from Figure 28 with the results from Figure 11 indicates that the curves bear a resemblance to one another. But there are some differences, mainly for the TankVC. For instance, at a tank pressure of 20 bars, the results in Figure 28 indicates a TankVC at approximately 33 CAD ATDC, while the results in Figure 11 indicates a TankVO at approximately 38 CAD BTDC. The difference of 6 CAD is due to the fact that IVC during AM is chosen in such way that the peak in-cylinder pressure is lower than the tank pressure when the tank valve opens, which can be seen in Figure 29. Thereby, the deficit in the pressurized air supply line is compensated for.
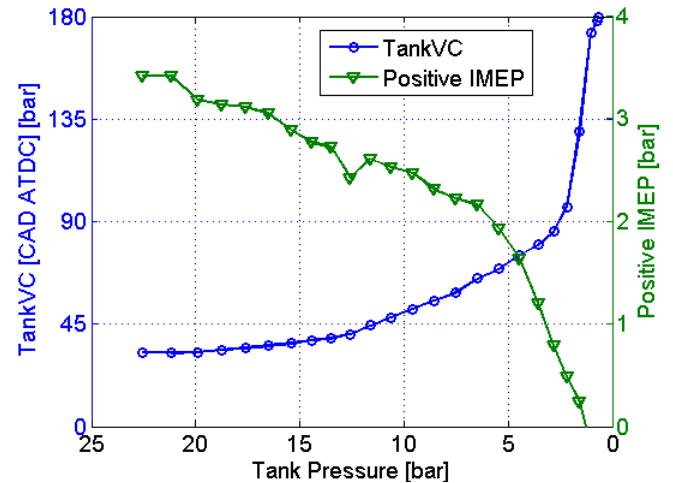

Figure 28 Optimized TankVO and corresponding positive IMEP during AM as a function of tank pressure for the large tank valve setup at an engine speed of 600 rpm
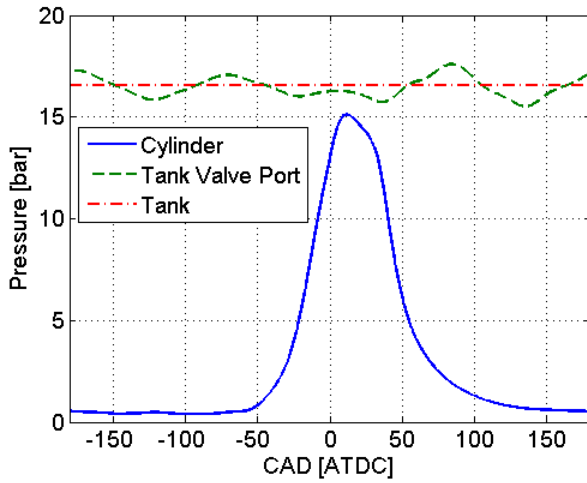
Figure 29 Illustration on the difference between the tank valve port pressure and the cylinder pressure at TankVO during AM operation

Figure 30 shows positive IMEP obtained with two different tank valve setups and valve strategies during AM operation. The small tank valve curve has been obtained with the constant valve timings displayed in Table 4. The large tank valve curve has been obtained with the optimal valve timings shown in Figure 28. The starting tank pressure is about 20 bars in both cases. It can be realized that, an increase in valve head diameter together with optimal valve timings, has a large impact on the AM operation. This will in turn lead to a considerable increase in the AM total efficiency. The reason why IMEP for the large tank valve setup is much higher throughout the whole test compared to the small tank valve setup, is that the pressurized air is used in a much more efficient way. A larger tank valve diameter contributes to less pressure losses over the tank valve and an optimized valve control strategy contributes to a more efficient use of the pressurized air, and together they contribute to a higher positive IMEP.
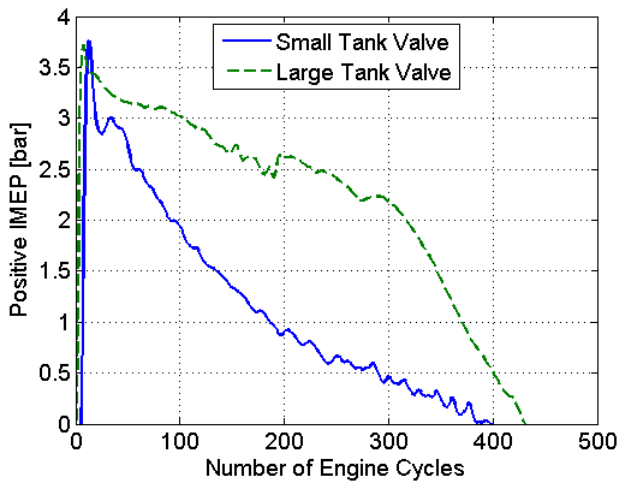

Figure 30 Positive IMEP for two different tank valve setups and valve strategies as a function of engine cycle number at an engine speed of 600 rpm during AM operation

Table 4 Valve timing used for the small tank valve setup during AM operation

IVO [CAD BTDC]	180
IVC [CAD BTDC]	0
TankVO [CAD ATDC]	-5
TankVC [CAD ATDC]	40

Figure 31 shows the tank pressure decrease for the small tank valve setup and large tank valve setup, obtained during the test displayed in Figure 30. With the large tank valve, the tank pressure decreases almost linearly. With the smaller valve, the tank pressure has a higher rate of discharge in the beginning, but after about 150 cycles the discharge rate starts to decrease. The reason for this behavior is that the valve timings with the small tank valve are set to a constant value. This means that in the beginning the tank valve duration is much longer than the optimal tank valve duration, and thereby the cylinder will be filled with more compressed air, thus leading to a higher rate of discharge of the tank pressure for this case. After a while, as the tank pressure decrease, the duration becomes too short and the cylinder is filled with less air than is optimal and thereby the tank pressure discharge will decrease.
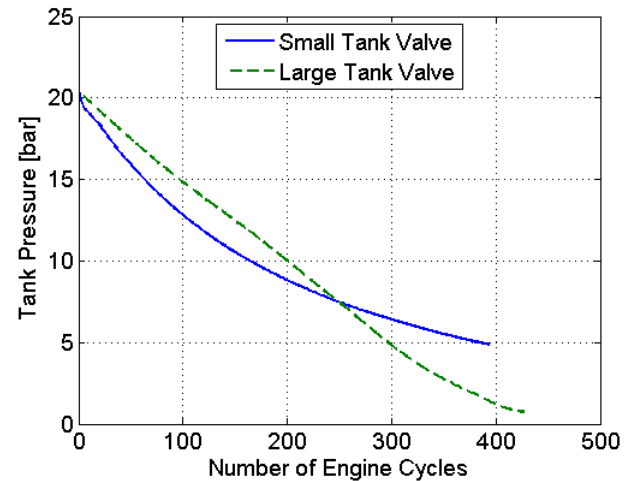

Figure 31 Mean tank pressure for two different valve geometries at an engine speed of 600 rpm

Figure 32 and Figure 33 illustrates PV-diagrams for both tank valve setups at tank pressures 16.5 bars and 6.5 respectively. There are evident differences in peak cylinder pressure between the small tank valve setup and the large tank valve setup in both figures. The reason is that the flow over the small tank valve will become chocked due to a very restricted flow area. With the larger tank valve, the flow area is increased more than three times compared to the small tank valve flow area and therefore the threshold for choked flow has been raised. Another issue with constant tank valve timing, which can be seen in Figure 33, is that one portion of the PV-curve indicates negative IMEP. Too

short tank valve duration at a certain tank pressure will lead to an expansion of the inducted pressurized air below atmospheric pressure thus generating vacuum. Generation of vacuum is an energy consuming process, at least in this case. Since the inlet valve opens at BDC, the vacuum is canceled by the induction of fresh air into the cylinder and thereby the vacuum created cannot be used as an upward-acting force on the piston as it moves towards TDC.
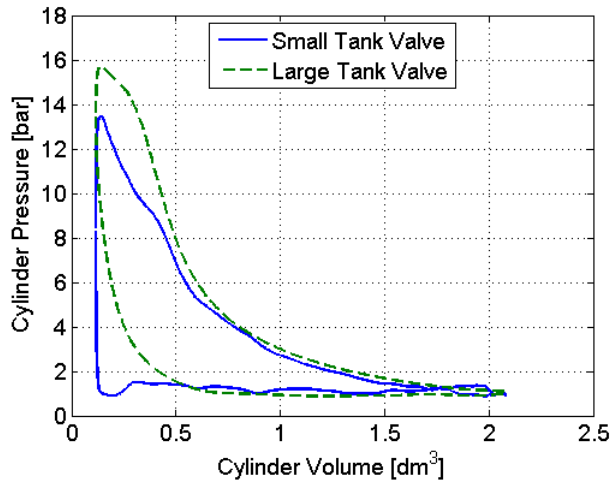

Figure 32 PV-diagram for two different tank valve geometries at a tank pressure of 16.5 bars and an engine speed of 600 rpm
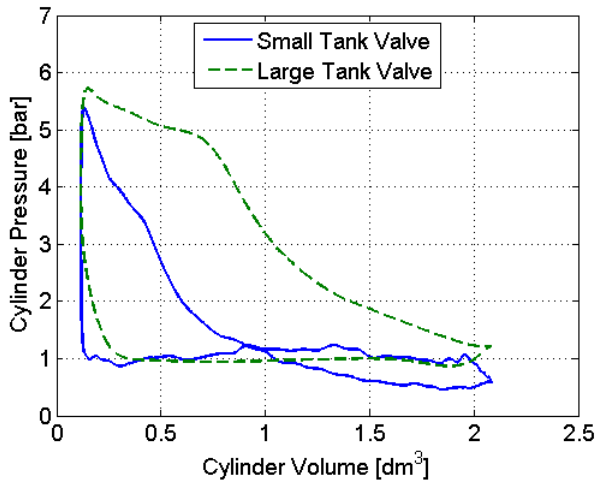

Figure 33 PV-diagram for two different tank valve geometries at a tank pressure of 6.5 bars and an engine speed of 600 rpm

During AM operation, the intake valve is controlled in such way that, the peak in-cylinder pressure should ideally be equal to the tank pressure. The reason is that in this way there will be a smooth filling of the cylinder when the tank valve opens. If the intake valve would close near TDC, the in-cylinder pressure at TDC would be close to atmospheric, and thus the compressed air from the pressure tank would rush into the cylinder as

the tank valve opens. Since a rush of compressed air into the cylinder would contribute with a higher air flow velocity compared to a smooth filling of the cylinder, the pressure drop over the vale, which increases with speed, would increase. Figure 34 shows the results obtained both from a test with constant IVC and from a test with open-loop controlled IVC. With the intake valve closing near TDC, positive IMEP reaches a level almost two bars higher than with the open-loop controlled intake valve. The reason behind this behavior is that, with IVC set to TDC, compression of inducted air, which is an energy consuming process, is eliminated.
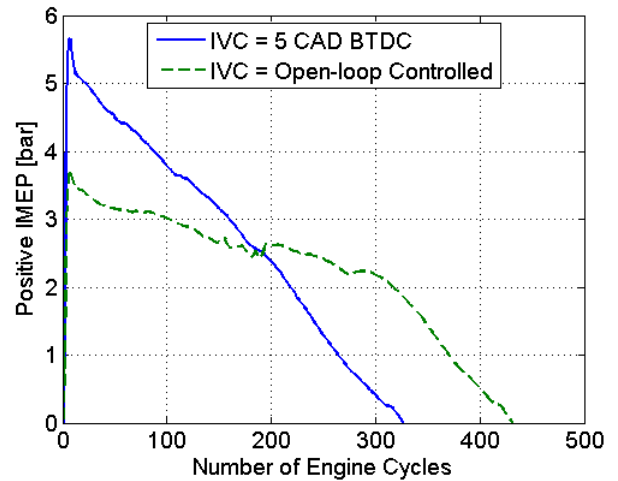

Figure 34 Positive IMEP during AM, solid line represents an AM test run with constant IVC while the dashed line represents an AM test run with IVC open-loop controlled

In Figure 34 the rate of decrease for positive IMEP is higher with constant IVC than with open-loop controlled IVC. This can be explained with the help of Figure 35, which shows the tank pressure as a function of engine cycles from the tests shown before in Figure 34. It can be seen that the rate of discharge is greater for the test with constant IVC, compared to the test with feedback controlled IVC. This implies that, the strategy with constant IVC, which leads to a rush of compressed air into the cylinder, contributes to higher compressed air consumption due to pressure losses over the tank valve.
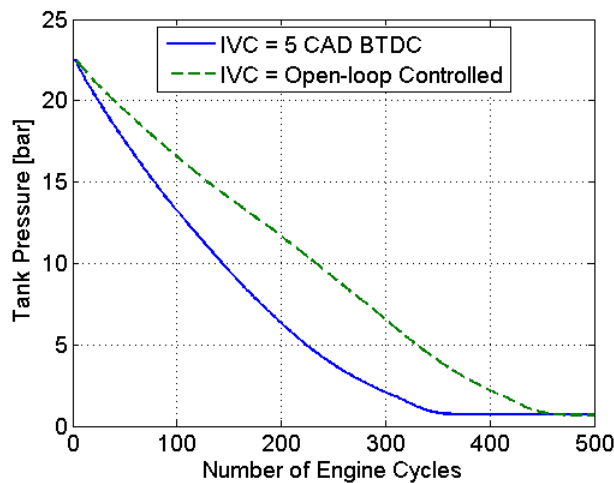
Figure 35 Tank pressure during AM, solid line represents an AM test run with constant IVC while the dashed line represents an AM test run with IVC open-loop controlled

Figure 36 shows torque for both constant IVC and open-loop controlled IVC. The result is quite impressive for a 2-litre engine operating without any combustion. The reason behind the large difference in maximum torque between the curves is that due to that rushing compressed air flow hits the piston with a huge force when the tank valve opens. With feedback controlled IVC, compressed air enters the cylinder smoothly and therefore no shock force will be generated.
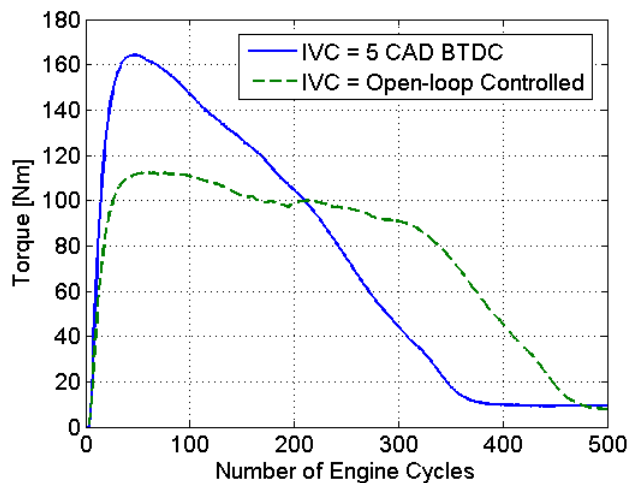

Figure 36 Torque during AM for both constant IVC timing and open-loop controlled IVC at an engine speed of 600 rpm

Figure 37, Figure 38 and Figure 39 illustrates PV-diagrams for both intake valve strategies at tank pressures 16.5 bars and 6.5 respectively. The pressure curve, obtained with constant IVC, has an overshoot at TDC compared to the curve obtained with open-loop controlled IVC. The reason is that as the compressed air starts to rush into the cylinder, a pressure wave is

generated which propagates though the cylinder and out again through the open tank valve. A close-up of the PV-diagrams in Figure 37 is illustrated in Figure 38. It can clearly be seen that with constant IVC, the cylinder pressure overshoots at first and then decreases bellow the cylinder pressure obtained with open-loop controlled IVC. This indicates that there is a pressure wave propagating through the cylinder.

Figure 37 PV-diagram obtained during AM at a tank pressure of 16.5 bar and at an engine speed of 600 rpm, solid line represents an AM test run with constant IVC while the dashed line represents an AM test run with IVC open-loop controlled

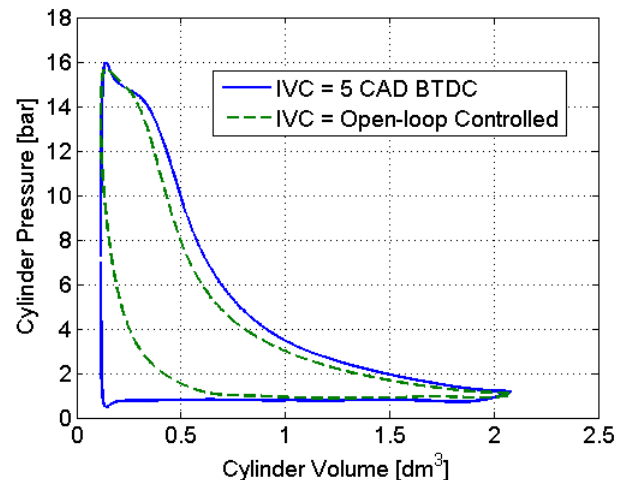**Figure 38 Close-up of the PV-diagrams at a tank pressure of 16.5 bars shown in Figure 37**

Figure 39 PV-diagram obtained during AM at a tank pressure of 6.5 bar and at an engine speed of 600 rpm, solid line represents an AM test run with constant IVC while the dashed line represents an AM test run with IVC open-loop controlled
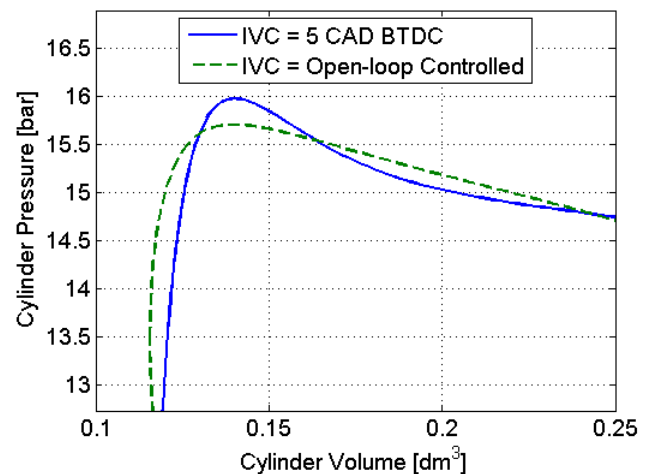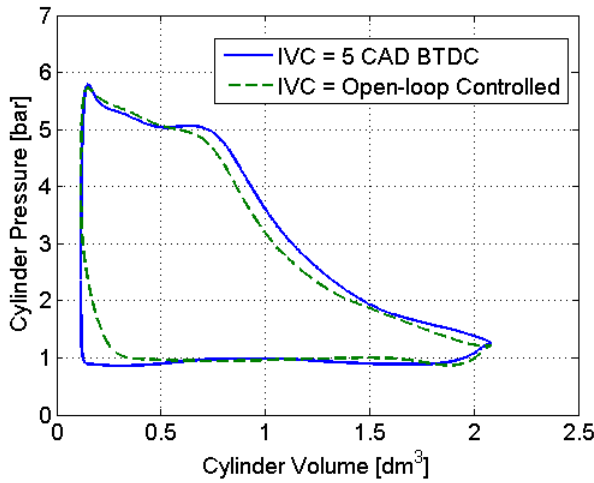
REGENERATIVE EFFICIENCY

In order to estimate the potential of the pneumatic hybrid, and the possibility to compare different tests with each other, a regenerative efficiency has to be calculated. The regenerative efficiency is the ratio between the energy recovered during AM and the energy consumed during CM. It can also be defined as the ratio between positive and negative IMEP:

$$\eta_{regen} = \frac{IMEP_+}{IMEP_-} \qquad (2)$$

Table 5 show the regenerative efficiency with different tank valve setups and valve strategies at three engine speeds. The regenerative efficiency obtained with the small tank valve setup is retrieved from [1]. It has a maximum value of 33% at 900 rpm. The reason why the efficiency is higher at 900 rpm than at 600 rpm, as explained by Trajkovic et al. [1], is that the unoptimized feedback controller by coincidence is better suited for the case at 900 rpm than at 600 rpm. The regenerative efficiency for the large tank valve setup indicates that with optimized tank valve timing, the maximum efficiency occurs at 600 rpm and decreases with increasing engine speed. A tremendous improvement has been achieved while switching from the small tank valve setup to the large tank valve setup. The improvement mainly depends on a larger tank valve head diameter and optimized tank valve timing during AM. A change in inlet valve strategy from constant IVC to open-loop controlled IVC, increases the regenerative efficiency further.

The pneumatic tank valve actuator consumes energy in the form of compressed air from the pressure tank. Since its energy consumption decreases the total energy stored in the pressure tank, it has to be seen as energy losses. These losses have automatically been taken into

account in the calculation of regenerative efficiency. This is only valid for the large valve setup, since the pneumatic tank valve used in the small tank valve setup has been feed with compressed air generated from an external source. This means that the regenerative efficiency calculated for the large tank valve setup, is lower than it would be if the pneumatic valve actuator energy losses were excluded from the calculation.

Table 5 Calculated total regenerative efficiency for different tank valve setups and valve strategies at three different engine speeds

	η_{regen}		
Engine speed	600	900	1200
Small tank valve setup	32	33	25
Large Tank valve setup, constant IVC during AM	44	40	37
Large tank valve setup	48	44	40

It should be noticed that the regenerative efficiency, described in this paper is actually an indicated efficiency, apart from the included pneumatic valve actuator energy losses. This means that a real vehicle cannot utilize the energy in the same extent due, among other things, to engine and driveline friction losses, which will lead to a lower regenerative efficiency.

CONCLUSION

A pressure compensated tank valve with a valve head diameter of 28 mm has been tested and evaluated. The pressure compensation has been achieved with an in-house developed pneumatic valve spring arrangement mounted on the cylinder head. The evaluation has shown that there exists some trouble with the pneumatic valve spring concerning tank valve actuation, mostly because the pneumatic valve actuator is driven by compressed air from the pressurize air. This can be resolved by the use of externally generated pressurized air in order to drive the pneumatic tank valve actuator.

Results from tests done with the pressure compensated tank valve have been compared with results from tests where a tank valve with a valve head diameter of 16 mm has been used. The results indicate that the increase in valve diameter reduces the pressure drop over the tank valve, contributing to a higher regenerative efficiency.

Feedback control of tank valve timing based on the polytropic compression law is not suitable for the pneumatic hybrid. Instead, optimal tank valve timings can be obtained from steady-state engine testing.

Optimization of both tank valve timing and inlet valve timing for CM and AM contributes to an increase of the regenerative efficiency.

Test during AM with constant IVC versus open-loop controlled IVC, shows that a much higher torque can be achieved with constant IVC due to the blowdown of compressed air. The drawback is that such AM operation lowers the AM efficiency due to higher pressure losses.

The total regenerative efficiency has been increased from 33% with the small tank valve setup to 48% with the large tank valve setup, primarily due to a larger valve head diameter and optimal valve timing,

REFERENCES

1. S. Trajkovic, P. Tunestål, and B. Johansson, "Introductory Study of Variable Valve Actuation for Pneumatic Hybridization", SAE Paper 2007-01-0288, 2007.

2. C. Thai, T-C Tsao, M. Levin, G. Barta and M. Schechter, "Using Camless Valvetrain for Air Hybrid Optimization", SAE Paper 2003-01-0038, 2003

3. M. Andersson, B. Johansson and A. Hultqvist, "An Air Hybrid for High Power Absorption and Discharge", SAE paper 2005-01-2137, 2005

4. M. Schechter, "Regenerative Compression Braking – A low Cost Alternative to Electric Hybrids", SAE Paper 2000-01-1025, 2000

5. M. Schechter, "New Cycles for Automobile Engines", SAE paper 1999-01-0623, 1999

6. P. Higelin, A. Charlet, Y. Chamaillard, "Thermodynamic Simulation of a Hybrid Pneumatic-Combustion Engine Concept International Journal of Applied Thermodynamics", Vol 5, No. 1, pp 1 – 11, ISSN 1301 9724, 2002

7. S. Trajkovic, A. Milosavljevic, P. Tunestål, B. Johansson, "FPGA Controlled Pneumatic Variable Valve Actuation", SAE Paper 2006-01-0041, 2006

CONTACT

Sasa Trajkovic, PhD student, Msc M. E.

E-mail: Sasa.Trajkovic@vok.lth.se

NOMENCLATURE

AM: Air-motor Mode

ATDC: After Top Dead Centre

BDC: Bottom Dead Centre

BMEP: Brake Mean Effective Pressure

BTDC: Before Top Dead Centre

CAD: Crank Angle Degree

CM: Compressor Mode

η_{regen}: Regenerative efficiency [%]

κ: polytropic exponent [-]

ICE: Internal combustion Engine

IMEP: Indicated Mean Effective Pressure

IVC: Inlet Valve Closing

IVO: Inlet Valve Opening

p: In-cylinder pressure [bar]

TankVO: Tank Valve Opening

TankVC: Tank Valve Closing

TDC: Top Dead Centre

RPM: Revolutions Per Minute

V: Cylinder volume [m^3]